ASSESSING THE ROLES OF STRIATIN ORTHOLOGS IN FUNGAL MORPHOGENESIS, SEXUAL DEVELOPMENT AND PATHOGENICITY

A Dissertation

by

CHIH-LI WANG

Submitted to the Office of Graduate Studies of
Texas A&M University
in partial fulfillment of the requirements for the degree of

DOCTOR OF PHILOSOPHY

August 2011

Major Subject: Plant Pathology

ASSESSING THE ROLES OF STRIATIN ORTHOLOGS IN FUNGAL MORPHOGENESIS, SEXUAL DEVELOPMENT AND PATHOGENICITY

A Dissertation

by

CHIH-LI WANG

Submitted to the Office of Graduate Studies of
Texas A&M University
in partial fulfillment of the requirements for the degree of

DOCTOR OF PHILOSOPHY

Approved by:

Chair of Committee,	Brian D. Shaw
Committee Members,	Won-Bo Shim
	Michael V. Kolomiets
	Xiaorong Lin
Head of Department,	Leland S. Pierson III

August 2011

Major Subject: Plant Pathology

ABSTRACT

Assessing the Roles of Striatin Orthologs in Fungal Morphogenesis, Sexual Development and Pathogenicity. (August 2011)

Chih-Li Wang, B.S.; M.S., National Chung Hsing University, Taiwan

Chair of Advisory Committee: Dr. Brian D. Shaw

Striatin family proteins contain a caveolin binding domain, a coiled-coil motif, a calmodulin binding domain, and a WD-repeat domain. Homologs of striatin protein have been identified in metazoans and fungi. The mammalian striatin homologs have been proposed to be scaffolding proteins that are involved in multiple signal transduction pathways. However, our knowledge of the function and the molecular mechanism of fungal striatin homologs is limited. Based on the conserved sequences of functional domains, I hypothesized that the fungal striatin orthologs also act as scaffolding proteins that are functionally conserved among fungal species and involved in multiple types of development in the diverse kingdom Mycota.

I used reverse genetic strategies to study the function of the *Aspergillus nidulans* striatin ortholog (*strA*) and the *Colletotrichum graminicola* striatin ortholog (*str1*). In assays of sexual development, the *strA* deletion strain (Δ*strA*) produces fewer ascospores with smaller cleistothecia, while the *str1* deletion strain (Δ*str1*) is defective in perithecia development. The Δ*strA* phenotypes indicate that StrA is associated with ascosporogenesis in cleistothecia. Both Δ*strA* and Δ*str1* are reduced in radial growth and

in conidia production. The Δ*str1* strain is also altered in its spiral growth pattern and morphology of conidia and hyphopodia, but it produces appressoria similar to wild type. The pairing of nitrate non-utilizing mutants demonstrates that Str1 is required for hyphal fusion. In pathogenicity, Δ*str1* is less virulent in maize anthracnose leaf blight and stalk rot. The phenotypes of Δ*str1* are complemented by the *Fusarium verticillioides* striatin ortholog (*fsr1*), indicating that Fsr1 and Str1 are functionally conserved. Over-expression of StrA reveals its positive role in conidiation and the sexual production. StrA::eGFP localizes mainly to the endoplasmic reticulum.

After comparing the results from these two species and other studied fungal species, I suggest that fungal striatins are involved in five types of development including hyphal growth, hyphal fusion, conidiation, sexual development, and virulence, and propose a model of fungal striatin protein interactions to account for these diverse phenotypes.

DEDICATION

TO

My parents, Chin-Fa Wang and Tsai-O Wu

My parents-in-law, Mau-Cheng Ku and Pi-Chu Ku Hsu

My wife, Chu-Chi Ku

My daughter, Chen-Yu Wang

For their love, support, and understanding

ACKNOWLEDGEMENTS

I would like to share my joy with sincere appreciation to my mentors and friends.

My greatest appreciation is to my academic adviser, Dr. Brian D. Shaw. His guidance and support directed me to be successful and to keep on the right track in my research and help me to be a scientist in molecular fungal biology. I also thank him for creating a friendly research environment, giving me the opportunity to interact with peers at scientific conferences, and being patient in our scientific debates during the past four years. This dissertation would not be finished without the expertise I acquired from him.

I thank my committee members, Dr. Won-Bo Shim and Dr. Xiaorong Lin, for their intelligent insight on my research in our monthly group meetings, and for kindly sharing their valuable experience with me. I also thank Dr. Michael V. Kolomiets, my other committee member, for teaching me a great deal about in plant-microbe interactions. I would like to express my gratitude to my former supervisor, Dr. Peter P. Ueng (USDA-ARS, Beltsville, Maryland), for continuously offering me caring advice on my personal life and future career.

I also would like to express my appreciation to my former and current lab members: Dr. Soo Chan Lee, for his friendship and many informative chats; Srijana Upadhyay, for teaching me many molecular techniques, generously sharing her research experience, and her generous encouragement; Dr. Dawoon Chung, for creating a delightful atmosphere in the lab and being an understanding lab member; Laura

Quintanilla, for being a nice lab member and sharing information about our Lifeact research.

I am indebted to the following post-doctoral fellows: Dr. Mala Mukherjee and Dr. Jung Eun Kim, for discussing the research of *fsr1*-interacting proteins; Dr. Shengli Ding, for assistance of western blot of StrA::S-tag; Dr. Yuanxin Yan, for sharing his knowledge and experience of maize development.

I would like to extend my gratitude to other faculty, staff, and students in the Department of Plant Pathology & Microbiology at Texas A&M University for giving me a great study experience. Especially, I would like to thank Dr. Dan Ebbole for giving me a broad knowledge of molecular fungal biology. I thank Eli Borrego, David Laughlin, Martha Malapi Nelson, Ghada Rawdan, Carlos Ortiz, and Iris Duarte for their friendship.

Finally, I thank my family for their support, especially my brother and sister, for their assistance with my parents while I was not able to be with them. I also thank God for bringing me to and through this journey.

NOMENCLATURE

A-ODN	antisense oligodeoxynucleotide
ALB	anthracnose leaf blast
ASR	anthracnose stalk rot
BFA	Brefeldin A
BSK	DJNK basket
CCM3	cerebral cavernous malformation
CKA	connector of kinase to AP-1
CM	complete medium
DFOS	*Drosophila* homolog of c-*fos*
DJNK	*Drosophila* homolog of JUN N-terminal kinase
DJUN	*Drosophila* homolog of c-j*un*
dpi	days post-inoculation
DPP	decapentaplegic
eNOS	endothelial nitric oxide synthase
ER	endoplasmic reticulum
ERα	estrogen receptor α
Fgfsr1	*Fusarium graminearum* striatin ortholog
Fsr1	*Fusarium verticillioides* striatin ortholog
GCK-III	germinal center kinase
GFP	green fluorescent protein

Ham3	*Neurospora crassa* striatin ortholog
HEP	DJNK kinase hemipterous
MAPK	mitogen-activated protein kinase
MM	minimal medium
MMC	minimal medium amended with chlorate
nit	nitrate non-utilizing
NLS	nuclear localization sequence
OE	over-expression
PDC	potato dextrose agar (PDA) amended with chlorate
PP2A	protein phosphatase 2A
Pro11	*Sordaria macrospora* striatin ortholog
RFP	red fluorescent protein
SLMAP	sarcolemmal membrane-associated protein
Str1	*Colletotrichum graminicola* striatin ortholog
StrA	*Aspergillus nidulans* striatin ortholog
STRIP 1/2	striatin-interacting protein 1/2
STRIPAK	striatin-interacting phosphatase and kinase
STRN	striatin
STRN3	SG2NA
STRN4	zinedin
Y2H	yeast-two hybrid

TABLE OF CONTENTS

CHAPTER Page

LIST OF FIGURES

Page

LIST OF TABLES

CHAPTER I

INTRODUCTION

Striatin family proteins contain a caveolin-binding domain, a coiled-coil motif, and a calmodulin-binding domain at the N-terminus, and a WD repeat domain at the C-terminus. Except for plants, they are found in all eukaryotes. Humans are representative of mammals in that they contain three homologs; STRN (striatin), STRN3 (SG2NA), and STRN4 (Zinedin) (Benoist et al., 2006). Among them, STRN3 is comprised of three isoforms, STRN3α (SG2NAα), STRN3β (SG2NAβ), and STRN3γ (SG2NAγ) (Benoist et al., 2006; Tan et al., 2008). Other metazoans, such as flies and fish, each contain one homolog (Chen et al., 2002; Ma et al., 2009). In the kingdom Mycota, filamentous fungi contain one homolog while the budding yeast, *Saccharomyces cerevisiae*, contains a striatin-like protein that lacks of the WD repeat domain (Kemp and Sprague, 2003). Phylogenetic analyses suggest that striatin family proteins in metazoans and filamentous fungi may have evolved from the same ancestral gene (Castets et al., 2000; Ma et al., 2009; Shim et al., 2006).

MAMMALIAN STRIATIN HOMOLOGS

Tissue and sub-cellular localization

Striatin was named from striatum, a subcortical part of the forebrain, due to its

---

This dissertation follows the style of Fungal Genetics and Biology.

predominant expression in the dorsal part of striatum (Castets et al., 1996). Striatin family proteins mainly localize to neurons of the central and peripheral nervous systems (Blondeau et al., 2003; Castets et al., 1996; Castets et al., 2000; Salin et al., 1998). Specifically, striatin family proteins are highly concentrated in the dendritic spines of neurons (Gaillard et al., 2006). All striatin homologs are abundant in the brain and cerebellum while the STRN3α (SG2NAα) was also found in muscle. Striatin family proteins are also weakly expressed in other tissues. For example, STRN (striatin) was also detected in lung and spleen. STRN4 (zinedin) was found in heart, kidney, lung, and spleen. STRN3α (SG2NAα) is ubiquitously expressed in all detected tissues including hart, kidney, lung, liver and spleen (Castets et al., 2000). In brain, striatin family proteins are distributed equally in the cytosol and on membrane (Castets et al., 2000). Moreover, the reticular and perinuclear subcellular localization of STRN and STRN3 has been shown, and the STRN3 localization is to the Golgi apparatus in the HeLa cells (Baillat et al., 2001; Moreno et al., 2001).

Function of striatin domains

The function of each domain of striain family proteins has been further verified in mammalian homologs. The caveolin-binding domain binds to caveolin-1, allowing striatin family proteins to attach to the membrane (Gaillard et al., 2001). Caveolin is a small protein that tightly binds to cholesterol in membrane. About 14-16 caveolins form a homo-oligomer as the coat of caveolae that derive from plasma membrane or the Golgi body. The function of caveolin is associated with the endothelial nitric oxide synthase

(eNOS) signaling, cholesterol homeostasis, vesicular trafficking, and other signaling pathways (Razani et al., 2002; Williams and Lisanti, 2004). The coiled-coil motif is highly conserved with 94 % identity among striatin family proteins (Castets et al., 2000). The coiled-coil motif of STRN3β is essential to localize the STRN3β to somato-dendritic spines, and required for the homo- and hetero- oligomerization of striatin family proteins (Gaillard et al., 2006). One of the features of striatin family proteins is that they are the only proteins known to contain a calmodulin-binding domain and WD repeat domains (Castets et al., 1996). STRN, STRN3 and STRN4 bind CaM-Sepharose through the calmodulin-binding domain in the presence of calcium *in vitro* (Castets et al., 1996; Castets et al., 2000). This interaction partially shifts the sub-cellular localization of STRN *in vivo* (Bartoli et al., 1998). Therefore, striatin family proteins are thought to respond the fluctuation of calcium and be involved in Ca^{2+}/calmodulin signaling. The function of the WD repeat domain of striatin family is still unknown. The crystal structure of Gβ indicates that the WD repeat forms a β-propeller structure to interact with other proteins. Interestingly, although WD repeat domains consistently form similar surfaces of 3D structure, proteins possessing WD repeat domain are involved in diverse functions in eukaryotic cells such as RNA processing, signal transduction, vesicular trafficking, regulation of sulfur metabolism and cytoskeleton assembly (Smith et al., 1999).

Phenotypes and molecular mechanisms

Rat brain was infused with a striatin A-ODN (antisense oligodeoxynucleotide), results in the down-regulation of striatin. The striatin A-ODN treated rat displays decreased nocturnal locomotor ability. While treated with the striatin A-ODN, the rate of spinal motoneurons is defective in dendritic outgrowth (Bartoli et al., 1999).

Analysis of striatin-interacting proteins is gradually uncovering the molecular mechanisms and sub-cellular functions of mammalian striatin homologs. PP2A A/C (Protein phosphatase 2A A/C) subunits are identified by co-immunoprecipitation with STRN and STRN3 (Moreno et al., 2000). The holoenzymes of PP2A are usually comprised of a PP2A A (structural) subunit, a PP2A B (regulatory) subunit and a PP2A C (catalytic) subunit, and promote activity of serine / threonine protein phosphatase in eukaryotes (Cohen, 1989). Many PP2A B subunits are expressed in specific cellular compartments and different developmental stages, and determine the substrate of the holoenzyme. Thus, the B subunits are the most diverse among the three classified subunits (Janssens and Goris, 2001; Lechward et al., 2001). STRN and STRN3 are proposed to interact with PP2A A/C subunits as a B subunit, and the STRN/STRN3-containing PP2A complexes provided the phosphatase activity in a Ca^{2+}-independent manner (Moreno et al., 2000).

Mob3/phocein is a component of the STRN/STRN3- containing PP2A complexes and co-localized with STRN3 to the Golgi apparatus (Baillat et al., 2001; Moreno et al., 2001). The mammalian striatin homologs are implicated in vesicular

trafficking, especially in endocytosis due to the direct interaction between Mob3 and EPS15 and nucleotide diphosphate kinase (Baillat et al., 2002; Bailly and Castets, 2007).

Upon the induction of estrogen, ERα (estrogen receptor α) may interact with a PP2A complex containing STRN or STRN3γ, respectively (Lu et al., 2004; Lu et al., 2003; Tan et al., 2008). Estrogen, through ERα, can induce both 'nongenomic' and the 'genomic' effects in a variety of tissues. In human vascular endothelial cells, STRN brings ERα to plasma membrane and forms a complex with Gαi. The protein complex is required to activate MAPK (mitogen-activated protein kinase), eNOS (endothelial NO synthase), and phosphatidylinositol 3–Akt kinase for signaling the nongenomic effects of estrogen. Disrupting the interaction of STRN and ERα blocks the signaling pathway (Lu et al., 2004). In rat uterine cells, STRN3γ-containing PP2A complex causes dephosphorylation of ERα, resulting in a decrease in ERα transcriptional activity, the genomic effects of estrogen (Tan et al., 2008).

APC (adenomatous polyposis coli), a multifunctional tumor suppressor protein, is involved in several cellular processes such as cell adhesion, organization of cytoskeleton, chromosome segregation and cell migration. Most colorectal cancer cells have been found containing a mutated APC gene (Polakis, 2000). Interactions between mammalian striatin homologs and APC contribute to the localization of the tight junction protein ZO-1 and to the organization of F-actin in epithelial tight junction compartment, suggesting a possible function of striatin members in cell-cell adhesion via rearrangement of the cytoskeleton (Breitman et al., 2008).

To summarize, mammalian striatin family proteins are involved in the development of neural dendrites, and are required for the nocturnal locomotor activity of rats. However, the molecular mechanism contributing to these functions is obscure. Evidence suggests that striatin family proteins are able to serve as a PP2A B sub-unit and form a holoenzyme with PP2A A/C subunits. These PP2A holoenzymes may function in vesicular trafficking or endocytosis through the interacting protein Mob3, and also interact with ERα to conduct the 'nongenomic' and 'genomic' effects of estrogen. In addition, mammalian striatin proteins may play a role in F-actin organization.

INSECT AND FISH STRIATIN ORTHOLOGS

Drosophila melanogaster

In *D. melanogaster*, epithelial cell sheet movement is essential during the processes of dorsal closure in embryo, and is regulated by the JUN N-terminal kinase (DJNK) and DPP (decapentaplegic) signal transduction pathways (Noselli and Agnes, 1999; Riesgo-Escovar and Hafen, 1997). Mutation of the fly striatin ortholog (CKA, connector of kinase to AP-1) results in the lethal dorsal open phenotype. In DJNK signaling pathway, CKA has been found to form a protein complex with four other components in which the interaction of CKA and HEP (DJNK kinase hemipterous) activates BSK (DJNK basket), and then the BSK phosphorylates DFOS (*Drosophila* homolog of c-*fos*) and DJUN (*Drosophila* homolog of c-j*un*) for triggering DPP

signaling pathway (Chen et al., 2002). This data suggests a striatin ortholog can activate kinases and transcriptional factors.

Goldfish, *Carassius auratus*

Goldfish produces two STRN3 transcripts, which is a homolog of human STRN3α. The goldfish STRN3 proteins are highly expressed in liver, spermary and heart, but are reduced in expression in brain, ovary and skeletal muscle. These proteins are increasingly expressed during the embryonic development with a few fluctuations. Several differences in the expression of mRNA and protein of the STRN3 demonstrate that there is post-transcriptional regulation to control protein expression in different tissues. STRN3, as seen in *Drosophila* CKA, also interacts with JUN N-terminus kinase in goldfish (Ma et al., 2009).

STRIATIN ORTHOLOGS IN FILAMENTOUS FUNGI

Common mutant phenotypes: sexual development and colony growth

The *Sordaria macrospora* striatin ortholog (*pro11*) was discovered by forward genetics after ethyl methanesulfonate mutagenesis and screening for the defective phenotypes of sexual development. The *S. macrospora pro11* mutant is significantly reduced in production of protoperithecia, and developmental processes of perithecia are arrested in the stage of protoperithecia (Pöggeler and Kück, 2004). Another homothallic fungus, *Fusarium graminearum*, also lost the sexual fertility when the striatin ortholog gene (Fg*fsr1*) was deleted (Shim et al., 2006). Strikingly, in two heterothallic fungi, *F.*

verticilloides and *Neurospora crassa*, the orthologous mutants are able to serve as the male strain for mating, but are female infertile (Shim et al., 2006; Simonin et al., 2010). In *N. crassa*, Δ*ham3*, while serving as a female strain, is able to perform the sexual chemotropic cell fusion, but subsequent sexual development is arrested. In addition, a homozygous cross of Δ*ham3* displays abnormal meiosis and ascospore formation (Simonin et al., 2010). In short, these data indicate that fungal striatin orthologs may be involved in early stages of perithecium development and the ascospore differentiation.

Altered colony growth is the other phenotype commonly found in filamentous fungal striatin mutants, though there is no discernable hyphal impairment reported. The reduced radial growth and short aerial hyphae are observed in *Fusarium verticillioides fsr1* mutants, *F. graminearum* ΔFg*fsr1* and *N. crassa* Δ*ham3* (Shim et al., 2006; Simonin et al., 2010). In contrast, an increased density of aerial hyphae is observed in the *pro11* mutant (Pöggeler and Kück, 2004).

Individual reported mutant phenotypes: virulence, hyphal fusion and conidiation

The *F. verticillioides* striatin ortholog (*fsr1*) was identified in a mutant screen with a significant defect in virulence of maize stalk rot. The *fsr1* mutant fails to expand disease symptoms from the inoculation site. The phenotype is also observed in another species of *Fusarium*, *F. graminearum*. ΔFg*fsr1* causes reduced disease symptoms of head blight of barley (Shim et al., 2006). This may implicate a conserved function of striatin orthologs in *Fusarium* species.

N. crassa wild type conidial germlings and hyphae tend to fuse between themselves when encountering each other through the formaiton of conidial anastomosis tubes. However, Δ*ham3* hyphae pass over each other without fusing. A quantitative heterokaryon assay demonstrates that Δ*ham3* is not able to fuse with the wild-type strain. These results indicate that *ham3* is essential for self- and nonself- fusion in *N. crassa*. In addition, Δ*ham3* also produces about 100 times fewer conidia than wild type (Simonin et al., 2010).

Gene expression

The gene expression of *S. macrospora pro11* is weak during the vegetative growth (Pöggeler and Kück, 2004). By using QRT-PCR (quantitative real-time polymerase chain reaction), *F. verticillioides fsr1* displays constitutive expression during the vegetative growth in various media and *in planta* (Shim et al., 2006). In contrast, the relevant gene expression of *pro11* is shown during the perithecium development (Bernhards and Pöggeler, 2011). This further supports the idea that fungal striatin orthologs play an important role in sexual development.

Domain functions and localization

Little is known about the function of each domain of fungal striatin orthologs. The N-terminal domains of *S. macrospora* Pro11 are required to remove the developmental arrest of perithecium development of the *pro11* mutant, but the amount of perithecium and ascospore production is still reduced (Pöggeler and Kück, 2004). The

coiled-coil motif of *F. verticillioides* Fsr1 is essential for the virulence of maize stalk rot and the vegetative radial growth (Yamamura and Shim, 2008). Pro11 is a membrane bound protein in cell fractionation assays (Pöggeler and Kück, 2004). As indicated above, the caveolin-binding domain plays an important role for mammalian striatin homologs to attach to membrane. There was, however, no caveolin homolog identified in sequenced fungal genomes (Pöggeler and Kück, 2004; Shim et al., 2006). This raises the question of what allows the association of striatin orthologs to membrane and to what membrane do striatin orthologs localize. In addition, it is still unknown what functions are mediated through the calmodulin binding domain and the WD repeat domain.

THE PUTATIVE PROTEIN COMPLEXES: FROM FUNGI TO HUMAN

In *S. cerevisiae*, Far8 (striatin-like protein) forms a protein complex with Far3, Far7, Far9, Far10 and Far11. Except for Far11, Far8 physically interacts with the other four proteins (Gavin et al., 2002; Ho et al., 2002; Ito et al., 2001; Kemp and Sprague, 2003; Uetz et al., 2000). Mutants of each gene phenocopy a pheromone arrest defect, which supports the notion that they are functional in the same pathway (Kemp and Sprague, 2003). The orthologs, Ham2 (ortholog of Far11), Ham3 (ortholog of Far8) and Ham4 (ortholog of Far 9 and Far10) are found in the *N. crassa* genome while there is no ortholog of Far3 and Far7. Although Far8 lacks the WD repeat domain of the striatin family, the protein complex was used as a model to explore gene functions in *N. crassa*. Due to the similar defects in hyphal fusion, aberrant meiosis, and abnormal ascospores,

Ham2, Ham3 and Ham4 are proposed to be functional together (Simonin et al., 2010). As mentioned above, Mob3 is a STRN-interacting protein in mammalian cells. *S. macrospora mob3* was characterized and compared to the *pro11* mutant. Mutants in both genes are impaired in perithecium development at early stages (Bernhards and Pöggeler, 2011). In addition, a hyphal fusion defect phenotype is observed in *mob3* mutants of *S. macrospora* and *N. crassa*, and the *N. crassa* Δham3 (Bernhards and Pöggeler, 2011; Maerz et al., 2009; Simonin et al., 2010), which implicates a potential interaction between Mob3 and fungal striatin orthologs. Although there is no experimental data demonstrating these protein-protein interactions, one may hypothesize that Ham2, Ham4, Ham3 and Mob3 form a protein complex in *N. crassa*, and that this complex is similar in other filamentous fungi.

Strikingly, a PP2A-related protein interaction was established in human cells. The STRIPAK (striatin-interacting phosphatase and kinase) complex was identified and comprises of striatin homologs, PP2A A/C subunits, Mob3, STRIP 1(striatin-interacting protein 1), STRIP2, CCM3 (cerebral cavernous malformation) protein, and members of the GCK-III (germinal center kinase) family of Ste20 kinases including STK24, STK25 and MST4 (Goudreault et al., 2009). The STRIP1 and STRIP2 are newly identified proteins in human and homologs of *N. crassa* Ham2. A sub-population of STRIPAK complex may further interact with CTTNBP2 proteins, which are associated with cytoskeletal protein cortactin, or with SLMAP (sarcolemmal membrane-associated protein), which is an ortholog of fungal Ham4 (Goudreault et al., 2009; Simonin et al., 2010). As indicated above, the orthologs of the four components of the putative fungal

striatin protein complex are present in the mammalian STRIPAK complex, implicating the molecular mechanism may be conserved from fungi to human through the evolution.

HYPOTHESIS

Mounting evidence indicates that mammalian striatin homologs are able to interact with several types of proteins, suggesting that striatin homologs are involved in multiple functions. Assuming that the putative protein complex of human striatin homologs is also conserved in filamentous fungi, and the fact that filamentous fungi are diverse in developmental structures and physiological processes for different niches, it is obvious that our knowledge of the functional roles of fungal striatin is limited. Due to the conserved functional domains among fungal striatin orthologs, **I formulated the hypothesis that fungal striatin orthologs mediate some conserved functions among the fungal species and play additional roles for individual adaption to varied environments.**

In my research, *Aspergillus nidulans* and *Colletotrichum graminicola* were chosen to characterize the functions of fungal striatin orthologs. One copy of striatin ortholog was identified in each organism by using *F. verticillioides* Fsr1 and bi-directional blast of the *A. nidulans* and the *C. graminicola* genome databases from the Broad Institute (http://www.broad.mit.edu/). Both predicted proteins contained the conserved domains that were characteristic of striatin family proteins (Figure 1.1). A summary of the characterized fungal striatin is shown in Table 1.1 Both *A. nidulans* and *C. graminicola* displayed several biological features different from *F. veritcillioides*, *S.*

macrospora, and *N. crassa*, which allowed me to explore the roles of fungal striatins in additional developmental processes. The conserved functions of fungal striatin orthologs were deduced from this study and previous research.

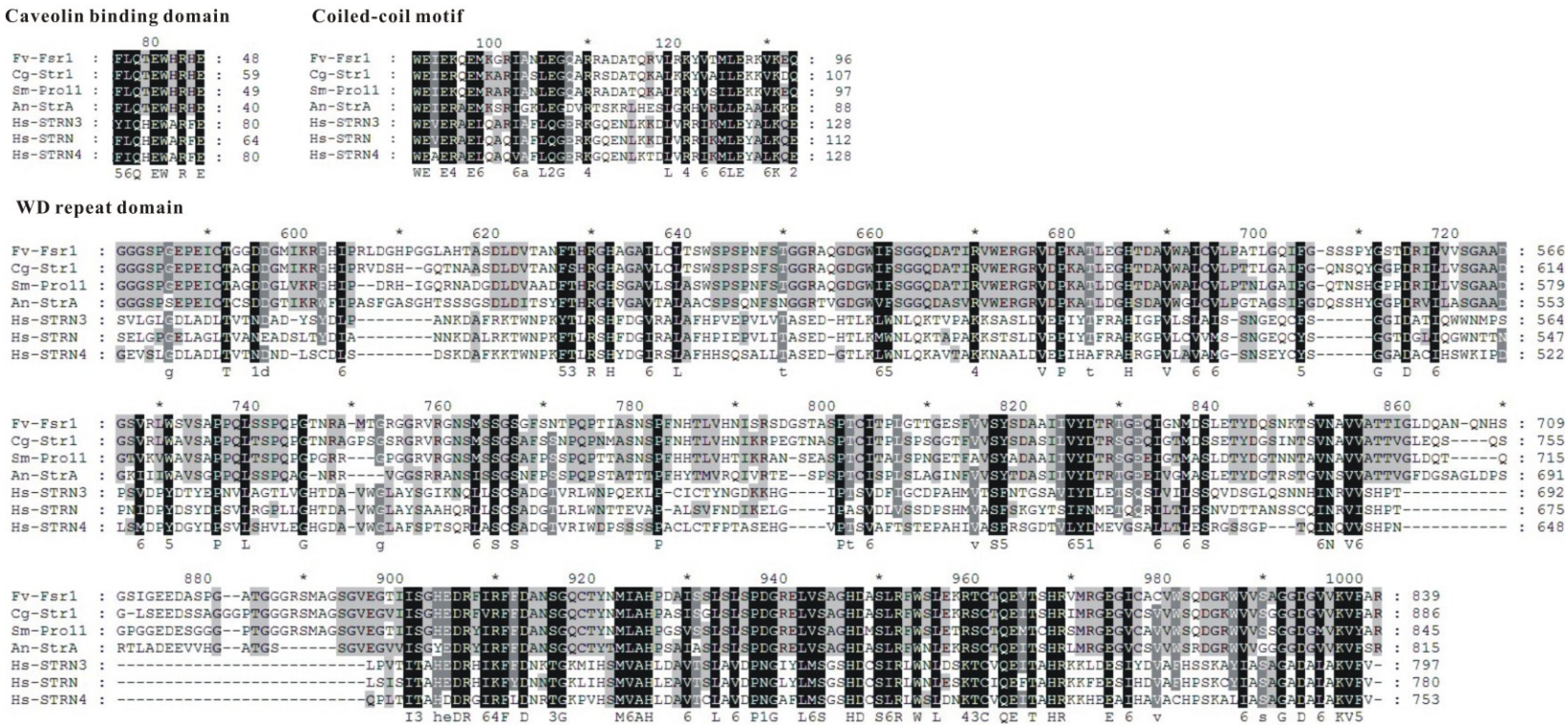

Figure 1.1 The putative conserved domain alignments of striatin family proteins.
Protein sequence for each species is shown. Conserved domains are highlighted by dark shading. Cg: *Colletotrichum graminicola*. An: *Aspergillus nidulans*. Fv: *Fusarium verticillioides*. Sm: *Sordaria macrospora*. Hs: *Homo sapiens*.

Table 1.1 Characteristics comparison of fungi and their striatin orthologs.

	Aspergillus nidulans	*Colletotrichum graminicola*	*Fusarium verticillioides*	*Sordaria macrospora*	*Neurospora crassa*
Class of classification	Eurotiomycetes	Sordariomycetes	Sordariomycetes	Sordariomycetes	Sordariomycetes
Life style	Saprophytic	Pathogenic (hemi-biotrophic)	Pathogenic (hemi-biotrophic) / Endophytic	Saprophytic	Saprophytic
Sexual compatibility	Homothallic	Unbalanced heterothallic	Heterothallic	Homothallic	Heterothallic
Ascoma	Cleistothecia	Perithecia	Perithecia	Perithecia	Perithecia
Asexual stage	Hyphomycete	Coelomycete	Hyphomycete	None	Hyphomycete
Striatin ortholog	StrA	Str1	Fsr1	Pro11	Ham3
Locus or accession No.[1]	ANID08071.1	GLRG_06260.1	FVEG_09767.3	Q70M86	NCU08741
Length of gene (nucleotides / amino acid)	2640 nt / 815 aa	2830 nt / 886 aa	2568 nt / 839 aa	2717 nt / 845 aa	2935 / 854 aa
E-Value[2]	3e-33	5e-32	1e-21	4e-21	2e-17

[1] The annotated genome sequences of *A. nidulans* A4 and *F. verticillioides* M3125, *N. crassa* RO74A, and the draft assembly sequence of *C. graminicola* M1.001 were acquired from the Broad Institute (http://www.broad.mit.edu/). The genome sequence of *S. macrospora* was available from NCBI (http://www.ncbi.nlm.nih.gov/). NA, not available.
[2] E-Values were measured with the amino acid sequence of *Homo sapiens* striatin (CAA11560.1).

CHAPTER II

Aspergillus nidulans STRIATIN (STRA) MEDIATES SEXUAL DEVELOPMENT AND LOCALIZES TO THE ENDOPLASMIC RETICULUM*

SUMMARY

Striatin family proteins have been identified in animals and fungi and are considered to be scaffolding proteins. In fungi striatin orthologs have been associated with sexual development and virulence to plants. In this study, we characterized the functions and localization of the striatin ortholog, StrA, in *A. nidulans*. ΔstrA strains showed multiple defects in conidium germination, mycelial radial growth, production of diffusible red pigment, and reduced conidiation. The most striking phenotype is the production of abnormally small cleistothecia that are defective in ascosporogenesis. Overexpression of *strA* enhanced cleistothecium development and increased the production of Hülle cells in shaking liquid cultures. In addition, we generated strains expressing StrA::eGFP under the endogenous promoter. By co-labeling with FM4-64 and co-localization with nuclear localized StuA(NLS)::DsRed or CxnA (an endoplasmic reticulum marker), we determined that StrA mainly localizes to endoplasmic reticulum and the nuclear envelope.

---

* This chapter is reprinted with permission from '*Aspergillus nidulans* striatin (StrA) mediates sexual development and localizes to the endoplasmic reticulum.' by Wang, C. L., Shim, W. B., and Shaw, B. D. 2010. Fungal Genet. Biol. 47: 789-799.

INTRODUCTION

The *Aspergillus nidulans* life cycle progresses through both asexual and sexual reproductive stages. Each is controlled by multiple diverse environmental factors such as light, oxygen, and nutrient availability. Generally, sexual reproduction is initiated after asexual conidiation and encouraged by oxygen limitation and lack of light. *A. nidulans* forms a closed fruiting body termed a cleistothecium. The details of cleistothecium formation have been described previously (Braus et al., 2002; Champe et al., 1994; Sohn and Yoon, 2002). Cleistothecium formation starts with a coiled structure formed by two hyphae. One hypha forms a 2-celled core structure while the other hypha wraps around the core structure. This primordium then enlarges and develops into the ascogenous system while the coiled hypha also develops to form the peridium. Simultaneously, a cluster of thick-walled Hülle cells develop from hyphae surrounding the developing primordia. Hülle cells are a unique cell type that are considered to be the first visible sign of sexual development and are always tightly associated with cleistothecia in nature. During the formation of cleistothecia, croziers and ascogenous cells develop in the centrum and expand the size of primordia. Ultimately, thousands of globular asci are produced in the mature cleistothecium. During ascosporogenesis, each ascus undergoes meiosis and post-meiotic mitosis to produce eight red-pigmented ascospores at maturity. Recently, several genes including *nsdD*, *veA*, *steA*, *rosA* and *nosA* have been demonstrated to have essential roles in sexual development of *A. nidulans*. Most of these encode transcription factors or other proteins localized to the nucleus (Han et al., 2001; Kim et al., 2002; Vallim et al., 2000; Vienken and Fischer, 2006; Vienken et al., 2005).

Sexual development is controlled by several cytoplasmic signaling pathways such as the MAP kinase (Wei et al., 2003) and the G-protein signaling pathways (Seo et al., 2004). However, the proteins mediating the signal transduction into nuclei are still poorly understood.

Striatin family proteins are thought to be molecular scaffolds that act as links between signal transduction and vesicular trafficking in animal systems (Benoist et al., 2006). They are mainly expressed in neurons and are highly concentrated in neuronal somato-dendritic spines (Castets et al., 2000). Three members of the striatin family; striatin, SG2NA and zinedin, have been identified in mammals and all contain four conserved domains: a caveolin-binding motif, a coiled-coil motif, a calmodulin-binding domain, and a WD-repeat domain (Castets et al., 1996; Castets et al., 2000; Muro et al., 1995). The caveolin-binding motif attaches striatin family proteins to membrane by binding to caveolin-1, an integral membrane protein of caveolae (Gaillard et al., 2001). The coiled-coil motif functions in homo- and hetero-oligomerization of these proteins, which is critical for striatin family proteins to localize to dendritic spines (Gaillard et al., 2006). In vitro studies demonstrated interactions between striatin family proteins and calmodulin through their calmodulin binding domain (Bartoli et al., 1998; Castets et al., 1996; Castets et al., 2000), suggesting striatin family proteins are able to sense Ca^{2+} fluctuation through the interaction with calmodulin. The WD-repeat domain can provide a platform for a protein to interact with other proteins (Smith et al., 1999).

Only one striatin ortholog is encoded by the genomes of sequenced filamentous fungi. Fungal striatin orthologs have been implicated in perithecium development

(Pöggeler and Kück, 2004; Shim et al., 2006; Simonin et al., 2010). Perithecia are ostiolate fruiting bodies produced in the Sordariomycetes, a class of Ascomycetes that includes all fungi where striatin orthologs have previously been characterized. *Sordaria macrospora* Pro11 is the first striatin ortholog characterized in filamentous fungi. It was determined to play a critical role in protoperithecia development (Pöggeler and Kück, 2004). In *Fusarium verticillioides* and *F. graminearum*, striatin orthologs were directly involved in virulence to plants via a coiled-coil motif and in female fertility (Shim et al., 2006; Yamamura and Shim, 2008). In *S. macrospora*, Pro11 was determined to be a membrane-bound protein (Pöggeler and Kück, 2004), suggesting that striatin attaches to either plasma membrane or organelle membrane. However, no caveolin ortholog has been identified to date in the genome sequences of *Neurospora crassa* and *F. verticillioides* (Pöggeler and Kück, 2004; Shim et al., 2006). To date, the diverse functions and the localization of the fungal striatin orthologs have not been fully explored.

Here, we demonstrate that the striatin ortholog also plays a role in sexual development in *A. nidulans*, a Eurotiomycete that produces cleistothecia. Sexual reproduction is not abolished in a *strA* mutant. Striatin over-expression enhanced initiation of sexual development, suggesting that striatin regulates cleistothecium formation. Our phenotypic analysis suggests that fungal striatin is also involved in conidiation. The subcellular localization of green fluorescent protein (GFP) tagged striatin illustrates that *A. nidulans* striatin localizes mainly to endoplasmic reticulum and the nuclear envelope.

MATERIALS AND METHODS

Strains, growth conditions, and reagents

Strains used in this study are listed in Table 2.1. Media included complete medium (CM) and minimal medium (MM) as previously described (Shaw and Upadhyay, 2005). For induction of the *alcA* promoter, 0.5% ethanol was added to MM (without glucose) when examining microscopically the germlings, while 1% ethanol, 1% glycerol was used for long-term growth studies. For *alcA* promoter repression, 1% glucose was added to the appropriate media (Flipphi et al., 2003). To measure radial growth, 10 µl conidia suspensions containing 10^5 conidia were inoculated at the center of medium plates with four replications for 5 days at 28 °C. To quantify conidia production, conidia suspended in 5 mL 1% water agar were overlaid on the medium and cultured for 5 days at 28 °C. Ten pieces of 1 cm diameter agar block with mycelial were randomly collected from each plate and vortexed with 20 mL 0.1% Tween 20 solution in a 50 ml centrifuge tube. The total number of conidia produced on collected agar blocks was counted with a hemocytometer. To quantify the formation of cleistothecia under various environmental conditions, 10^5 conidia in 5 mL 1% water agar were overlaid on appropriate medium in parafilm sealed petri dishes and incubated for two weeks. To evaluate the rate of germ tube emergence, conidia were cultured on coverslips submerged in liquid CM. Three replicates of 200 conidia each were counted. A conidium was scored as having germinated if a germ tube was discernable from the conidium. To evaluate the effects of *strA* over-expression in shaking liquid medium, conidia were incubated in 50 ml or 75 ml liquid MM in a 125 ml flask at 28 °C 200 rpm incubator for

Table 2.1 Strains used in this study.

Strains	Genotype	Source
A4	Wild type	FGSC
A773	*pyrG89; wA3; pyroA4; veA1*	FGSC
TN02A25	*pyrG89; argB2; pabaB22; ΔnkuA::argB; riboB2; veA1*	(Nayak et al., 2006)
ASL91	*argB2; pyrG89; wA3; veA1*	(Chung et al., 2011)
A126	*pabaA1; yA2; wA3; veA*	FGSC
CL206	*pyroA4; wA3; veA*	This study
StrAKOD2-3c	*ΔstrA::pyr4; pyrG89; wA3; pyroA4; veA1*	This study
StrAKOcs	*ΔstrA::pyr4; pyrG89; wA3; veA1*	This study
StrAKO18	*ΔstrA::pyr4; pyrG89; argB2; wA3; veA1*	This study
StrAKO217	*ΔstrA::pyr4; wA3; veA*	This study
StrAcomD32	*ΔstrA::pyr4; pyrG89; strA(p)::strA::argB; argB2; wA3; veA1*	This study
A91GFP5a	*alcA(p)::strA::sGFP::argB; pyrG89; argB2; wA1; veA1*	This study
StrAove3	*alcA(p)::strA::sGFP::argB; ΔstrA::pyr4; pyrG89; argB2; wA3; veA1*	This study
StrAGFP135	*strA::eGFP::pyrG-AF; pyrG89; ΔnkuA::argB; argB2; pabaB22; riboB2; veA1*	This study
StrAGFP140	*strA::eGFP::pyrG-AF; pyrG89; ΔnkuA::argB; argB2; pabaB22; riboB2; veA1*	This study
AJW11	*alcA(p)::stuA*(NLS)*::DsRed::argB; pyrG89; argB2; wA3*	Toews et al. (2004)
StrAGFP135w2	*strA(p)::strA::eGFP::pyrG-AF; pyrG89; argB2; wA3; veA1*	This study
StrAGFP140G2	*strA(p)::strA::eGFP::pyrG-AF; pyrG89; ΔnkuA::argB; argB2; pabaB22; veA1*	This study
AJ135w2-4	*strA(p)::strA::eGFP::pyrG-AF; pyrG89; alcA(p)::stuA*(NLS)*::DsRed::argB; argB2; wA3; veA1*	This study
StrA135w2-cnxA9	*strA(p)::strA::eGFP::pyrG-AF; pyrG89; alcA(p)::cnxA::mRFP1::argB; argB2; wA3; veA1*	This study

Fungal Genetic Stock Center (McCluskey, 2003).

one week in the dark. Diagnostic PCR reactions were performed with *Taq* DNA polymerase (New England Biolabs, Ipswich, MA, USA). All fusion PCR reactions were performed by the using Expand High Fidelity PCR system and the Expand Long Template PCR system (Roche Diagnostics, Indianapolis, IN, USA).

DNA extraction and Southern blot analysis

Genomic DNA extraction and Southern blotting were conducted by following standard procedures (Sambrook and Russell, 2001). To verify the *strA* deletion, genomic DNA from *strA* wild-type strain (A773) and Δ*strA* candidates were digested with *Pst*I, *Msc*I and *Sac*I and separated on 1% agarose gels. Digested DNA samples were transferred from the agarose gel to a Hybond-N+ nylon membrane (Amersham Biosciences). Hybridization probe A (429 bp) spanned the 3'-flanking region of *strA* and was amplified with primers downF and downR (all primers listed in Table 2.2) while probe B (599 bp) spanned the coding region of *strA* and was amplified with primers fsrApR and AnfsrGFPF. The probes were labeled by using a random primer labeling kit, Prime-It II (Stratagene, La Jolla, CA) and (γ-^{32}p)CTP. For verification of the StrA::eGFP strains, *Pst*I, *Ssp*I and *Hind*III were used to digest genomic DNA of *strA* wild-type strain (TN02A25) and selected candidates. The hybridization probe spanned the 3'-flanking region (429 bp) of strA and was amplified with primers downF and downR and labeled as described above.

Table 2.2 Oligonucleotides used in this study.

oligo	Sequence (5'-3')
upF	TTCCTTGGCGGACGTAATAA
upR	GGGATGAGCGTCGGTACCCCGAGGGAGATTGCCAAGACAT
Pyr4F	GGGGTACCGACGCTCATCCCAGTCATAT
Pyr4R	GCTCTAGACTCAACCTCTCGATTCTTCC
downF	CGAGAGGTTGAGTCTAGAGCATTCCCGAGCATTTGTAACG
downR	CGATAATTCTCAGCCCAGGA
GatfsrAF	**CACC**ATGTCTGGAGGTGGAGGGTT
GatfsrAR	TCTCGAGAACACCTTGACTACTCC
fsrGFP1	ACCTTGAGCTATCGAACCAT
fsrGFP2	GGCACCGGCTCCAGCGCCTGCACCAGCTCCTCTCGAGAACACCTTGACTA
GFP-F	GGAGCTGGTGCAGGCGCT
GFP-R	CTGTCTGAGAGGAGGCACTGAT
fsrGFP3	CATCACGCATCAGTGCCTCCTCTCAGACAGCGCAGTGGATGTGGCCTGAT
fsrGFP4	CTTCGCAGTAGCCGTAACAG
AnfsrGFPF	CGATCAAGCGGTGGTTTATT
AnfsrGFPR	AAACTGCGGGCTGACTATGT
fsrApR	GATACAAGTGGGCGAAGGTG
Pyr4endF	CAGAGGTTGGACTGCTTGAC
Anfsr-ComF	CGGTACCACCCAGGTTCCTTTGCGATA
Anfsr-ComR	CACTAGTCGATAATTCTCAGCCCAGGA
GatCalAF	**CACC**ATGCGTCTCAACACAGCTCT
GatCalAR	CTCCGCAGACGATCGGGTGGT
veAF	TGTGTTATCCCATCAAGAGG
veAR	CTTGGCGCTGTAGACGATAA

Note: The underline indicates the overhang for fusion PCR, the double underlines are inserted enzyme restriction sites, and the bold is the overhang for Gateway cloning.

Generation of *strA* deletion strain

The *strA* deletion cassette was made by fusing *N. crassa pyr*-4 between *strA* 5'- and 3'- flanking regions, using techniques previously described (Yu et al., 2004). The *N. crassa pyr-4* (orotidine 5'-phosphate decarboxylase) supplied positive selection and was amplified from pGEM-pyr4 (Lee and Shaw, 2007) with primers pyr4F and pyr4R. The *strA* 5'- flanking region was amplified from 672 bp upstream of the *strA* start codon from A4 wild-type strain by primer upF and upR (with 20 bp homologous sequence overlapping the primer pyr4F). The *strA* 3'- flanking regions were amplified from 514 bp downstream of the *strA* stop codon from A4 wild-type strain by primer downF (with 20 bp homologous sequence overlapping the primer pyr4R) and downR. The three amplicons were purified using the QIAquick Gel Extraction Kit (Qiagen, Valencia, CA, USA). Fusion PCR was performed by primers upF and downR and followed previously described procedures (Yu et al., 2004). *A. nidulans* strain A773 was transformed with the *strA* deletion cassette using a previous described method (Shaw and Upadhyay, 2005). The selected pyrimidine prototrophic transformants were further screened for homologous recombination at the strA locus by PCR with primers pyr4end and AnfsrGFPR. Southern blot analysis of transformants then confirmed deletion of the native locus. A putative deletion strain StrAKOD2-3c was crossed with ASL91 (Chung et al., 2011). Several progeny including StrAKOcs and StrAKO18 (both Δ*strA*; *veA1*) were obtained from the cross. Deletion of the *strA* locus was confirmed by Southern analysis (Figure 2.1) and sequencing.

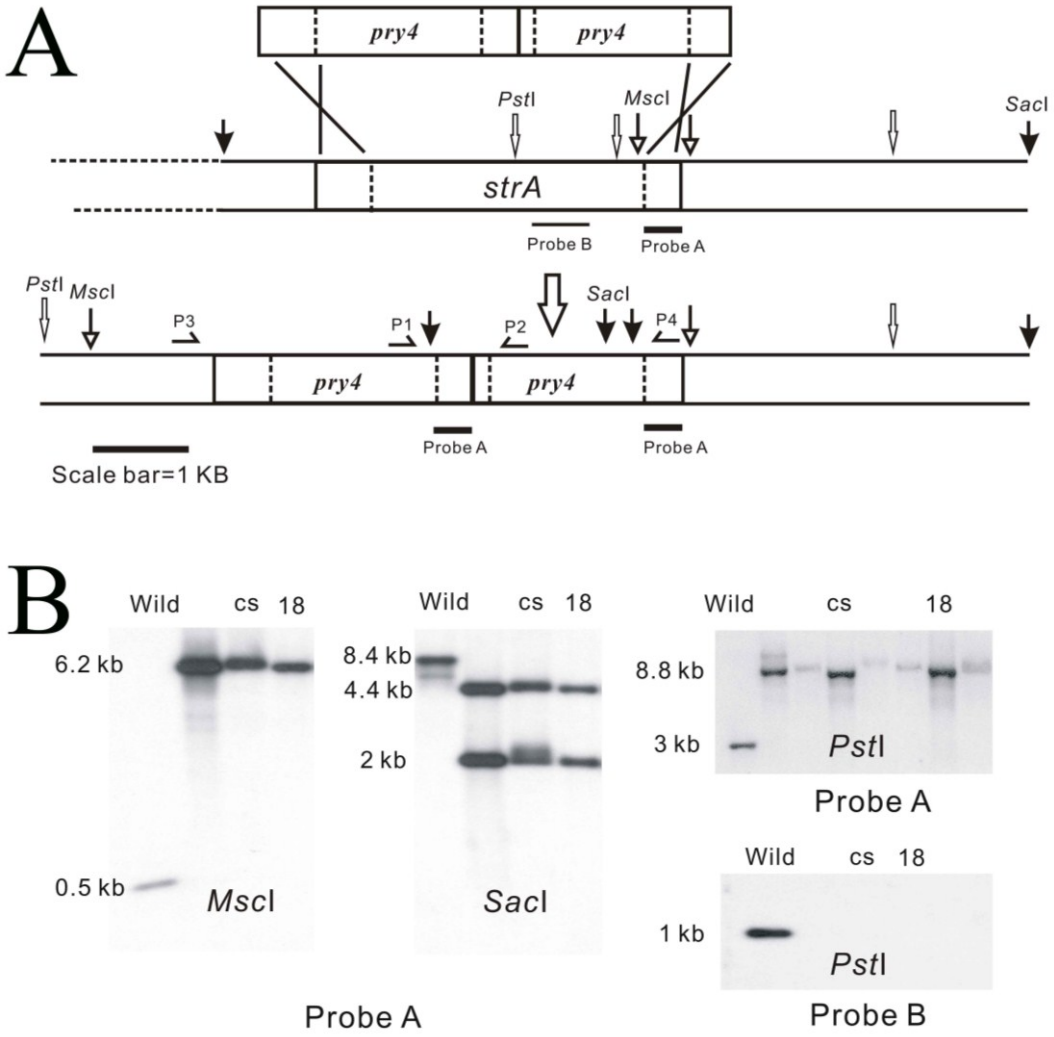

Figure 2.1 *strA* gene replacement.
(A) Schematic representation of gene replacement of *StrA* in *A. nidulans* by two tandem fused deletion cassettes with *pyr4* as the selectable marker. Restriction sites of *Msc*I, *Sac*I and *Pst*I are indicated by arrows. Probe A (heavy line) located at the 3'- flanking region of *strA* and probe B (light line) spanned the coding region of *strA* are indicated. PCR primer pairs of Pyr4endF (P1) / upR (P2) and Anfsr-comF (P3) / AnfsrGFPR (P4) were used to sequence and to verify the tandem deletion construct. (B) Southern analysis of several progeny from a cross of the Δ*strA* strain and wild-type strain ASL91. Genomic DNA of the wild-type strain and Δ*strA* strains were digested with *Msc*I, *Sac*I and *Pst*I, respectively. With probe A two Δ*strA* progeny (cs: StrAKOcs; 18: StrAKO18) used in this study clearly show *strA* was replaced by the deletion cassette. Probe B was used to re-confirm that *strA* was deleted in these two progeny.

The *veA1* allele is involved in regulating sexual development (Bayram et al., 2008; Kim et al., 2002). Since our deletion strain carries this allele, we generated a Δ*strA* strain carrying the wild-type *veA* locus by crossing StrAKO18 (Δ*strA*; *veA1*) with strain A126 (*veA*). Progeny CL206 (*strA*; *veA*) and StrAKO217 (Δ*strA*; *veA*) were selected by their colonial phenotypes in continuous light or dark conditions, and further verified by PCR. A 687 bp amplicon representing the *veA* allele was amplified at 54 °C annealing temperature with primers veAF and veAR.

Complementation of *strA* deletion strain

The *strA* gene including 733 bp of the promoter region and 552-bp of the down stream untranslated region was amplified with primers Anfsr-ComF (containing a *Kpn*I site) and Anfsr-ComR (containing an *Spe*I site) and cloned into pTA-argB at the position preceding *argB*, resulting in pTA-fsrA. The complementation construct containing *strA* and the selectable marker *argB* was released by *Kpn*I and *Not*I digestion, resulting in a linear fragment of 5.7 kb that was then transformed into AStrAKO18 (Δ*strA*; *argB2*). Transformation followed the previously described method except for the initial step of protoplast preparation where the conidia suspension of AnStrAKO18 was cultured in liquid CM where 1% glucose was substituted to 0.8% fructose to increase the conidium germination rate (Serlupi-Crescenzi et al., 1983).

Generation of StrA::eGFP strains

To study StrA subcellular localization, we generated a strain carrying StrA::eGFP sequence inserted at the *strA* locus that was driven by the *strA* endogenous promoter. The fusion PCR methodologies for tagging eGFP to a native target gene have been previously described (Yang et al., 2004). Briefly, an eGFP::pyrG-AF (Aspergillus fumigatus pyrG) construct with a five Gly-Ala repeat (GA-5) linker at the N-terminus was amplified from pFN03 with primers GFP-F and GFP-R. The 1974-bp fragment upstream of the stop codon of *strA* from strain A4 was initially amplified with primers fsrGFP1 and fsrGFP2 (with 30-bp homologous sequence overlapping the 5' end of the eGFP::pyrG-AF construct). The 1971-bp fragment downstream of the stop codon of *strA* was amplified with primers fsrGFP3 (with 30-bp homologous sequence overlapping the 3' end of the eGFP::pyrG-AF construct) and fsrGFP4. The three amplicons were purified and used as the template for fusion PCR with the nested primers AnfsrGFPF and AnfsrGFPR. The final amplicon, from the 5'-end to the 3'-end, contains 1227-bp upstream of the stop codon of *strA*, the GA-5::eGFP::pyrG-AF construct, and 1309-bp downstream stop codon of *strA*. The final amplicon was cloned into the pGEM-T Easy vector (Promega, Madison, WI) to produce pG-AnfsrGFP10 and then released by *Eco*RI digestion and transformed into *A. nidulans nkuA* strain TN02A25 (Nayak et al., 2006). Seven transformants were recovered including StrAGFP135 and StrAGFP140. A single homologous insertion at the *strA* locus was confirmed by Southern blot for these strains. We noted auto-fluorescence in medium containing riboflavin that hampered observation of the weak StrA::eGFP signal. StrAGFP135 and StrAGFP140 were crossed with

ASL91 to select riboflavin prototrophic progeny. Ten riboflavin prototrophic progeny displayed the same StrA::eGFP localization pattern. Two StrA::eGFP strains, StrAGFP135w2 and StrAGFP140G2, were used in this study.

To verify that StrA localizes to nuclear envelope, a StrA::eGFP strain (StrAGFP135w2) was crossed with AJW11 which expresses the nuclear localization of StuA(NLS)::DsRed (Toews et al., 2004) under control of the inducible *alcA* promoter. Strains with dual expression were selected when grown in *alcA* promoter inductive conditions (0.5% ethanol in MM without glucose).

Generate StrA::sGFP and CnxA::mRFP1 strains under the control of *alcA* promoter

To generate *alcA(p)::strA::sGFP* strains and *alcA(p)::cnxA::mRFP1* strains, the *alcA(p)::strA::sGFP* and *alcA(p)::cnxA::mRFP1* constructs were generated by using the Gateway cloning system (Invitrogen) as previously described (Toews et al., 2004). Calnexin, *cnxA*, is an endoplasmic reticulum marker in *A. oryzae* (Watanabe et al., 2007). The *strA* gene was amplified using primers GatfsrAF (with CACC overhang for Gateway cloning) and GatfsrAR (that omits the stop codon) and *cnxA* gene (AN3592.3) using primers GatCalAF (with CACC overhang) and GatCalAR. The cloned *strA* and *cnxA* genes were then transferred from the entry plasmid to the expression plasmid pMT-sGFP and pMT-mRFP1 (Toews et al., 2004), respectively. The resulting plasmid containing the *alcA(p)::strA::sGFP* construct and *argB* was transformed into strain ASL91. Ten arginine prototrophic transformants showed the same GFP expression

pattern under the *alcA* inductive conditions. One, A91GFP5a, was crossed with StrAKO18 (Δ*strA*;*argB2*) to generate StrAove3, hereafter referred to as OE*strA*. To show StrA::eGFP localizes to ER, the plasmid containing *alcA(p)::cnxA::mRFP1* and *argB* was transformed into an *argB2* auxotrophic strain, StrAGFP135w2 that carried *strA::eGFP*. Five transformants were obtained and all displayed the same localization pattern. Strain StrA135w2-cnxA9 (*strA::GFP;cnxA::mRFP1*) was imaged in this study.

Microscopy

To visualize GFP and FM4-64 stain in live cells, germlings were grown on coverslips submerged in liquid MM with appropriate supplements. After 10 h of incubation at 28 °C, the liquid medium was removed and the coverslips with germlings were overlaid on microscopy slides with fresh liquid medium containing 12.5 μM of FM4-64 and glass spacers made from broken coverslips to avoid mechanical perturbation of the cells. The FM4-64 staining was documented after 5 min, 10 min, 20 min, 30 min, 45 min, and 60 min. An Olympus BX51 microscope (Olympus America, Melville, NY, USA) was used for observation. A detailed description of features used for imaging fluorescence with this microscope and the image processing has been described (Shaw and Upadhyay, 2005). The system now includes a 100× (UPlanSApo NA 1.40) objective. To visualize the dual expression of StrA::eGFP and StuA(NLS)::DsRed or CnxA::mRFP1, germlings were grown on coverslips submerged in liquid MM without glucose, but with 1% ethanol and appropriate supplements.

RESULTS

Multiple functions of *strA* in *Aspergillus nidulans*

We identified one striatin ortholog, ANID_08071.1 in the *A. nidulans* genome database (http://www.broad.mit.edu/) by bi-directional blast analysis with *F. verticillioides fsr1* and named it *strA*. We had previously referred to this gene as *fsrA* due to its orthology to the Fusarium Stalk Rot 1 (*fsr1*) gene (Shim et al., 2006; Wang et al., 2009). The predicted 816-amino-acid StrA protein contains all four putative domains common to the striatin family: a caveolin-binding motif (aa 30 - 40), a coiled-coil motif (aa 40 - 97), a calmodulin-binding domain (aa 68 - 83), and a WD-repeat domain (aa 390 - 816). The StrA protein shares 48%, 47%, and 24% overall amino acid identity with *F. verticillioides* Fsr1, *S. macrospora* Pro11, and *Homo sapiens* striatin, respectively.

To explore the functional role of *strA*, we generated *strA* deletion (Δ*strA*) strains. This deletion was confirmed in two *veA1* strains StrAKOcs and StrAKO18 by Southern blot (Figure 2.1 B). To assess whether observed phenotypes associated with Δ*strA* were affected by *veA1* we also created wild type and Δ*strA* strains carrying the wild-type *veA* allele. A Δ*strA;veA* strain (StrAKO217) was obtained by crossing StrAKO18 (Δ*strA;veA1*) with A126 (*veA*). The Δ*strA;veA1* strain was crossed with *strA* wild-type strain A773 to confirm phenotypic segregation with the deleted locus. Analysis of the progeny from a cross revealed a 1:1 segregation ratio (184 wild type, 156 mutant, n = 340; not significant different from 1:1 after χ^2 analysis, $p < 0.05$) of the mutant and wild-type phenotypes, indicating a single locus is responsible for the observed phenotypes. Further confirmation was provided by restoration of wild-type phenotypes

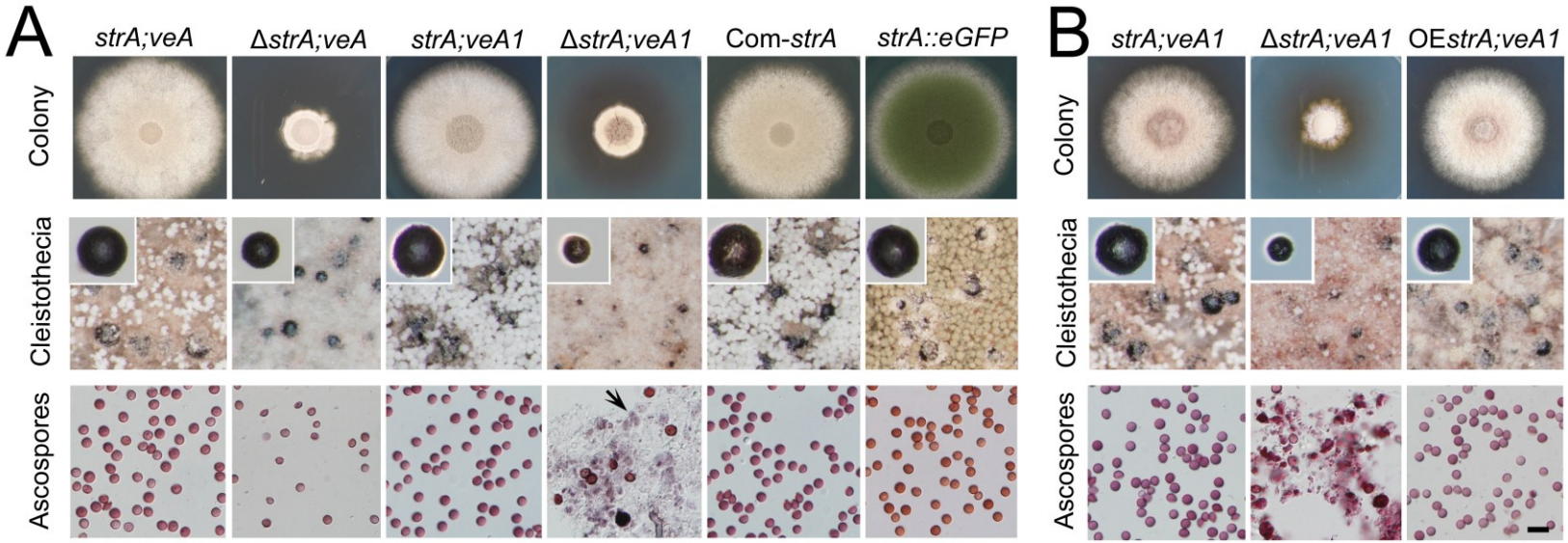

Figure 2.2 Phenotypes of Δ*strA* strains.
(A) The Δ*strA* mutants (Δ*strA;veA* and Δ*strA;veA1*) displayed reduced mycelial radial growth, small cleistothecia, and defective ascosporogenesis on complete medium in contrast with wild types (*strA;veA* and *strA;veA1*). Non-differentiated asci were found in the centrum Δ*strA;veA1* (arrow). All phenotypes of Δ*strA* strains were complemented by introduction of the native *strA* gene (strain Com-*strA*). The *strA::eGFP* strain displayed identical wild-type phenotypes, indicating that the *GFP* fused to *strA* locus did not alter the functionality of StrA. (B) All strains were grown in complete medium with *alcA* promoter-permissive condition. The OE*strA* strain (StrAove3, *alcA(p)::strA::sGFP*) complemented cleistothecia production and ascosporogenesis. Scale bar = 10 μm.

by complementation with the wild-type *strA* allele (see below).

Mycelia of Δ*strA* strains showed reduced radial growth on complete medium with the accumulation of a diffusible red pigment (Δ*strA;veA*: 20.7 ± SE 0.5 mm, $n = 4$; Δ*strA;veA1*: 20.5 ± SE 0.3 mm, $n = 4$) when compared to wild type (*strA;veA*: 60 ± SE 0.7 mm, $n = 4$; *strA;veA1*: 57.5 ± SE 0.3 mm, $n = 4$) (Figure 2.2 A). We did not observe significant defects in hyphal growth or morphology on CM. During germination, conidia of Δ*strA* strains continue isotropic growth with a delay in germ tube emergence of 2 h when compared with the wild type (Figure 2.3 A). The Δ*strA* strains did not show significant alterations in conidiophore morphology, but produced fewer conidia. Compared with wild type (*strA;veA*), the Δ*strA;veA* strain produced 35% of conidia in continuous light (data not shown) and less than 1% total conidia in the dark (Figure 2.3 B). Conidia production of Δ*strA;veA1* was 17% of that of *strA;veA1* in the dark (Figure 2.3 B).

Mammalian striatin family proteins have been implicated in participating in endocytosis because one of their interacting proteins, phocein, has been characterized to interact with other endocytosis associated components (Baillat et al., 2002; Baillat et al., 2001; Bailly and Castets, 2007). To examine if fungal striatin orthologs are involved in endocytosis, we incubated ΔstrA strain with FM4-64, a lipophilic styryl dye, which can be taken up by endocytosis to ultimately stain the endomembrane system (Fischer-Parton et al., 2000; Peñalva, 2005). We did not observe a difference in FM4-64 uptake in Δ*strA* compared to wild type, leading us to conclude that StrA does not participate directly in an endocytic process that can be monitored by FM4-64 uptake (Figure 2.4).

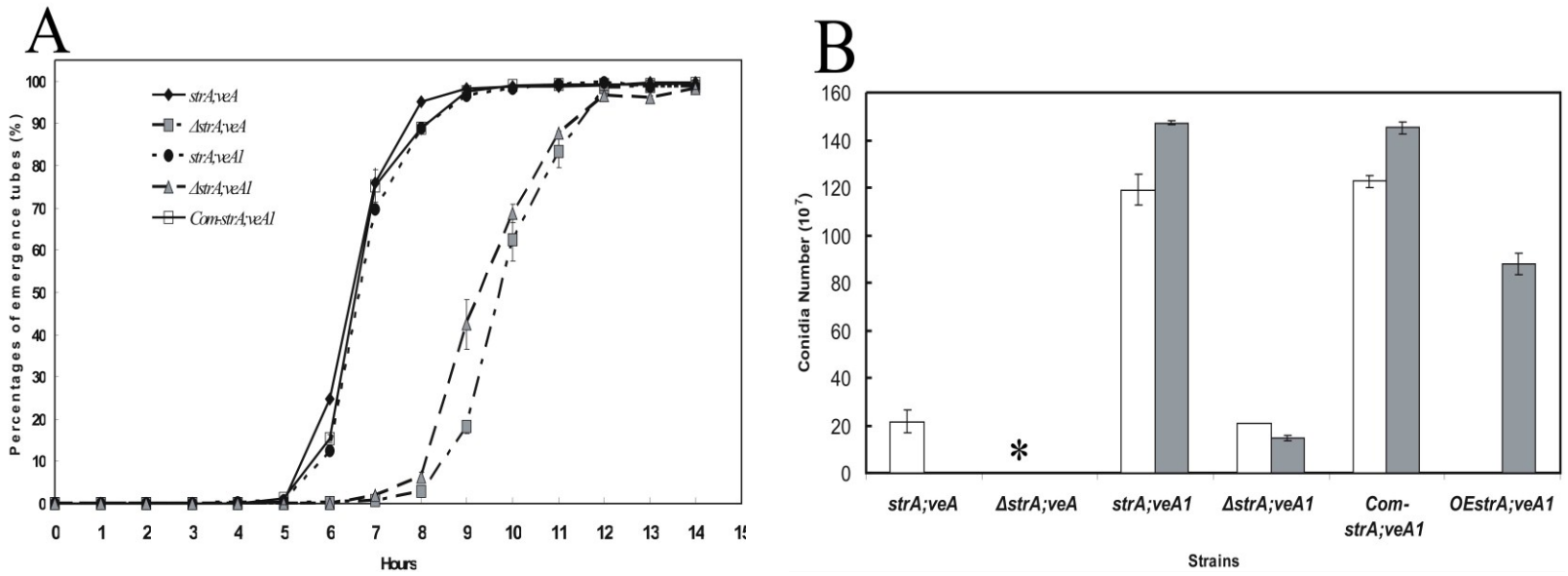

Figure 2.3 Effects of Δ*strA* on germination and conidium production.
(A) In the Δ*strA* strains (Δ*strA;veA* and Δ*strA;veA1*) germ tube emergence was delayed 2 hours in comparison with wild types (*strA;veA* and *strA;veA1*) and the complemented strain (Com-*strA;veA1*). (B) Conidium production was evaluated in the dark. Compared with the wild types (*strA;veA* and *strA;veA1*) and the complemented strain (Com-*strA;veA1*), the Δ*strA* strains (Δ*strA;veA* and Δ*strA;veA1*) produced fewer conidia in *alcA* promoter repressive conditions (white column). To examine the effects of OE*strA* (OE*strA;* Δ*strA; veA1*), *veA1* strains were compared in *alcA* permissive conditions (grey column). The Δ*strA;veA1* remained defective in conidium production while OE*strA* strain only partially restored the defect. * Conidium production of Δ*strA;veA* was less than $1x10^7$ in this evaluation.

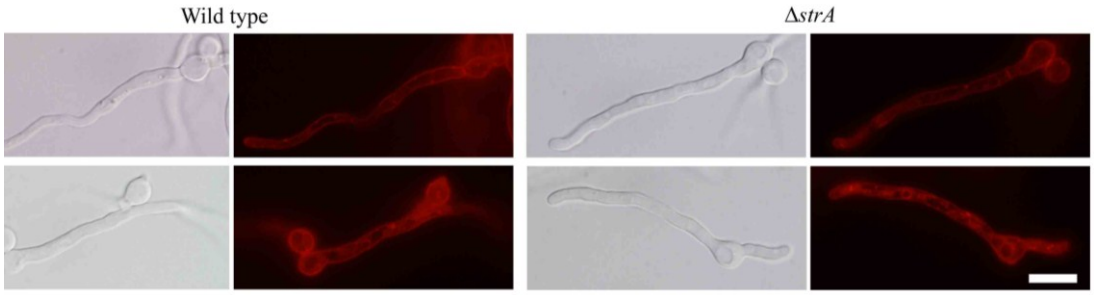

Figure 2.4 FM4-64 uptake via endocytosis.
Δ*strA* and wild type were incubated in FM4-64, 10 min and 20 min are shown. At 10 min (upper images), only cell membrane, septa and few punctate spots were visible in both strains while at 20 min (lower images), vacuoles and vesicles structures are stained. There is no significant difference in timing and staining patterns between the strains at any observed time point. Scale bar = 10 μm.

The Δ*strA* strains were defective in sexual development

Cleistothecium production was observed to examine the role of *strA* in sexual development in *A. nidulans*. The wild-type strains produced abundant darkly pigmented cleistothecia with a wealth of ascospores, while Δ*strA* strains produced fewer cleistothecia with delayed development (Table 2.3). Compared with wild-type cleistothecia (diameter 267 μm ± SE 7 μm, *n* = 20), ΔstrA strains produced smaller cleistothecia. The cleistothecia of Δ*strA;veA1* (diameter 98 μm ± SE 5 μm, *n* = 15) were smaller than those produced by Δ*strA;veA* (diameter 166 μm ± SE 4 μm, *n* = 15). The Δ*strA;veA* strain produced fewer ascospores, but 11% of those ascospores were abnormal in shape or were not fully separated from neighboring spores (Figure 2.5 D and E). The defects in ascosporogenesis were more pronounced in the Δ*strA;veA1* strain. Fifty-three percent of observed cleistothecia from Δ*strA;veA1* contained no ascospores. Many asci that were not fully developed are found in the Δ*strA;veA1* cleistothecia (Figures 2.2 A and 2.5 G). Some developed to produce normal ascospores, but some developed to produce ascospores that were not separated from other ascospores, ascospores that were not released from the ascus, and ascospores of different sizes (Figure 2.5 H and I). Occasionally we were able to observe larger ascospores, approximately 1.5 times the size of normal ascospores (Figure 2.5 J). Ascospores derived from the Δ*strA* strains were viable (Figure 2.5 K and L).

To complement the Δ*strA* mutation, a Δ*strA;veA1;argB2* strain was transformed with a fragment released from pTA-fsrA carrying wild-type *strA* and *argB* for nutritional selection. We examined a strain (Com-*strA;veA1*) that was wild type for all observed

Table 2.3 The effect of Δ*strA* and OE*strA* on cleistothecium, ascospore and Hülle cell production.

	strA;veA	Δ*strA;veA*	*strA;veA1*	Δ*strA;veA1*	OE*strA;veA1*
Glucose[1]	M +++/H[2]	I++/H	M ++/H	P +/H	ND
Ethanol	M++/ H	I++/H	M ++/H	P +/H	M++++/H

[1]. Complete medium used as the basal medium contains 1% glucose or substituted by 1% ethanol. Cultures were incubated at 28 °C in the dark for two weeks.
[2].Cleistothecia/Hülle cells. Average number of cleistothecia per cm^2 of 15 agar blocks from 3 plates: - = 0; + = 1-300; ++ = 301-600; +++ = 601-900; ++++ > 900. H: the presence of Hülle cells. ND: not determined. M: mature cleistothecia with ascospores. I: immature cleistothecia without ascospores. P: protocleistothecia.

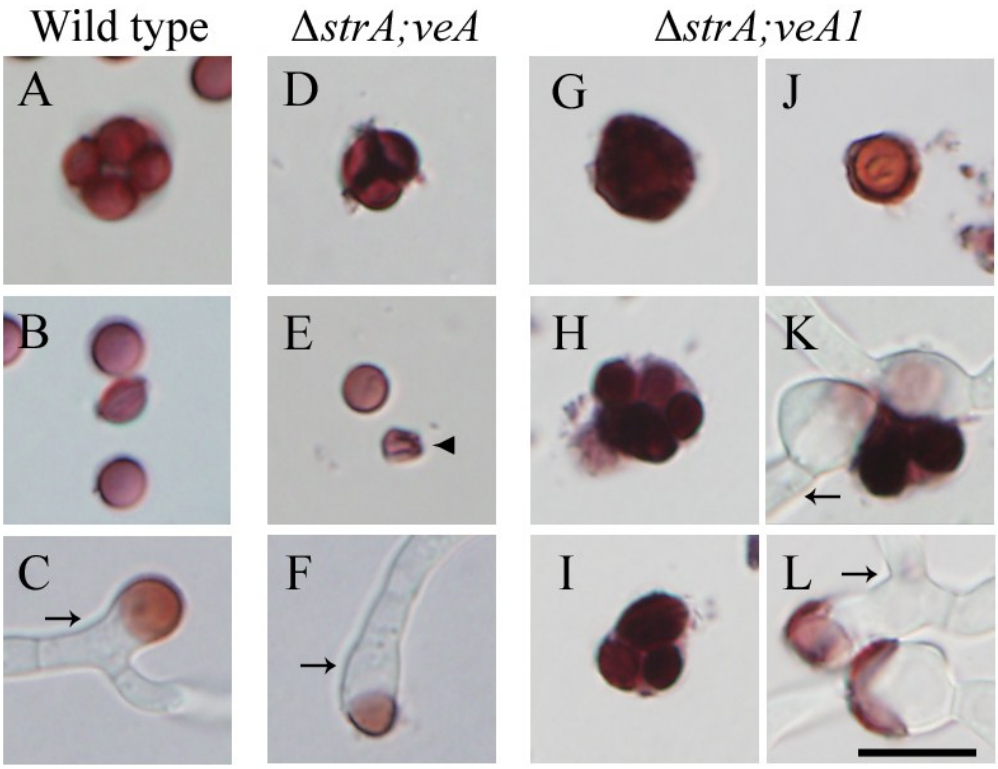

Figure 2.5 Disrupted ascosporogenesis in Δ*strA* stains.
(A-C) Ascus and ascospores of wild type. D-F. Δ*strA;veA*. (D) Connected ascospores. (E) An aberrant ascospore (arrowhead). G-L. Δ*strA;veA1*. (G) An abortive ascus. (H) Ascospores in an ascus that have not separated. (I) Ascospores of different sizes. (J) A larger ascospore. (K) Germination of connected ascospores. (L) Germination of ascospores of different sizes. Arrows indicate germination tubes. Scale bar = 10 μm.

mutant phenotypes indicting that deletion of *strA* was responsible to the altered phenotypes observed in Δ*strA* strains (Figures 2.2 and 2.3).

StrA::eGFP localized to endoplasmic reticulum and nuclear envelope

To visualize the subcellular localization of StrA in a living cell, we generated strA::eGFP strains that express the StrA::eGFP fusion product from the *strA* locus via the endogenous promoter. Homologous insertion of this product was verified by Southern blot (Figure 2.6). We noted no phenotypic difference between the recipient wild-type strain (TN02A25), and *strA::eGFP* expressing strains in conidium production (data not shown), in radial growth, nor in cleistothecia development (Figure 2.2 A) demonstrating the functionality of the fusion protein. StrA::eGFP localized to prominent circular structures with punctate points within the circular structure (Figure 2.7 B, green arrow heads) and irregularly dispersed tubular and punctate structures (Figure 2.7 B). StrA::eGFP was not found at the plasma membrane, septa, or cytosol. Since the *S. macrospora* striatin ortholog, Pro11, was characterized as a membrane-bound protein (Pöggeler and Kück, 2004), we hypothesized that StrA::eGFP localizes to components of the endomembrane system. Germlings expressing StrA::eGFP were incubated in FM4-64 to simultaneously image StrA and the endocytosis-related endomembrane systems. The major subcellular localization of StrA::eGFP (green arrow heads) and FM4-64 stained endomembrane structures (red arrow heads) were distinct and only a few minor regions (yellow arrow heads) overlapped, indicating a lack of co-localization (Figure 2.7 C and D). This suggested that the StrA::eGFP localized to the endomembrane structures

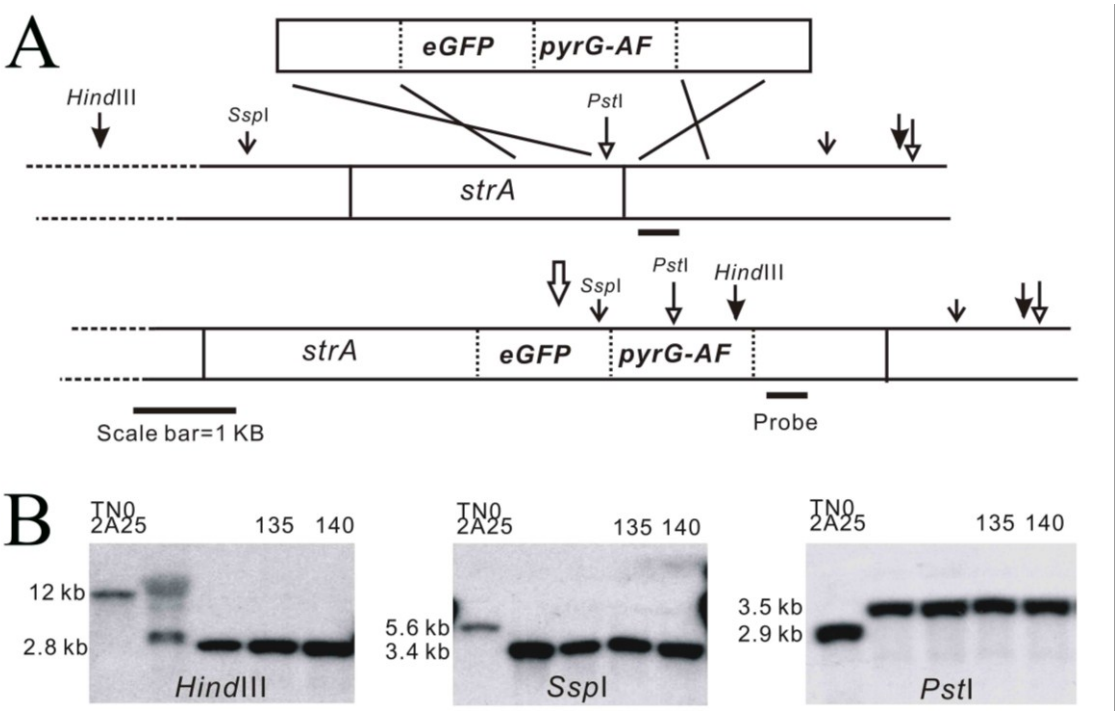

Figure 2.6 Generation of *strA::eGFP* strains.
(A) Schematic diagram *strA::eGFP* construct. A cassette containing *eGFP* with a GA-5 linker (not shown) at the N-terminus and *pyrG-AF* (*A. fumigatus pyrG*) at the C-terminus was integrated into the genome at the *strA* locus of *A. nidulans* strain TN02A25 by homologous recombination. Restriction sites of *Pst*I, *Ssp*I and *Hind*III are indicated by arrows. Probe used for Southern blotting was located at the 3'- flanking region of *strA*. The transformants were selected using the *pyrG-AF* marker. (B) Southern analysis of four transformants including StrAGFP135 (135) and StrAGFP140 (140) and wild type (TN02A25). Genomic DNA of wild type and selected transformants were digested with *Hind*III, *Ssp*I and *Pst*I, respectively. The hybridization probe spanned the 3'-flanking region of *strA* detected only a single band with expected size in each enzyme digestion, indicating homologous recombination at the *strA* locus.

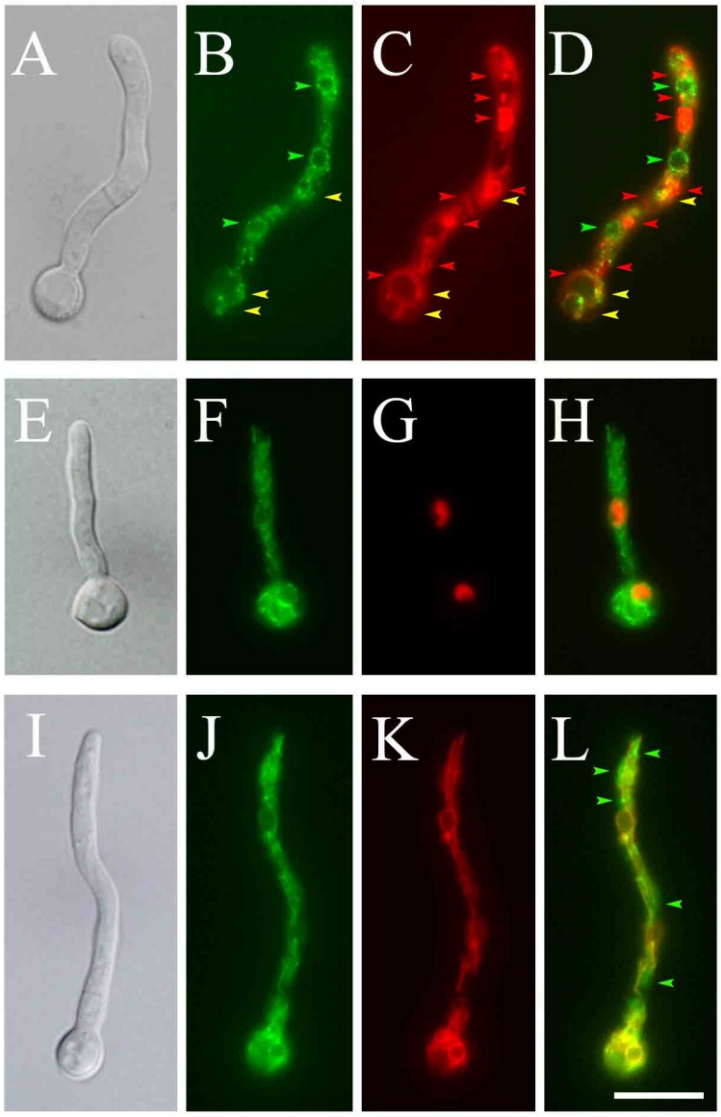

Figure 2.7 Subcellular localization of StrA::eGFP.
(A-D) StrA::eGFP localization and FM4-64 staining. (B) StrA::eGFP (green) localized to circular (green arrowheads) and irregularly dispersed endomembrane. Concentrated points of localization were observed in the circular endomembrane structure (C) FM4-64 (40 minutes) stained the vacuole, septum, and vesicles (red arrowheads). The merged image (D) revealed limited co-localization that is rendered yellow (yellow arrowheads in panels B-D). The prominent circular structures did not co-localize with the FM4-64 stained endomembrane. (E-H) The dual expression of StrA localization and nuclei. (F) StrA::eGFP (green) expressed via the strA promoter and (G) StuA(NLS)::DsRed (red) (NLS, Nuclear Localization Signal) expressed via the alcA promoter. The merged image (H) showed that the prominent circular endomembrane structure consistently surrounded the nuclei (red), indicating that StrA::eGFP localizes in part to the nuclear envelope. (I-L) StrA::eGFP colocalized with an ER marker, calnexin (CnxA::mRFP1).
(J) StrA::eGFP (green) expressed via the strA promoter. (K) CnxA::mRFP1 (red) expressed via the alcA promoter. (L) the merged image with significant colocalization rendered in yellow. Some StrA::eGFP did not colocalize with CnxA::mRFP1 (green arrowheads). Scale bar = 10 μm.

which are only weakly stained by FM4-64, such as endoplasmic reticulum and nuclear envelope (Peñalva, 2005).

To determine if StrA::eGFP co-localized with the nuclear envelope, we generated a strain that expresses StrA::eGFP and the StuA(NLS)::DsRed construct that labels nuclei (Toews et al., 2004). In this strain, StrA::eGFP consistently surrounded the nuclei (Figure 2.7 E-H), indicating that it is present in the nuclear envelope. StrA::eGFP also localized to a tubular system that was distinct from the nuclear envelope. The endoplasmic reticulum (ER) membrane system has been shown to connect with the outer membrane of the nuclear envelope (Bowman et al., 2009; Wedlich-Soldner et al., 2002). To verify localization of StrA::eGFP to the ER, we next generated a strain expressing StrA::eGFP and CnxA::mRFP1. Calnexin (CnxA) is a chaperon that functions in assisting protein folding and quality control on ER membrane that is widely used as an ER marker in animal cells (Halaban et al., 2000; Qi and Mochly-Rosen, 2008) and its localization to ER has been demonstrated in *Aspergillus oryzae* with ER-Tracker (Watanabe et al., 2007). StrA::eGFP and CnxA::mRFP1 fusion proteins co-localized at the nuclear envelope and throughout the ER tubular network (Figure 2.7 I-L). Additionally, we observed areas of StrA::eGFP that did not contain CnxA::mRFP1, suggesting the StrA::eGFP may also localize to another unknown cellular component or that CnxA::mRFP1 does not localize to all components of the ER equally. To test if StrA also localized to Golgi equivalents, the strA::eGFP strain was treated with Brefeldin A (BFA), a drug that blocks membrane flow from the ER to Golgi equivalents. We did not

see a significant change in the localization pattern (Figure 2.8), indicating that these additional structures are likely not Golgi equivalents.

Effects of *strA* over-expression

Previous work has demonstrated that the fungal striatin ortholog is constitutively expressed at very low levels (Pöggeler and Kück, 2004; Shim et al., 2006). This led us to question the effect of over-expression (OE) of *strA*. Because the deletion of *strA* resulted in aberrant sexual development and conidiation, we next hypothesized that *strA* over-expression would also alter these developmental processes. OE*strA* strains over-expressing StrA::sGFP under the control of the conditional *alcA* promoter in Δ*strA* background were generated. The *alcA* promoter is the regulatory element of the alcohol dehydrogenase gene and is highly induced by ethanol or L-threonine, but repressed in the presence of glucose (Felenbok, 1991). Glycerol neither induces nor represses the *alcA* promoter and is used to support growth (Flipphi et al., 2003). The StrA::sGFP fusion utilized a commonly used Gateway vector system (Toews et al., 2004) that allowed us to monitor localization and qualitative differences in expression level of the OE*strA* construct. In this experiment each strain carried the *veA1* allele. Under inductive conditions, the localization of StrA::sGFP was indistinguishable from that of StrA::eGFP expressed by endogenous *strA* promoter, indicating both GFP-tagged StrA fusion proteins localized to the same subcelluar localizations (Figure 2.9). Compared with StrA::eGFP expressed from the *strA* promoter, the qualitatively brighter GFP signal from OE*strA* strains also indicated a higher concentration of StrA in the OE cells

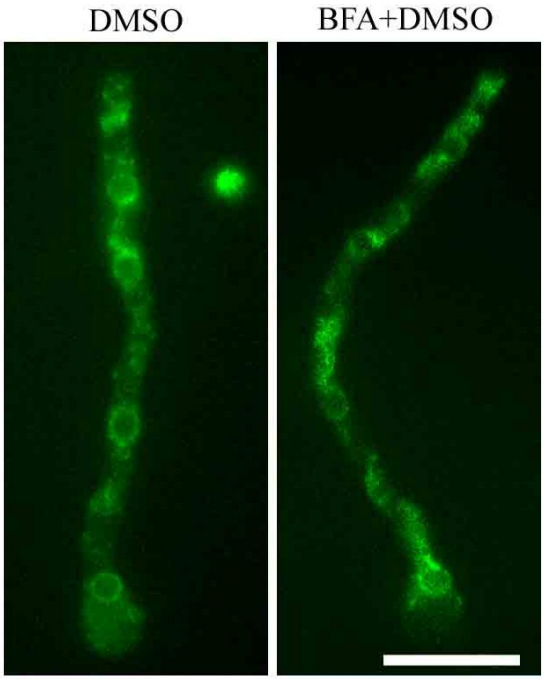

Figure 2.8 Effect of Brefeldin A treatment on StrA::eGFP subcellular localization.
The StrA::eGFP expressing strain (StrAGFP140G2) was exposed to DMSO or BFA+DMSO for 30 min and the StrA::eGFP localization was examined. There is no significantly difference in StrA::eGFP localization between the two treatments and in comparison with that of Figure 2.7 B, F, and J. Scale bar = 10 μm.

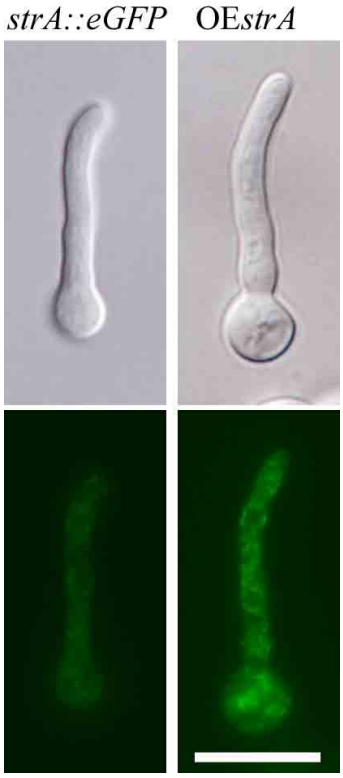

Figure 2.9 StrA subcellular localization of OE*strA*.
Compared with Figure 2.7, OE*strA* strain overexpressing StrA::sGFP displayed similar localization patterns to ER and nuclear envelop. OE*strA* showed brighter and enriched GFP signals in comparison to StrA::eGFP expressed by *strA* endogenous promoter. Note: all GFP micrographs were taken under the same photographic parameters. Scale bar = 10 μm.

(Figure 2.9).

OE*strA* strains displayed a mycelial colony similar in appearance to that of wild type (Figure 2.2 B). Conidia production by the OE*strA* strain was only 60% of that in the wild type (Figure 2.3 B). The OE*strA* strains developed Hülle cells, cleistothecia and ascospores morphologically comparable to wild type (Figure 2.2 B) but the number of cleistothecia produced was significantly greater in comparison with wild type (Table 2.3, in ethanol containing medium). Similarly, on 0.6 M KCl amended medium that conventionally represses sexual development, wild type produced three times fewer protocleistothecia (<300 per cm^2 agar block) than did the OE*strA* strain (>900 per cm^2 agar block). The Δ*strA* strain produced Hülle cells but lacked cleistothecia or protocleistothecia in this medium. In shaking liquid medium, Hülle cell formation and conidiation were inhibited in the wild-type strain, but some Hülle cells were produced by the Δ*strA* strain. Interestingly, the OE*strA* strain produced profuse Hülle cells from submerged mycelia (Figure 2.10 C). The increased formation of cleistothecia and Hülle cells indicates a positive role of StrA in sexual development. In addition, the OE*strA* strain produced sparse conidiophores that were morphologically normal with the accumulation of a brown pigment (Figure 2.10 D). Only very rare abnormal conidiophores (conidiophores without phialides, or phialides developed directly from a hypha) were observed in wild type and Δ*strA* when cultured in shaking liquid medium (data not shown). These results suggest that OE*strA* bypasses the repression of conidiation in liquid culture. It is of note that no strain produced Hülle cells or conidiophores from submerged mycelia in stationary cultures suggesting that available

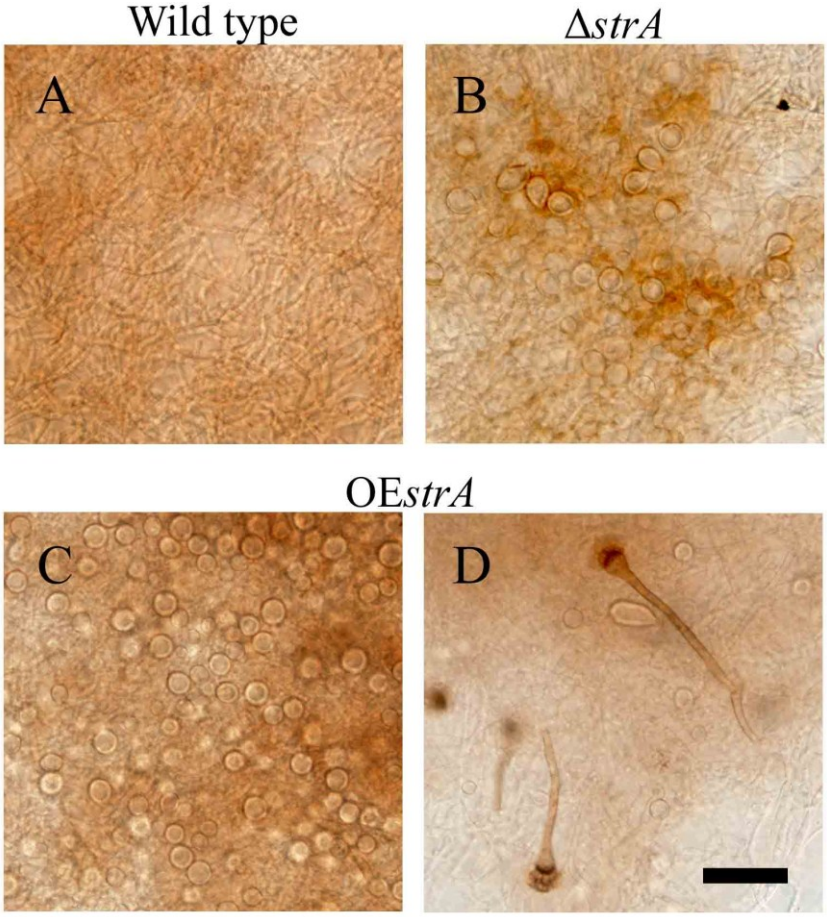

Figure 2.10 Hülle cell formation and conidiation in shaking liquid culture.
The OE*strA* strain produced Hülle cells (C) and conidiophores (D) in shaking liquid culture in *alcA* inductive minimal medium while both structures are suppressed in wild type (A). Some Hülle cells are produced in the Δ*strA* strain in shaking liquid culture but not conidiophores (B). Note: The two images of the OE*strA* strain were taken from different areas of the same sample. Scale bar = 100 μm.

dissolved air may be required or that starvation conditions induce differentiation in the OE*strA* strain.

DISCUSSION

In humans, striatin is required for the polarized development of dendritic spines (Bartoli et al., 1998). Polarized development is also a defining trait of the filamentous fungal lifestyle. The *strA* deletion strains showed delayed germination, but there was no significant defect in hyphal morphology. The reduced mycelial radial growth was also observed in *F. verticillioides* Δ*fsr1* while an increased density of aerial mycelia was produced by the *S. macrospora pro11* mutant (Pöggeler and Kück, 2004; Shim et al., 2006). These studies suggested that disruption of striatin orthologs affects fungal growth at the colony level, but not hyphal polarity.

The *A. nidulans* Δ*strA* strains produced smaller cleistothecia than wild type and these cleistothecia did produce ascospores. In contrast, the *F. verticillioides fsr1* mutant and *N. crassa* striatin (*ham3*) mutant fail to form perithecia as a female, but could fertilize protoperithecia as the male (Shim et al., 2006; Simonin et al., 2010). The *S. macrospora pro11* mutant was arrested in sexual development during the transition from protoperithecia to perithecia and formed fewer protoperithecia and lacked ascospores (Pöggeler and Kück, 2004). Therefore, striatin orthologs were important not only in the formation of perithecia (ostiolate ascocarps), but also in cleistothecia (closed ascocarps). Wild-type *A. nidulans* produces a wealth of normal ascospores in either *veA* or *veA1* backgrounds. In contrast, the Δ*strA;veA* strain produced significantly fewer ascospores

and 11% of those ascospores were abnormal. Interestingly, defects in ascosporogenesis were more pronounced in the Δ*strA;veA1* background. The Δ*strA;veA1* strain produced undifferentiated asci, ascospores that were misshapen and larger than normal, and ascospores that appeared to be fused with neighboring ascospores. Similarly, the *N. crassa* striatin (Δ*ham3*) mutant also showed a meiotic malfunction and abnormal ascospores in a homozygous cross (Simonin et al., 2010). Since both Δ*strA;veA* and Δ*strA;veA1* strains were defective in ascospore formation, it is clear that StrA plays an important role in ascosporogenesis and that there is a synthetic hypermorphism introduced in the Δ*strA;veA1* background indicating a genetic interaction between *strA* and *veA* in this process. Since the role of VeA in regulating sexual development is linked to its localization to either the cytoplasm or the nucleus (Bayram et al., 2008; Stinnett et al., 2007), it is tempting to hypothesize that the punctate points of localization in the nuclear envelope may play a role for entry of VeA into the nucleus. Further work will be necessary to clarify this connection.

Cleistothecium formation and ascosporogenesis were complemented in the Δ*strA* background by expression of *strA* from its endogenous promoter and by over-expression of *strA* using the OE*strA* construct. Moreover, OE*strA* promoted cleistothecium development in media with 0.6 M KCl (repressive for cleistothecium development in wild type) and developed abundant Hülle cells in shaking liquid culture. Therefore, our results suggest that StrA positively regulates cleistothecium development. Previous studies demonstrated that over-expressing the positive sexual regulators *nsdD* and *veA* promoted cleistothecium development on solid media and induced Hülle cells in shaking

liquid culture (Han et al., 2001; Kim et al., 2002). Unlike the wild-type strain, the Δ*strA* strain also produces Hülle cells in shaking liquid culture. Therefore the influence of StrA on Hülle cell formation is complex. A similar effect was noted for the protein kinase ImeB (Bayram et al., 2009) where overproduction of cleistothecia was noted from Δ*imeB* and over-expression of *imeB*. Further work is needed to clarify the role of StrA in Hülle cell formation.

Here we also demonstrated that Δ*strA* produced fewer conidia than wild type. Similarly, the *N. crassa* striatin deletion strain (Δ*ham3*) was also defective in conidia production (Simonin et al., 2010). Unlike the wild type and Δ*strA* strains, the OE*strA* strain developed fully formed conidiophores in shaking liquid cultures. This demonstrates an important role for StrA in either inducing conidiation or in removing a block on conidiation. One may argue that StrA served as an inhibitor of conidiation due to the fact that the OE*strA* strain produced fewer conidia than wild type. Previous studies suggest that the physiological conditions that favor cleistothecium development may discourage conidiation and *vice versa* (Tsitsigiannis et al., 2004). Two putative dioxygenase genes, *ppoA* and *ppoC*, regulate the ratio of conidia and ascospores production through two feedback loops associated with the expression of *nsdD* and *brlA*, which are required for cleistothecium development and conidiation, respectively. The Δ*ppoC* and Δ*ppoA*;Δ*ppoC* strains displayed an increase in Hülle cells and cleistothecia production, but decreased conidia production, while the wild type and Δ*ppoA* mutant produced more conidia but fewer Hülle cells and cleistothecia (Tsitsigiannis et al., 2004). Although we do not know whether the OE*strA* strain expressed altered levels of *nsdD*

and *brlA*, the changes in cleistothecia production and conidiation of OE*strA* are indirectly supported by this view.

The presence of a caveolin binding domain in striatin family proteins strongly suggests a function at membranes (Williams and Lisanti, 2004). Mammalian striatin family proteins were detected in cytosolic and the membrane fractions (Castets et al., 2000). *S. macrospora* Pro11 was also detected in a membrane fraction (Pöggeler and Kück, 2004). A caveolin ortholog is not found, however, in the *A. nidulans* genome, nor was one identified in *N. crassa*, or *F. verticillioides* (Pöggeler and Kück, 2004; Shim et al., 2006). Therefore, the role of the caveolin binding domain in these fungi remains unknown. Its conservation indicates an important role, perhaps in binding to some other membrane proteins. We did, however, identify the specific membrane to which StrA::eGFP localizes. In this study, we demonstrated that the subcellular localization of StrA::eGFP is mainly to the ER and nuclear envelope. Phocein, a protein known to interact with striatin in rat, localizes to ER and the Golgi apparatus in neurons and to the Golgi apparatus in HeLa cells (Baillat et al., 2001). Since *A. nidulans* StrA did not change the localization pattern after Brefeldin A (BFA) treatment, we concluded that it does not localize to Golgi equivalents. We also showed there is a small population of StrA::eGFP localization in endomembrane that did not co-localize with the CnxA::mRFP1 ER marker. This indicated that either StrA::eGFP localizes to endomembrane distinct from the ER, or that CnxA::mRFP1 does not uniformly localize to all ER organelles.

The four conserved domains of StrA (caveolin-binding motif, a coiled-coil motif, a calmodulin-binding domain, and a WD-repeat domain) are found in striatin family proteins from fungi to humans. Functional conservation was also demonstrated by complementation of the *S. macrospora pro11* mutant with mouse striatin cDNA (Pöggeler and Kück, 2004). The structural and functional conservation implicate the molecular mechanisms of striatin proteins may be evolutionarily conserved from fungi to animals. Interactions of striatin family proteins with three protein complexes (Ca^{2+}/calmodulin, Phocein, and Jun) have been demonstrated.in animal and human cells (see below). First, animal striatin homologs bind to calmodulin in a Ca^{2+}-dependant manner and are thought to be involved in the neuron-specific Ca^{2+} signaling events (Bartoli et al., 1998). It is of particular note that ER is a Ca^{2+} storage site in fungal cells (Bowman et al., 2009). The ER localization of StrA in *A. nidulans* indirectly supports the idea that StrA may be involved in Ca^{2+}/calmodulin signaling pathways via its calmodulin-binding domain. A role for Ca^{2+} in striatin function was demonstrated in human where protein phosphatase 2A (PP2A) A/C heterodimers and Mob1 formed a protein complex with human striatin homologs in a Ca^{2+} signaling pathway (Moreno et al., 2001; Moreno et al., 2000). *A. nidulans* homolog of human PP2A catalytic subunit (PP2Ac), An*ppg1*, has been characterized (Son and Osmani, 2009) to display a reduced growth rate and a reduced germination rate, both similar to phenotypes of Δ*strA*. Additionally, human Mob1 was thought to be a substrate of PP2Ac (Moreno et al., 2001). Deletion of *mob1* in *N. crassa* also resulted in a reduction in growth rate and in conidiation (Maerz et al., 2009). Furthermore, a cross of wild type with

ΔNc*mob1*+Nc*mob1*$^{+}$ conidia resulted in a frequent formation of larger than usual, viable ascospores (Maerz et al., 2009). This phenotype recalled the un-separated ascospores and variant sizes of ascospores in the defective ascosporogenesis in Δ*strA*.

Phocein, another striatin interacting protein, has been demonstrated to associate with Esp15 and NDPK by a yeast two-hybrid screen and to partially co-localize with Dynamin I in rats (Baillat et al., 2002; Baillat et al., 2001). Eps15 and NDPK serve as functional neighbors of Dynamin I, a GTPase that plays a critical role in endocytosis. Therefore, a role for striatin in endocytosis was suggested in animal cells. Since the phocein ortholog is found in *A. nidulans* (ANID06190.1), it is possible that striatin also plays a role in endocytosis in fungi. Here we show that FM4-64 uptake is not affected in the Δ*strA* strain, and StrA::eGFP localizes to the nuclear envelope and endoplasmic reticulum but not to the plasma membrane. Although our results do not support a role of StrA in endocytosis, it is worth noting that the detailed mechanisms of FM4-64 uptake and endocytosis in filamentous fungi are still not fully understood (Fischer-Parton et al., 2000). Thus, a Striatin/Phocein complex may be involved in an alternative endocytic pathway or alternately in intracellular vesicle trafficking. Interestingly, the deletion strains of *N. crassa* phocein homolog (ΔNc*mob3*) produced few, smaller and less developed protoperithecia. Wild-type protoperithecia that were fertilized with ΔNc*mob3* conidia generated few viable ascospores (Maerz et al., 2009). Those phenotypes resemble the general cleistothecium development defects of Δ*strA*, suggesting that it will be necessary in the future to determine if phocein interacts with StrA in *A. nidulans* and plays a role in cleistothecium development.

The *Drosophila melanogaster* striatin homolog (*cka*) formed a complex with DJun (the homolog of mammalian *c-Jun*) an AP-1 transcription factor, and other kinases to function in the JUN N-terminal kinase (DJNK) and decapentaplegic signal transduction pathways (Chen et al., 2002; Hou et al., 1997; Riesgo-Escovar and Hafen, 1997). The *A. nidulans* homolog of c-Jun and DJun (CpcA) negatively regulated cleistothecium development and is induced by the 'cross-pathway control' network upon amino acid starvation (Hoffmann et al., 2000). The induction of CpcA results in a block in sexual development at the microcleistothecia stage. Although CpcA and StrA play opposing roles in cleistothecium development, their connection in *D. melanogaster* warrants further examination in fungi.

In summary, we have demonstrated that the *A. nidulans* striatin ortholog, StrA, localizes to the ER and nuclear envelope. Deletion of *strA* results in decreased ability to produce cleistothecia and in defects in ascosporogenesis and vegetative growth. Over-expression of *strA* increases production of cleistothecia and Hülle cells. Striatin proteins contain multiple interacting domains suggesting they play a role in interacting with numerous partners. We propose that StrA is a scaffolding protein localizing to ER where Ca^{2+} serves as a signal to trigger Ca^{2+}/calmodulin signaling pathways. StrA may also interact with AnPpg1 and Mob1 to regulate vegetative growth and conidiation. By coupling with the phocein signaling pathway, and perhaps CpcA regulated pathways, StrA is involved in mediating cleistothecium development and ascosporogenesis. Further work is needed to clarify which of these interactions occur in *A. nidulans*.

CHAPTER III

THE *Colletotrichum graminicola* STRIATIN ORTHOLOG (STR1) IS INVOLVED IN HYPHAL FUSION, CONIDIATION, SEXUAL DEVELOPMENT AND VIRULENCE

SUMMARY

Colletotrichum graminicola is one of major pathogens that can cripple maize production in the US. Little is known about the molecular biology of the fungus and its interaction with maize. Fungal striatin orthologs have been reported to play multiple roles in fungal development, and the striatin ortholog (Fsr1) in *Fusarium verticillioides* is essential for the virulence to maize stalk. Here, we investigated the function of *C. graminicola* striatin ortholog (*str1*) by generating a gene knock-out mutant. The mutant strain (Δ*str1*) was reduced in radial growth, displayed altered hyphal spiral growth, and was compromised in hyphal fusion. The mutant also produced fewer conidia and was defective in sexual development. The Δ*str1* produced functional appressoria, but produced hyphopodia that were less lobed than the wild-type strain. The Δ*str1* mutant was still pathogenic to maize but was less virulent than wild type, which was demonstrated by production of smaller lesions on leaves and stalks. By complementing Δ*str1* with *fsr1*, we concluded that striatin orthologs in *Fusarium* and *Colletrotricum* are structurally and functionally conserved.

INTRODUCTION

Colletotrichum graminicola, the anamorph of *Glomerella graminicola*, is a hemi-biotrophic fungus, which causes anthracnose leaf blast (ALB) and anthracnose stalk rot (ASR) of maize (*Zea mays*). *C. graminicola*-associated ASR and ALB is common in US corn fields since 1970s. The ASR results in a significant reduction in maize yields even on Bt-resistant maize hybrids (Bergstrom and Nicholson, 1999; Gatch et al., 2002; Gatch and Munkvold, 2002). The falcate conidia of *C. graminicola* on corn debris are the major primary inoculum source in fields, and are disseminated by splashing rain to maize seedlings (Bergstrom and Nicholson, 1999). After making contact with the host cell wall, conidia germinate and subsequently form appressorium at the tip of germ tubes to penetrate through the cell wall of the host (Mims and Vaillancourt, 2002; Politis and Wheeler, 1973). The invasive hyphae establish a short biotrophic phase and then shift to a necrotrophic phase while expanding the hyphal network. The hyphae preferentially colonize the fiber cells of vascular bundles and the stalk rind of maize (Venard and Vaillancourt, 2007a). The fungus also produces oval conidia inside the host tissue during colonization (Panaccione et al., 1989). *C. graminicola* also produces lobed hyphopodia from hyphae that may play an important role in root infection and serve as a survival structure on corn debris (Sukno et al., 2008). The role of oval conidia is obscure. It was proposed that oval conidia are important for establishing a discontinuous infection site in the stalk (Venard et al., 2008). Sexual development proceeds to generate perithecia from a single strain or two sexually compatible strains in certain culture conditions though it has rarely been found in nature (Politis, 1975; Vaillancourt and Hanau, 1991). The

molecular mechanisms behind these biological events remain obscure in *C. graminicola*.

Striatin family proteins are comprised of a caveolin-binding domain, a calmodulin-binding domain and a coiled-coil motif at the N-terminus, and a WD-repeat domain at the C-terminus. Mammals encode three striatin family proteins: STRN (striatin), STRN3 (SG2NA) and STRN4 (zinedin) are found in human. They mainly localize to neurons of central and peripheral nervous system, especially at the somato-dendritic spines (Benoist et al., 2006). A large protein complex identified in human cells is referred to as STRIPAK (Striatin-interacting phosphatase and kinase) which suggests that the mammalian striatin homologs are functionally related to PP2A (protein phosphatase 2A) A and C subunits, Mob3, the newly identified STRIP 1(striatin-interacting protein 1) and STRIP2, CCM3 (cerebral cavernous malformation) protein, and members of the GCK-III (germinal center kinase) family of Ste20 kinases (Goudreault et al., 2009). Thus, mammalian striatin homologs may act as a scaffolding protein that coordinate multiple signal transduction pathways including Ca^{2+}-signaling pathway, the PP2A signaling pathway, endocytosis, and estrogen regulated pathways (Bailly and Castets, 2007; Bartoli et al., 1998; Lu et al., 2004; Moreno et al., 2000; Tan et al., 2008).

Little is known about how fungal striatin orthologs involve in the signal transduction pathways. A striatin-like protein (Far8) in *Saccharomyces cerevisiae* forms a protein complex with five other Far proteins and is involved in maintaining cell cycle arrest responding to pheromone signaling (Kemp and Sprague, 2003). In *N. crassa*, similar defects of hyphal fusion and sexual development were observed in mutants of the

Ham2, Ham3 (striatin homolog), and Ham4. Since these proteins are homologs of the Far8 protein complex in *S. cerevisiae*, they may also form a putative protein complex in *N. crassa*. Moreover, a putative Pro11 (striatin homolog)/Mob3 complex was proposed in *Sordaria macrospora* (Bernhards and Pöggeler, 2011; Simonin et al., 2010). The increasing number of evidences indicates that striatin orthologs of filamentous fungi may contribute to hyphal growth, hyphal fusion, conidiation, and sexual development (Pöggeler and Kück, 2004; Simonin et al., 2010; see Chapter II). However, the conserved functions of fungal striatin orthologs are still under investigation. More importantly, the striatin ortholog (Fsr1) of *Fusarium verticillioides* has been reported to be essential for maize stalk rot (Shim et al., 2006). Here, I utilized the recently established genome sequence of *C. graminicola* to study the role of the striatin ortholog in virulence for foliar infection and formation of penetration structures. I also used *C. graminicola* to examine what phenotypes may be shared among fungal striatin mutants.

MATERIALS AND METHODS

Strains, inoculum preparation, and growth conditions

Strains of *C. graminicola* in this study (listed in Table 3.1) are derived from two sexually compatible wild-type strains, M1.001 and M4.001. Except where indicated, strains were grown at room temperature under continuous light to induce the production of falcate conidia. For preparation of inoculum, falcate conidia were harvested from 2-3-week-old PDA (potato dextrose agar, Difco) plates just before use. Conidia were washed with 40 ml of sterile water twice, and then concentrated to indicated concentrations. To

Table 3.1 Strains and plasmids used in this study.

Strains	Genotype	Origin
M1.001	Wild type	(Vaillancourt and Hanau, 1991)
M4.001	Wild type	(Vaillancourt and Hanau, 1991)
ΔCg*str1*-124	Δ*str1*::*hph*	M1.001; this study
Cg*str1*com1	Δ*str1*::*hph*; *str1*; *ble*	ΔCg*str1*-124; this study
Cg*fsr1*comA5	Δ*str1*::*hph*; *fsr1*:: *ble*	ΔCg*str1*-124; this study
Nit-1	*nit1*	M1.001; this study
Nit-2	*nit1*	M1.001; this study
Nit-9	*nitM*	M1.001; this study
Nit-13	*nit1*	M4.001; this study
Nit-16	*nitM*	M4.001; this study
Nit-23	Δ*str1*::*hph; nitM*	ΔCg*str1*-124; this study
Nit-25	Δ*str1*::*hph; nit1*	ΔCg*str1*-124; this study
Nit-30	Δ*str1*::*hph*; *str1*; *Sh ble; nitM*	Cg*str1*com1; this study
Nit-34	Δ*str1*::*hph*; *fsr1*::*Sh ble; nitM*	Cg*fsr1*comA5; this study
Nit-23com1	Δ*str1*::*hph*; *nitM; str1*; *Sh ble*	Nit-23; this study
Plasmids	Genes contained	Background
pBP15	*Hph*	(Li et al., 2005)
pGEM-T Easy	TA cloning vector	Promega
pCgStr1-SM1	5'UTR of *str1*::N-*hph*	pGEM-T Easy; this study
pCgStr1-SM2	C-*hph*::3'UTR of *str1*	pGEM-T Easy; this study
pAN8-1	*gpdA*(p):: *ble*::*trpC*(t)	(Punt and van den Hondel, 1992)
pCgStr1	*str1*	pGEM-T Easy; this study
pFvfsr1	*fsr1*	pGEM-T Easy; this study
pANFvfsr1	*fsr1*::*ble*	pAN8-1; this study

determine the radial growth rate, agar blocks of 6 mm diameter were placed at the center of PDA and V8 medium plates (1L contains V8 juice 200 ml, $CaCO_3$ 3 g, and agar 20 g), and incubated at 30 °C with continuous light for 6 days. The diamter of colonies was recorded daily. To quantify falcate conidia production, 4 agar blocks of 6 mm diameter close to the colony center from each 2-week-old PDA plate were sampled. Conidia were suspended into 1 ml sterile water with 0.05% Tween 20, and counted with a hemocytometer. The size of conidia was measured with an eyepiece reticle. To stimulate perithecia production, a conventional crossing method was adapted (Politis, 1975; Vaillancourt and Hanau, 1991). Briefly, two sexually compatible strains were inoculated at two ends of an autoclaved maize leaf strip placed on a layer of autoclaved coral gravel. The moisture level of the plates was maitained by adding sterile water to the gravel every few days. The plates were incubated at at room temperature with continuous fluorescent light and observed for 1-3 months to determine the perithecium development. Appressoria were induced by suspending conidia in sterile water and incubating on a cover slide (VWR, West Chester, PA, USA) overnight. To induce hyphopodia, each strain was inoculated on top of a 15 mm^2 PDA agar block that was placed on a glass cover slip. Hyphae that grew through the agar and made contact with the cover slip differentiated hyphopodia.

Generation of *str1* deletion strains

The *str1* deletion (Δ*str1*) strains were generated using the split-marker gene deletion method (Catlett et al., 2002) with hygromycin phosphotransferase gene (*hph*) as

the selectable marker. The *hph* was amplified from pBP15 (all plasmids listed in Table 1). All primers used in this study are listed in Table 3.2. Two deletion cassettes were generated. Using the fusion PCR (Yu, 2004), 1,021-bp 5'UTR (untranscribed region) of *str1* was amplified with primers Cgfsr1 and Cgfsr2, and fused with 1,251-bp fragment generated from the N-terminus of *hph* that was amplified using primers M13R-F and HY-R. The 475-bp 3'UTR of *str1* was amplified with primers Cgfsr3 and Cgfsr4, and fused with 856-bp C-terminus of the *hph* that was amplified with primers YG-F and M13F-R. There was 466-bp overlapping between the N- and C-termini of *hph*. The two deletion cassettes were isolated with gel electrophoresis, purified with the QIAquick Gel Extraction Kit (Qiagen, Valencia, CA, USA) and cloned into the pGEM-T Easy vector (Promega, Madison, WI, USA). The resultant vectors, pCgStr1-SM1 and pCgStr1-SM2, were used for the amplification of the two deletion cassettes, respectively. The two deletion cassettes were transformed into *C. graminicola* M1.001 using a previously described protocol (Panaccione et al., 1988; Rasmussen et al., 1992). Transformants were verified with primers Cgfsr5R and M13R-F to confirm homologous recombination at the *str1* locus. Colonies generated from single conidium were selected from a hygromycin containing medium, and further verified by Southern blot for recombination at the *str1* locus.

DNA isolation and Southern blot analysis

Standard procedures and reagents were used for DNA isolation and Southern analysis (Sambrook and Russell, 2001). For the verification of Δ*str1* strains, genomic

Table 3.2 Oligonucleotides used in this study.

Oligo	Sequence (5' – 3')
Cgfsr1	TCACTAATCAAGGGGAGAGGAG
Cgfsr2	GAGGAAAAGGAGATGTCGGTAAAATCATGGTCATAGCTGTTTCC
M13R-F	GGAAACAGCTATGACCATGATT
HY-R	GGATGCCTCCGCTCGAAGTA
Cgfsr3	TCACTGGCCGTCGTTTTACAATTGGGCATAGCAGAGGTAGAAA
Cgfsr4	GCAATGTCGTCGTTTATTCTG
YG-F	CGTTGCAAGACCTGCCTGAA
M13F-R	TTGTAAAACGACGGCCAGTGA
Cgfsr5R	GACAAGCTCAACGACCTCAA
hphFS	AACTCACCGCGACGTCTGT
hphRS	CGGCGAGTACTTCTACACA
CgfsrCpF	CAGGAGATGAAGGCGAGGA
CgfsrCpR	AGAGAGGAGGAGGCGAAGG
FSR1-D4t[a]	AATCATGGTCATAGCTGTTTCCTGATTCACTTCGCTGCAAGGTTCCAC
FSR1-U4[a]	AGGATAACAGCAGTAGATGGCAGC
Fvfsr1F2	GGTCACGCAGGAGCAATTCTGT
Fsr1UR	CCTGTCTGAAGCAGATGCAA

Note: The underline indicates the overhang for fusion PCR.

[a] The sequences and names of the primers were adopted from a previous work (Shim et al., 2006).

DNA of transformants was digested with *Pst*I and *Sac*I restriction enzymes. The digested DNA fragments were separated on a 1% agarose gel and then transferred onto a Hybond-N+ nylon membrane (Amersham Biosciences). A 966-bp PCR product amplified from the sequence of *hph* with primers hphFS and hphRS was used as a template for probe A to detect the number of integrations of each of the gene deletion cassettes. A 530-bp PCR product amplified from the sequence of *str1* with primers CgfsrCpF and CgfsrCpR was used as a template for probe B to confirm the deletion of *str1*. Probes were amplified with the random primer labeling kit, Prime-It II (Stratagene, La Jolla, CA) and labeled with (γ-^{32}p) CTP.

Complementation of *str1* deletion strains

The Δ*str1* strain was transformed with *C. graminicola str1* and *F. verticillioides fsr1* to examine the ability of each to complement the mutation. The *C. graminicola str1* gene containing 1,121-bp 5' upstream sequence and 670-bp 3' downstream sequence was amplified with primers Cgfsr1 and Cgfsr4, and cloned into the pGEM-T Easy vector, resulting in pCgStr1. The pCgstr1 and the pAN8-1 that contained the *Sh ble* gene conferring resistant to phleomycin were co-transformed into Δ*str1* strain. The *F. verticillioides fsr1* gene including 730-bp 5'UTR and 800-bp 3'UTR was amplified with primers FSR1-D4t and FSR1-U4, and cloned into pGEM-T Easy vector, resulting in pFvfsr1. The *fsr1* gene was released from pFvfsr1 with *Eco*RI, and ligated into digested pAN8-1 at the *Eco*RI cutting site, resulting in pANFvfsr1 for the transformation of Δ*str1* strain. Due to the low production of falcate conidia of Δ*str1* strain, we followed the

transformation procedures of *A. nidulans* to generate protoplasts from young hyphae, and to transform DNA into Δ*str1* and Δ*str1;nitM* (Yelton et al., 1984). After incubating with the PTC solution for 20 min, the transformed protoplasts were incubated in regeneration broth (100 ml contains sucrose 34.23 g and yeast extract 0.02 g) with 100 rpm at 30 ℃ overnight, and then mixed with the *C. graminicola* regeneration medium containing phleomycin (75 ng / mL). Colonies generated from single conidia of transformants was isolated from the phleomycin-amended PDA plates. Primers hphFS and hphRS were used to confirm the deletion of *str1* in candidate transformants. Primers CgfsrCpF and CgfsrCpR were used to verified the presence of complemented *str1* while primers Fvfsr1F2 and Fsr1UR were used for complemented *fsr1*.

Generation of nitrate non-utilizing (*nit*) mutants

To generate *nit* mutants, 1 cm diameter agar blocks of M1.001, M4.001, Δ*str1*, Δ*str1*;*str1*, and Δ*str1*;*fsr1* strains were placed onto PDA amended with chlorate (PDC) and minimal medium amended with chlorate (MMC). For PDC, 1 L of potato dextrose broth (Difco) was added with agar 20 g and chlorate 20 g. For MMC, 1 L of a basal medium was prepared as previously described (Brooker et al., 1991), and combined with D-glutamate 1.6 g, $NaNO_3$ 2 g, chlorate 20 g (Vaillancourt and Hanau, 1994). Fast-growing colony sectors on PDC and MMC may indicate the occurrence of spontaneous *nit* mutants. A small piece of mycelia from the sectors was transferred to PDA and basal medium amended with $NaNO_3$ ($NaNO_3$BM). The *nit* mutants grew as wild type on PDA, but with sparse and lose aerial hyphae on $NaNO_3$BM. To characterize the mutated loci,

the feeding tests and the mutant designation were followed as previously described (Brooker et al., 1991).

Pathogenicity assays

The B73 inbred maize line was used for all pathogenecity assays. In leaf infection assays, V3-stage maize seedlings were laid on a tray and leaves were afixed to paper towel with clear adhesive tape. A 10 ul drop of of falcate conidia (10^6 / mL) suspended in 0.01% Tween 20 solution was placed on the third or fourth leaf of the seedling to a total of four inoculation sites per plant. The inoculated plants were kept in moisture by wetting the paper towel and sealing the tray with transparent plastic wrap. After 24 hours, the plants were removed from trays and grown in an upright position in a growth chamber at 25 °C with 60% humidity for 7 days to allow the development of disease symptom. For stalk infection assays, 8-week-old maize stalks (about 1.7 cm of diameter) were stabbed to a depth of 0.5 cm with dissecting needle. A cotton swab infested with falcate conidia suspension (10^6 conidia / ml) was placed on the wound site. Parafilm strips sealed the cotton swab on the wound site during the assay for 7 days. Lesion areas of leaf and stalk infection assays were scanned and measured with Image J.

Imaging

The microscopic images with differential interference contrast (DIC) were taken through an Olympus DP70 camera outfitted on an Olympus BX51 microscope (Olympus America, Melville, NY, USA) using DP70-BSW software (version 01. 01). Images of

disease symptoms were scanned and prepared with Adobe Photoshop version 7.0.1 (Adobe, Mountain View, CA, USA).

RESULTS

Identification and deletion of the striatin ortholog in *C. graminicola*

The sequence of the *C. graminicola* striatin ortholog was identified using the 'tblastn' algorithm with the amino acid sequence of *F. verticillioides* striatin ortholog (Fsr1) as the query sequence against the un-assembled sequence of *C. graminicola* M5.001 deposited in the database of the Genomic Survey Sequence at NCBI (http://www.ncbi.nlm.nih.gov/). The *C. graminicola* gene was contained on two assembled DNA sequences that were not joined. I sequenced the missing 56-bp located in the promoter region by sequencing using inverse PCR. The gene identity of the assembled sequence was confirmed by querying the *F. verticillioides* translated genome with the deduced Fsr1 protein sequence. The sequenqce was also identified as GLRG_06260.1 in the the Broad Institute (http://www.broad.mit.edu/) genomic sequence of *C. graminicola* strain M1.001, and I named the gene *str1*. The putative Str1 protein was 886 amino acids in length. Compared with the predicted domains contained in *F. verticillioides* Fsr1 (Shim et al., 2006), the amino acid sequence identity between Str1and Fsr1 was 100% in the caveolin-binding domain, 86% in the coiled-coil motif, 39% in the calmodulin-binding domain and 86% in the WD repeat domain.

To study the function of Str1 in *C. graminicola*, I used the split-marker gene deletion method to generate *str1* deletion (Δ*str1*) strains. Fourteen single conidium

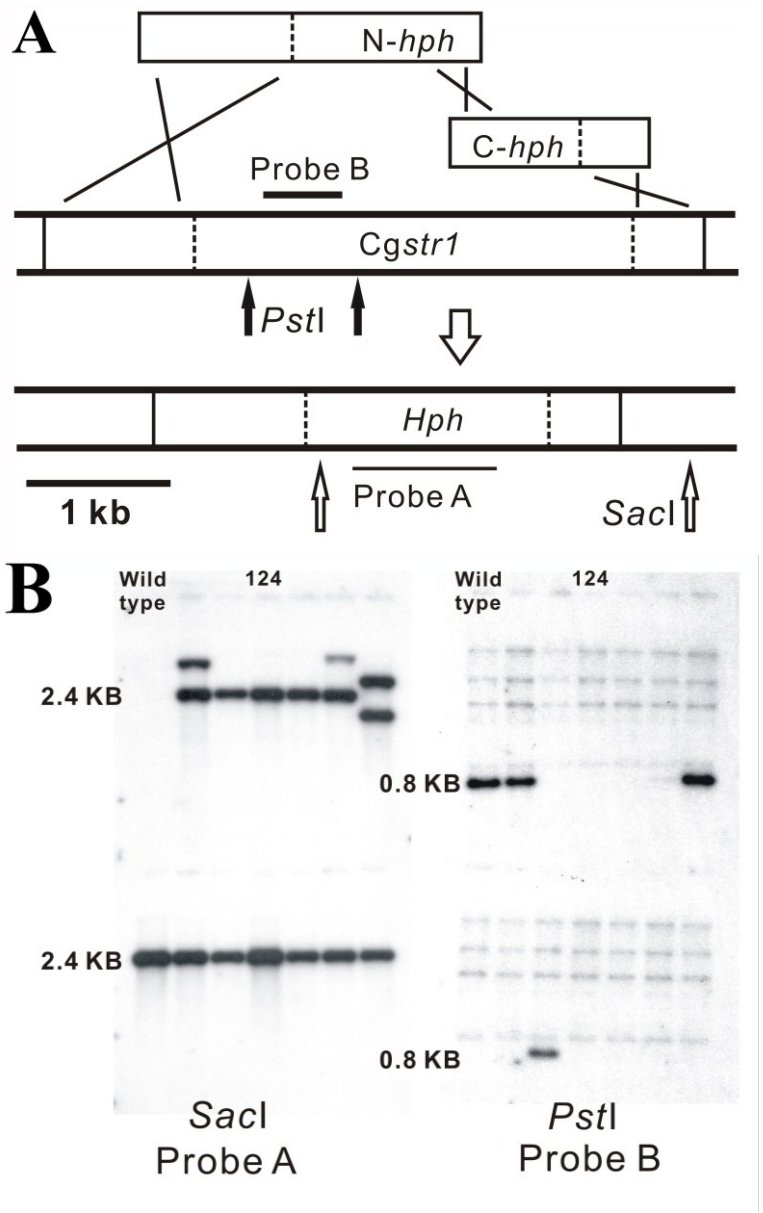

Figure 3.1. Schematic diagraph of gene replacement of Cg*str1* by split-marker deletion. (A) N- and C- terminal fragments of hygomycin phosphotransferase (*hph*) were fused to the upstream and downstream flanking region of Cg*str1*, respectively. Restriction sites of *Sac*I and *Pst*I are indicated. Probe A spanned the coding region partially overlapping the N- and C- terminal fragments. Probe B located in Cg*str1* was used to detect the presence of the gene. (B) With Probe A, several transformants including Cgstr1-124 (124) displayed a single integration event at the *str1* locus. Probe B re-confirmed that Cg*str1* was deleted in most transformants, but not wild type. Faint non-specific bands are evident in all lanes.

isolates derived from 10 transformants were examined for homologous integration of a single copy of the deletion cassettes at the *str1* locus by Southern blot (Figure 3.1). Nine out of the 14 isolates were confirmed to be Δ*str1*. The 9 isolates displayed similar conidial and colonial phenotypes that were distinct from wild-type strain (see below). One of the 9 isolates, ΔCg*str1*-124, was chosen as a representative of the Δ*str1* strains for the following experiments.

Δ*str1* altered the colony appearances

Fungal striatin orthologs have been reported to be involved in colony development. In the *C. graminicola* mutant, the germ tube emergence rate of Δ*str1* was comparable to wild type (data not shown), but the radial growth of the colony was reduced (Figure 3.2). The wild-type strain displayed clock-wise spiral growth on PDA while Δ*str1* showed no spiral pattern or slightly counterclock-wise on the same medium (Figure 3.3). The Δ*str1* displayed an obvious counterclock-wise spiral growth pattern on V8 medium while wild type grew more straight on the same medium (data not shown). I complemented Δ*str1* with *str1* to confirm that the observed phenotypes were linked to the deletion of the gene and with *F. verticillioides fsr1* to examine if the functional domains are conserved between *C. graminicola* and *F. verticillioides*. The complemented strains Δ*str1;str1* (Cg*str1*com1) and Δ*str1;fsr1* (Cg*fsr1*comA5) rescued the phenotypes of radial growth and spiral growth (Figures 3.2 and 3.3). It is of note that the colony of Δ*str1;str1* seemed to be less pigmented than wild type, which may be a consequence of the ectopic insertion of the marker gene or the complementing gene.

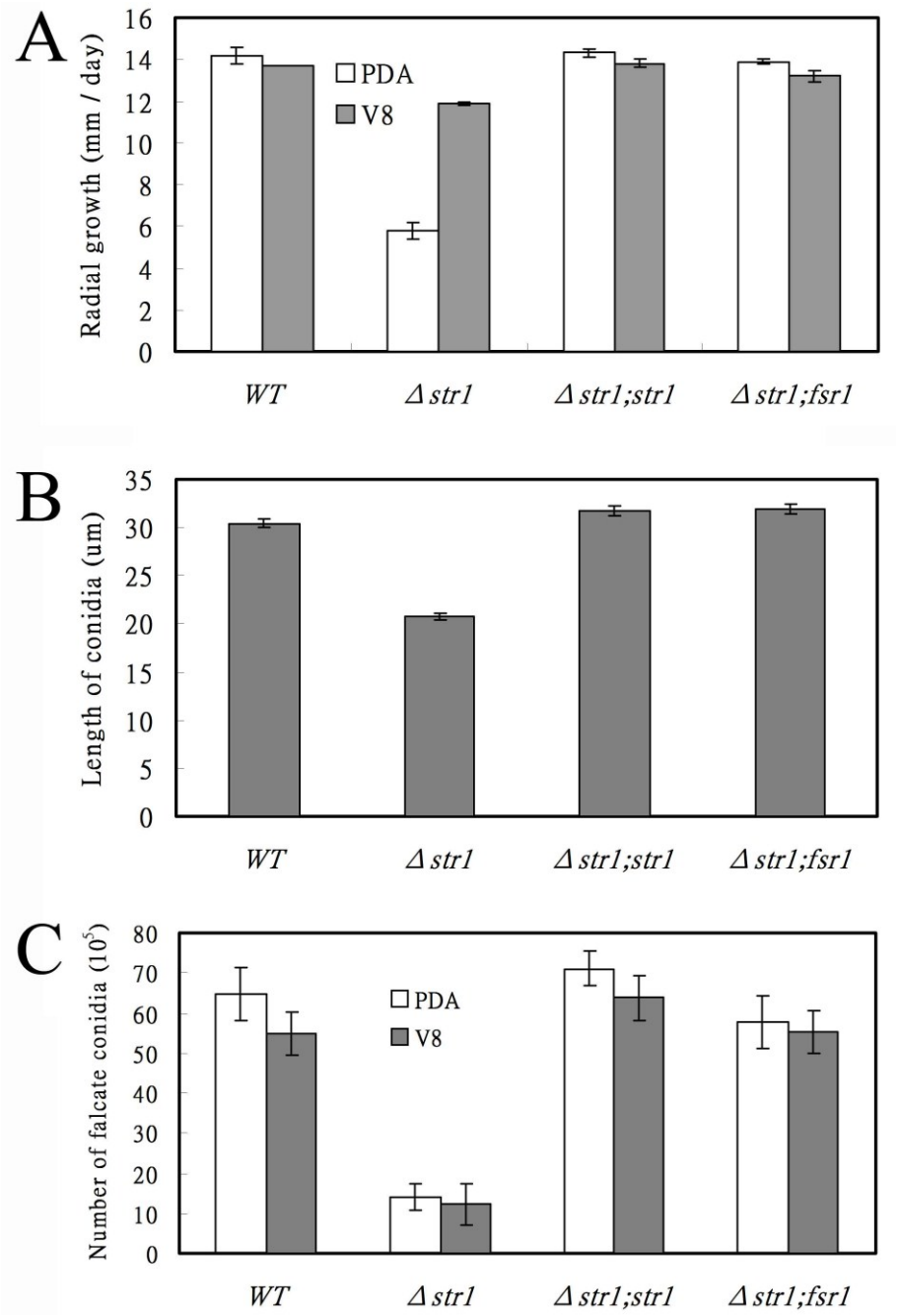

Figure 3.2 Δ*str1* shows reduced radial growth and conidia production.
Compared with the wild-type strain and mutant strains complemented by the *str1* (Δ*str1;str1*) and by *F. verticillioides fsr1* (Δ*str1;fsr1*), Δ*str1* was reduced in growth on V8 and PDA media (A), produced shorter conidia (B) and fewer conidia (C). Bars represent standard error.

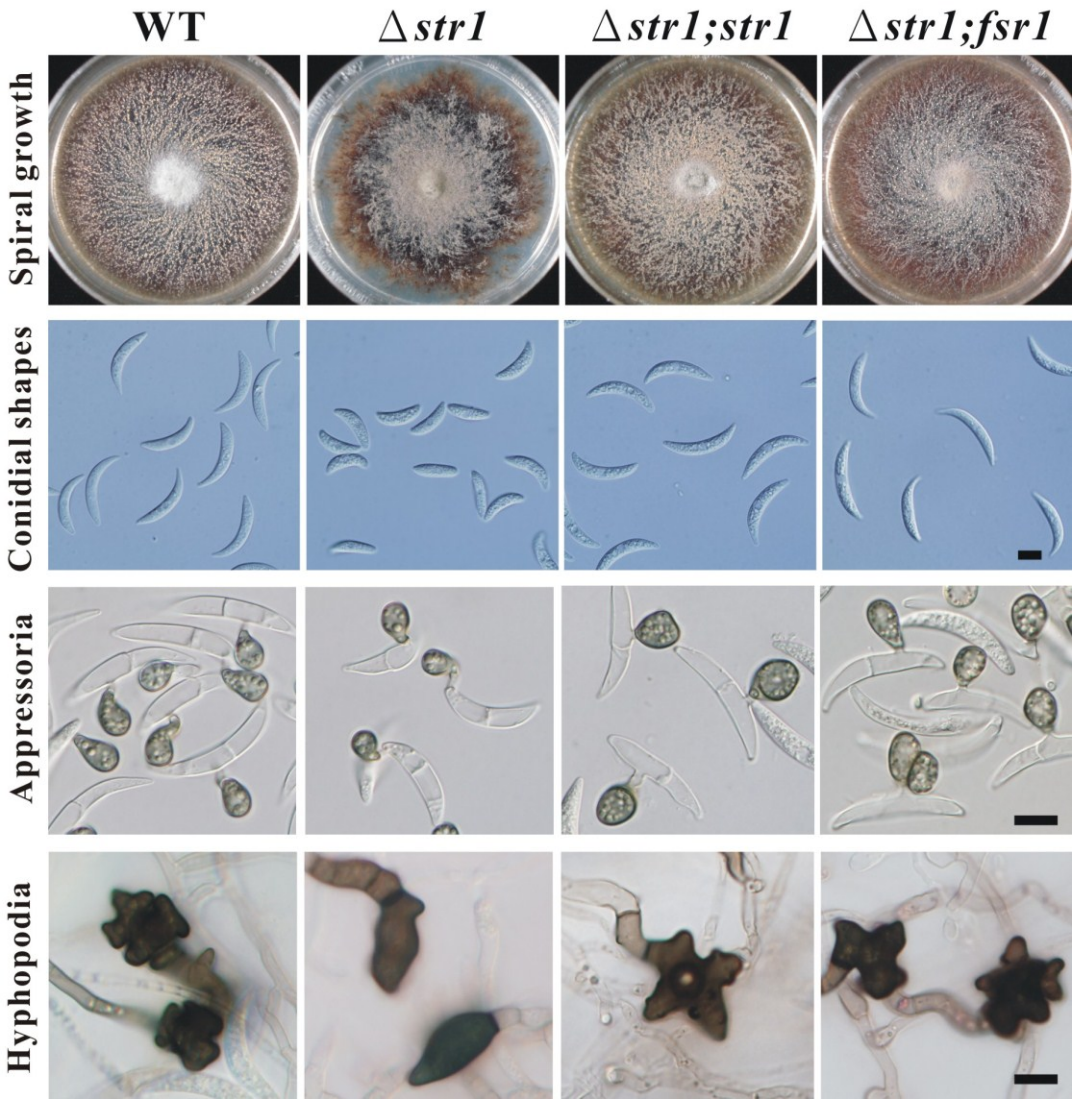

Figure 3.3 Phenotypes of Δ*str1* compared with wild-type strain and mutant strains complemented with *str1* (Δ*str1;str1*) or *F. verticillioides fsr1* (Δ*str1;fsr1*).
The Δ*str1* displayed slightly counterclock-wise spiral growth on PDA medium compared with clock-wise growth of other strains. Conidia of Δ*str1* were shorter and straighter. All strains produced appressoria similar to wild-type in morphology, but hyphopodia of Δ*str1* were altered in morphology, being less lobed. Scale bars = 10 um.

Str1 is involved in conidiation and sexual development

The conidiophores of fungi in which striatin orthologs have been characterized, including *F. verticillioides*, *A. nidulans*, and *N. crassa,* produced exposed conidia at maturity. In contrast, *C. graminicola* produces falcate conidia that are enclosed at maturity inside of an acervulus. Therefore, the examination of the connection between conidiation and striatin function is the first example found in a fungus that has traditionally been categorized a Coelomycetes. Falcate conidia of *C. graminicola* are the major inoculum for dissemination during the course of disease progression. When grown in culture, falcate conidia production is stimulated by light and aggregates in mass on a cluster of conidiogenous cells. The Δ*str1* produced fewer clusters of conidiogenous cells and fewer conidia in comparison to wild type (Figure 3.2). Moreover, the conidia of Δ*str1* were shorter and straighter compared to wild type (Figures 3.2 and 3.3). The reduced conidia production and conidial morphology were complemented in strain Δ*str1;str1* and strain Δ*str1;fsr1* (Figures 3.2 and 3.3), indicating that deletion of *str1* was responsible for these phenotypes.

As mentioned above, fungal striatin orthologs are involved in the production of sexual structures in several fungi. We followed a conventional sexual cross method to examine the effect of Δ*str1* on production of perithecia. There were no fertile perithecia produced when Δ*str1* was crossed with a sexually compatible wild-type strain (M4.001). Occasionally, 1~2 protoperithcium-like structures were observed that never contained ascospores. In contrast, many fertile perithecia were produced in a cross between two wild-type strains (M1.001 and M4.001) (Figure 3.4).

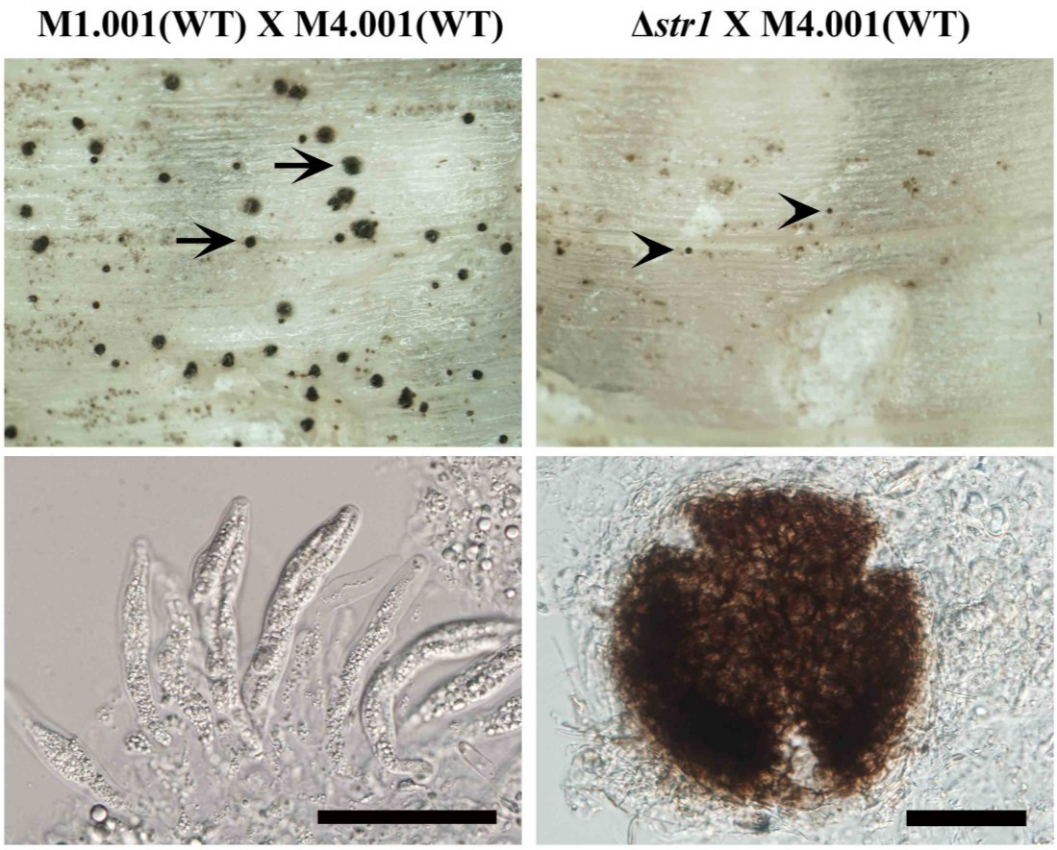

Figure 3.4 Δ*str1* was defective in sexual development.
Wild type (M1.001) and Δ*str1* (derived from M1.001) were crossed with a sexually compatible wild-type strain (M4.001). Many perithecia (arrows) formed between the colonies of M1.001 and M4.001. However, in a cross between Δ*str1* and M4.001, only a few poorly developed stromata (arrow heads) were observed, and ascospores were not found in these protoperithecia. Scale bar = 50 um.

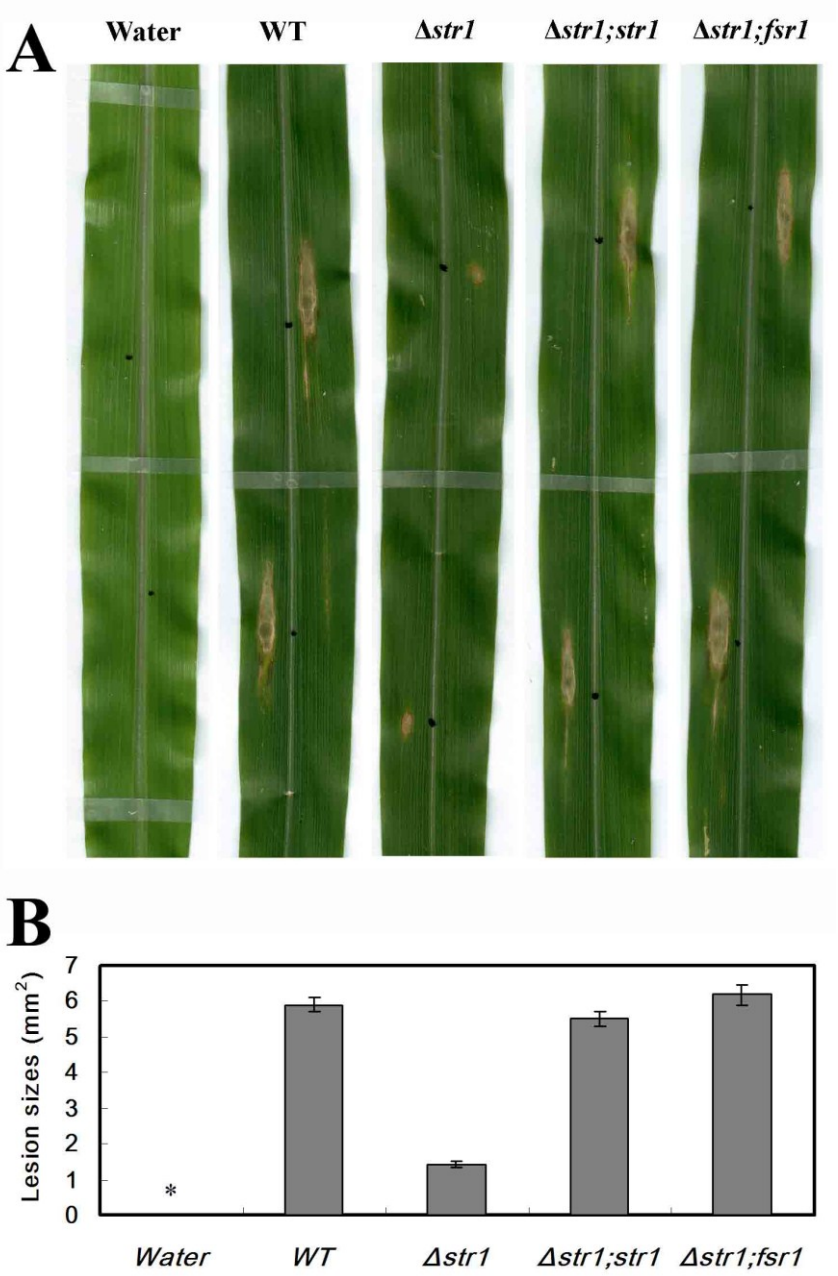

Figure 3.5 Δ*str1* was less virulent for anthracnose leave blight.
Drops of conidial suspension were point inoculated, and areas of nectrotic lesions were measured at 7 day post inoculation. Δ*str1* caused oval lesions (A) in samller areas (B) while other strains generated long oval lesions in larger areas. * Water treatments did not cause necrosis.

Δ*str1* is less virulent to maize

C. graminicola forms appressoria and hyphopodia, which allow the pathogen to actively penetrate through host cells in the absence of wounds or natural openings (Bergstrom and Nicholson, 1999; Sukno et al., 2008). The Δ*str1* formed appressoria that were morphologically similar to wild type (Figure 3.3). However, hyphopodia of Δ*str1* were less lobed than wild type (Figure 3.3). The altered hyphopodia were restored to wild-type morphology in complemented strains Δ*str1;str1* and Δ*str1;fsr1* (Figure 3.3). For leaf infection assays, the wild-type strain caused entensive lesions while the Δ*str1* strain produced restricted oval lesions at the inoculation site at 7 dpi (days post-inoculation) (Figure 3.5). This result implied that the appressoria of Δ*str1* were functional and allowed the fungus to penetrate host cells, but Δ*str1* is limited in developing disease symptoms compare to the wild-type progenitor. The possibility remains, however, that naturally occurring wounds on the leaf facilitated penetration. A further observation indicated that Δ*str1* was still capable of expanding the restricted lesions with additional incubation. The virulnence of complemented strains, Δ*str1;str1* and Δ*str1;fsr1* was comparable to the wild-type strain. For stalk infection assays, conidia suspensions of tested strains were inoculated on a wound made by a dissecting needle, which mimics field coniditions where stalk rot is often initied through a wound made by the larvae of European corn borers (*Ostrinia nubilalis*) (Gatch and Munkvold, 2002; Keller et al., 1986). After 7 dpi Δ*str1* discolored the stalk tissues in a smaller area compare to wild-type strain. It also produced oval conidia *in planta* similar to the wild-type strain (data not shown) and initiated the secondary infection along the rind under

the epidermal cells (Figure 3.6).

Hyphal fusion is defective in Δ*str1*

Hyphal fusion or anastomosis is implicated in colony development, sexual reproduction, and virulence (Read et al., 2010). A connection of fungal striatin to hyphal fusion was demonstrated in *N. crassa* where the striatin ortholog mutant diplayed a hyphal fusion defect (Simonin et al., 2010). It is reasonable to hypothesize that *C. graminicola* Δ*str1* is also defective in hyphal fusion. In *C. graminicola*, hyphal fusion occurred more often in the inner area of colony than the periphery. In my observation I was never able to document hyphal fusion in Δ*str1* (data not shown). To unequivocally document the presence or absence of hyphal fusion we generated the auxotrophic nitrate non-utilizing (*nit*) mutants to examine the ability of hyphal fusion of Δ*str1*. The *nit* mutants have been widely used for testing vegetative compatibility, hyphal fusion, and heterokaryon formation (Correll et al., 1987; Correll et al., 1989; Craven et al., 2008; Prados Rosales and Di Pietro, 2008; Vaillancourt and Hanau, 1994). Several spontaneous *nit* mutants from wild-type strains (M1.001 and M4.001) and Δ*str1* were selected from chlorate containing media. These *nit* mutants were identified and designated as *nit1* or *nitM* mutants following the previous designation for *Colletotrichum* spp. *nit* mutants. The *nit1* designation indicated that the mutation was defective in gene of nitrate reductase. The *nitM* designation indicated the mutant was defective in assembly of molybdenum cofactor, resulting in impairing the activity of nitrate reductase (Brooker et al., 1991). Tested strains were grown on the basal medium containing

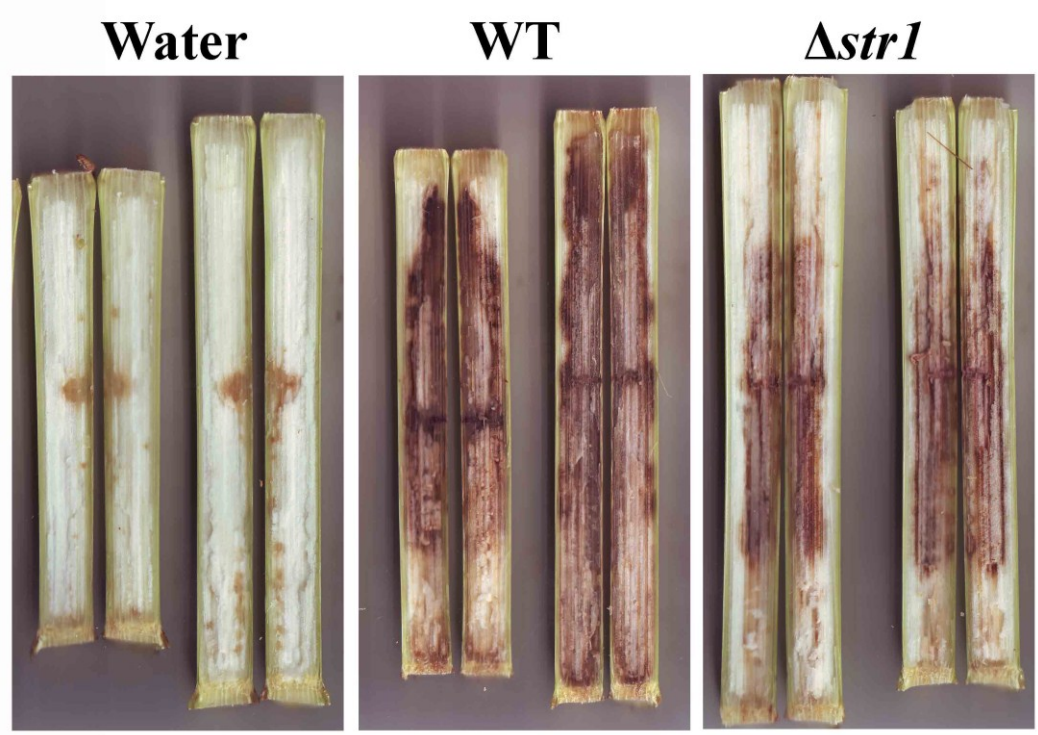

Figure 3.6 Δ*str1* was less virulent for anthracnose stalk rot.
Conidial suspensions of each strain were inoculated on a wounded internode of maize stalk. Discoloration of stalk was examined at 7 days post inoculation. Discolored areas of Δ*str1* were smller and lighter in color.

sodium nitrate as sole nitrogen source ($NaNO_3$BM). On this medium *nit* mutants grow sparsely but when a heterokaryon is established thorugh anastomosis, complementary *nit* mutants grow vigorously in the margin between each colony. The *nit* mutants in wild-type M1.001 background established a clear line of vigorous hyphal growth on the colony border between M1-*str1;nit1* (strain Nit-1) and M1-*str1;nitM* (strain Nit-9) on $NaNO_3$BM, indicating the occurrence of hyphal fusion and the genetic complementation between *nit1* and *nitM* genes in the heterokaryon (Figure 3.7 B). In contrast, there was no visible zone of complementation formed when tested with two non-complementary *nit* mutants or when a Δ*str1* strain was used, including tests between M1-*str1;nit1* (strain Nit-1) and M1-*str1;nit1* (strain Nit-2) (Figure 3.7 A); Δ*str1;nitM* and M1-*str1;nit1* (strain Nit-23) (Figure 3.7 C); Δ*str1;nitM* and Δ*str1;nit1* (strain Nit-25) (Figure 3.7 D); Δ*str1;nit1* and M1-*str1;nitM* (data not shown). To rule out the possibility that the hyphal fusion defect was caused by a random mutation while generating spontaneous *nit* mutants, I complemented the strain Nit-23 (Δ*str1;nitM*) with *str1* (Δ*str1;nitMcom*), and then tested its ability to undergo anastomosis. The Δ*str1;nitMcom* (Nit-23com1) and M1-*str1;nit1* strains fused and formed a zone of complementation on $NaNO_3$BM, indicating that the hyphal fusion phenotype depends on the presence of *str1* (Figure 3.7 E compared to C). These results demonstrated that the presence of *str1* in both strains was necessary for hyphal fusion. The hyphal fusion defect of Δ*str1* was rescued in *nit* mutants with *str1*- or *fsr1*- complemented background (Δ*str1;str1;nitM* (Nit-30) or Δ*str1;fsr1;nitM* (Nit34)), indicating that Str1 was responsible for the defect and that *F. veritcillioides* Fsr1 was effective to restore the function of hyphal fusion in *C.*

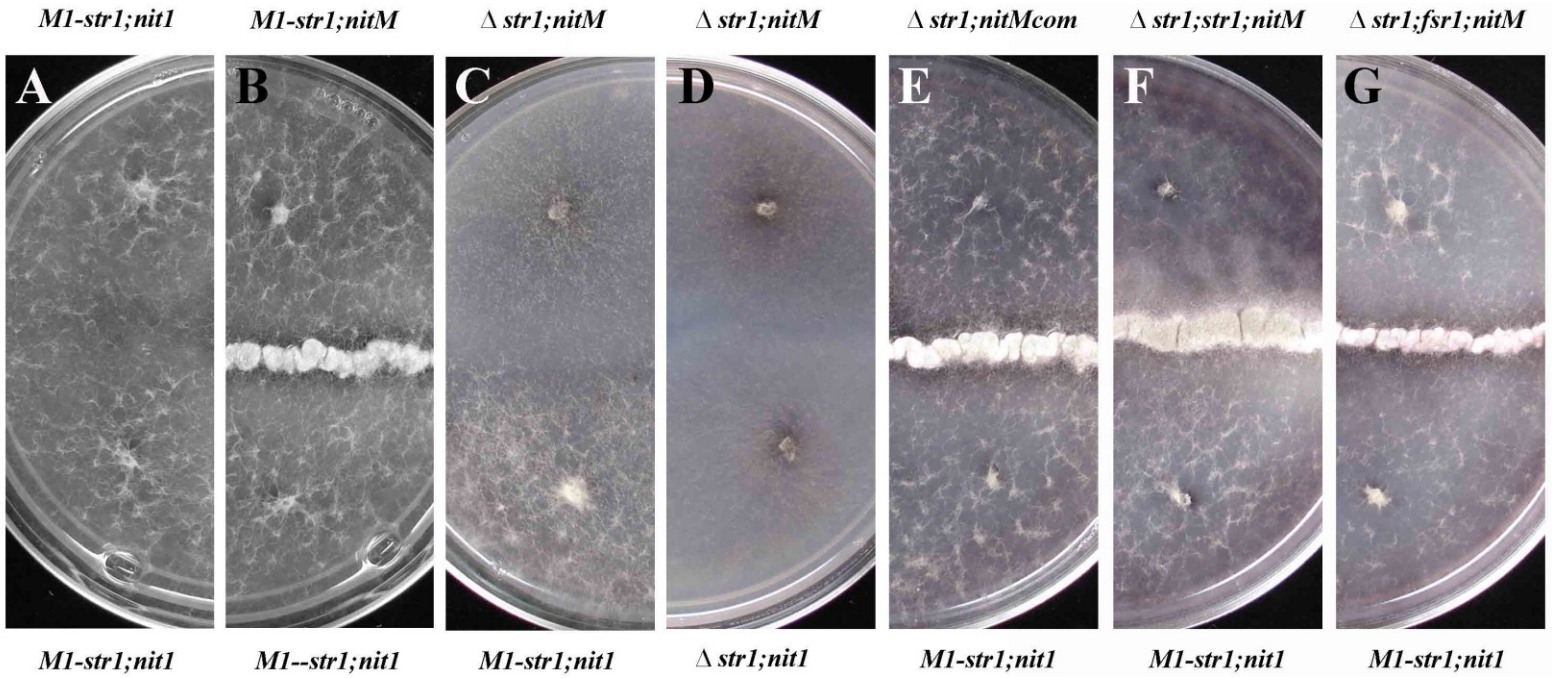

Figure 3.7 The *str1* is required for hyphal fusion.
Hyphal fusion was tested by complementation of *nit1* and *nitM* mutations in a pairing of two vegetatively compatible strains on $NaNO_3$BM medium. The *nit* mutants grew sparsely on the medium and a line of vigorous hyphal growth indicated a positive hyphal fusion and heterokaryon formation between two strains. (A) A negative control of *str1* wild-type strains. (B) A positive control of *str1* wild-type strains. (C & D) Δ*str1* was not able to fuse with a wild-type strain or with itself. (E) Complementation of *Δstr1;nitM* strain shown in (C) with *str1* rescued the anastomosis, indicating *str1* was responsible for the ability of anastomosis rather than a potential random mutation in this *nit* strain background. (F & G) complementation of Δ*str1* with *str1* or *fsr1* rescued hyphal fusion.

graminicola (Figure 3.7 F and G). Although M1.001 and M4.001 are sexually compatible strains they were not able to vegetativly fuse with each other. The M1-*str1;nit1* (Nit-1, derived from M1.001) and M4-*str1;nitM* (Nit-16, derived from M4.001) strains were not able to fuse with each other (data not shown). The same result was also observed between M1-*str1;nitM* (Nit-9) and M4-*str1;nit1* (Nit-13) strains (data not shown).

DISCUSSION

All fungal striatin orthologs examined so far are associated with sexual development. In heterothallic fungi, e.g. *F. verticillioides* and *N. crassa*, striatin mutants are female sterile, but are male fertile (Shim et al., 2006; Simonin et al., 2010). The female sterility phenotype may be due to the defect in hyphal fusion. The *N. crassa* striatin (*ham3*) mutant is impaired in hyphal fusion, but not in conidium-trichogyne fusion (Simonin et al., 2010). This result indicates that the fungal striatin mediates vegetative hyphal fusion, and that sexual cell fusion may be controlled by different molecular mechanisms. The striatin orthologs in *A. nidulans* and *N. crassa* are also involved in ascosporogenesis. These mutants produce abnormal ascospores, and this defect is due to aberrant meiosis (Simonin et al., 2010; see Chapter II). Here I concluded that *C. graminicola* Δ*str1* was not able to develop perithecia. Rarely, few protoperithecia-like structures formed but these were always void of ascospores. The biological process of *C. graminicola* sexual development is still not documented fully. It is unknown what the male and female gametes are, and what factors induce the gamete

formation and differentiation. Therefore, I was not able to differentiate between male and female function in the sterility phenotype. Since perithecia of *C. graminicola* are formed at the interface between the two crossing strains, I speculate that vegetative hyphal fusion is required for the sexual development. The *nit* mutant pairings, however, indicate that M1.001 and M4.001, two sexually compatible strains, are not able to form a heterokaryon. A similar lack of fusion between two sexually compatible wild-type strains was observed previously and in that case vegetative incompatibility was implicated (Vaillancourt and Hanau, 1994). There are two possible explanations for this lack of fusion between the two wild-type strains that can mate: (1) Vegetative hyphal fusion is not required for sexual development. (2) Vegetative hyphal fusion occurs and the vegetative incompatibility is suppressed during sexual crossing, but not during vegetative growth.

Appressoria and hyphopodia are thought to be equivalent structures in initiating of pathogenesis, and the morphological difference may be due to their origins from different cell types (Howard, 1997). However, appressoria of Δ*str1* are morphologically identical to the wild-type progenitor and function normally in disease initiation. However, hyphopodia of Δ*str1* were altered in morphology. This result suggests that distinct regulatory mechanisms regulate the development of two specialized cells. Additionally, the hyphopodia of Δ*str1* were less lobed than the wild type. It can be argued that the altered hyphopodia may be functionally compromised, resulting in altered adhesion to the surface, which may explain in part the reduced virulence of the Δ*str1* mutant. In case of appressoria-mediated penetration, the tight adhesion to the host

surface is required while a penetration peg invades the host cell wall. Many *Colletrotrichum* spp. also require appressoria to be tightly attached to the host surface for infection (Prusky et al., 2000). Although it is unknown if hyphopodia of *C. graminicola* play any role in leaf blight and stalk rot infection, hyphopodia do develop during root infection. *C. graminicola* infects root tissue through hyphae and hyphopodia that developed from runner hyphae, and colonizes root tissues intercellularlly and intracellularlly (Sukno et al., 2008). Some infections result in asymptomatic colonization from root to the aboveground stem and leaves. During leaf senescence, hyphopodia develop on the leaf sheath. It has been proposed that hyphopodia also serve as a survival structure on maize residues (Sukno et al., 2008).

The fungal striatin orthologs of *F. verticillioides* (*fsr1*) and *F. graminearum* (Fg*fsr1*) are essential in their virulence to maize and barley, respectively (Shim et al., 2006). Since filamentous fungi possess a striatin ortholog, I used *C. graminicola* to examine if fungal striatin orthologs mediate virulence in pathogenic fungi other than *Fusarium* species. Compared with *F. verticillioides*, *C. graminicola* not only causes stalk rot on maize, but also induces foliar lesions. The pathogenicity assays of Δ*str1* indicate that the Δ*str1* is less virulent in anthracnose stalk rot and anthracnose leaf blight as well. Although Δ*str1* is less virulent than wild type, the symptom reduction of Δ*str1* is less prominent than that of the *F. verticillioides fsr1* mutant strain (Shim et al., 2006). The mechanism of striatin-mediating virulence is unknown. Since both *fsr1* mutant and Δ*str1* displayed reduced radial growth in culture media, these mutants may also grow slowly in maize tissue. When compared to wild type, Δ*str1* virulence is more impaired on leaves

than on stalks. *C. graminicola* mostly colonizes mesophyl cells on leaves and fiber cells on stalks (Venard and Vaillancourt, 2007a; Venard and Vaillancourt, 2007b). In contrast to the non-living fiber cells, the living mesophyl cells are more capable of mounting an active defense response. Thus, it is also possible that the slower growth of the mutant allowed the host tissue to mount a defense response that reduced the disease progress. In a wound-healing assay during stalk rot inoculations it was demonstrated that the longer the wound-healing time before inoculation, the less *C. graminicola* colonization was present (Muimba-Kankolongo and Bergstrom, 2011). Slower hyphal growth may not fully explain the observed reduction in virulence. When considering necrotrophic and hemibiotrophic fungi, effectors or toxins rather than hyphal growth are the key virulence factors that are required to kill host cells or damage the defense mechanisms preceding hyphal arrival. For example, in the necrotrophic fungus *Sclerotinia sclerotiorum*, mutants deficient in oxalic acid production are non-pathogenic though hyphal growth was only slightly reduced on media (Godoy et al., 1990). The hemibiotrophic rice blight fungus, *Magnaporthe oryzae*, translocates the effectors, PWL2 and BAS1, into uninfected host cells before hyphal invasion (Khang et al., 2010). *C. graminicola*, a hemibiotrophic fungus, may apply a similar invasion strategy during maize colonization.

Hyphal fusion is also referred to as anastomosis. A role for hyphal fusion in pathogenicity is documented. The Fmk1 protein of *F. oxysporum* and Amk1 of *Alternaria brassicicola* are orthologs of *N. crassa* Mak-2 that is required for hyphal fusion. The Δ*fmk1* and Δ*amk1* mutants are defective in hyphal fusion and unable to infect tomatoes and cabbage, respectively (Cho et al., 2007; Di Pietro et al., 2001). The

Fso1 protein of *F. oxysporum* and Aso1 of *A. brassicicola* are orthologs of *N. crassa* So. Both *fso1* and *aso1* are also required for efficient hyphal fusion (Craven et al., 2008; Prados Rosales and Di Pietro, 2008). The Δ*aso1* mutant is able to invade the host plant, but is defective in colonization of plant tissue (Craven et al., 2008), which is similar to the defects of Δ*fmk1* and Δ*amk1*. Assuming that fusion of hyphae is a conserved function of fungal striatin orthologs, the significant reduction of virulence in *F. verticillioides* Δ*fsr1* also supports the idea that hyphal fusion contributes to the pathogenicity. However, the *F. oxysporum* Δ*fso1* is only reduced slightly in virulence (Prados Rosales and Di Pietro, 2008). Similarly, *C. graminicola* Δ*str1* showed a severe defect in hyphal fusion, but it still colonized maize stalk. The unresolved role of hyphal fusion contributing to virulence and pathogenicity may depend on the infection and colonization strategies of the pathogens in their targeted host systems.

The conserved functions of fungal striatin orthologs that have been documented in multiple fungi include sexual development and hyphal growth. Functions revealed in fewer fungi include virulence, hyphal fusion, and conidiation. However, what are the conserved functions of striatin orthologs in fungi? Here I used *C. graminicola* that posseses multiple biological characteristics that allow us to examine these phenotypes in Δ*str1*. My results indicate that *C. graminicola* striatin ortholog is important for five functions including hyphal growth, hyphal fusion, conidiation, sexual development, and virulence. To confirm the functional conservation at the molecular level, we transformed Δ*str1* with *F. verticillioides fsr1*. It should be noted that the phenotypes of macroconidia production and hyphal fusion were not determinated in Δ*fsr1* (Shim et al., 2006), and *F.*

verticillioides is not a foliar pathogen on maize. The transformant Δ*str1;fsr1* was still able to complement all the observed phenotypes. Thus, I propose that these five functions, if applicable, are conserved among striatin orthologs of filamentous fungi.

CHAPTER IV

CONCLUSIONS

SUMMARY

The functional domains of striatin family proteins suggest that these proteins are molecular scaffolds that mediate multiple signal transduction pathways. The functional analyses of mammalian striatin-interacting proteins also support this idea. In addition, a putative STRIPAK protein complex and its interacting partners further broaden the potential functions of striatin homologs in mammals (see Chapter I). The molecular mechanisms of striatin homologs characterized in mammalian systems including the molecular function of Mob3, calcium/CaM signaling and PP2A signaling pathways may be conserved in fungal striatin orthologs. However, the developmental phenotypes associated with striatin family members may be diverged in different kingdoms through evolution.

Filamentous fungi are diverse in the presence of asexual and sexual stages in their life cycle and in the the morphology and ontogeny of these structures, parasitic and saprophytic life styles, and unique physiological processes for their fitness in different environmental conditions. The role of striatin orthologs in fungal development was still obscure. I, therefore, proceeded to characterize fungal striatin orthologs in *A. nidulans* and *C. graminicola*. I identified one striatin ortholog in *A. nidulans* (*strA*) and *C. graminicola* (*str1*), respectively. The two proteins contain putative domains that are conserved in striatin family. I knocked out each gene and examined their functions in

fungal development. The following is comprehensive summary of the role of fungal striatin orthologs in fungal development.

Hyphal growth and hyphal fusion

All reported fungal striatin mutants display phenotypes where colonial growth or colony appearance is effected. Reduced aerial hypha production is also found in the *F. verticillioides fsr1* mutant and *N. crassa* Δ*ham3* while an increase in aerial hypha production is found in the *S. macrospora pro11* mutant. In the *C. graminicola* Δ*str1*mutant, a conspicuous colonial phenotype includes an alteration in spiral growth. To date, no discernable defect in vegetative hypha growth other than growth rate is known to account for these changes in colonial phenotypes.

Another significant function of fungal striatin orthologs is hyphal fusion. The Δ*str1* mutant of *C. graminicola* and Δ*ham3* of *N. crassa* reveal that fungal striatin orthologs are essential components for anastomosis. Although the function of hyphal fusion was not examined in other fungal striatin studies, in each case sexual development has been altered, and a necessary step in sexual reproduction is the fusion of two cells. Therefore, I presume that striatin mutants of *F. verticillioides* (*fsr1*), *F. graminearum* (Fg*fsr1*) and *S. macrospora* (*pro11*) possess a similar defect in hyphal fusion. The presumption is supported by evidence that mutants of Mob3, a putative striatin-interacting protein, of *N. crassa* and *S. macrospora* were defective in hyphal fusion.

Sexual development and conidiation

Fungal striatins are involved in sexual development, including perithecium and cleistothecium development. In *A. nidulans*, StrA is important but not essential for cleistothecium development. In the over-expression strain in *A. nidulans*, StrA is a positive regulator of sexual development and facilitates the transition from vegetative growth to the early stages of sexual development. In contrast to cleistothecia, striatin orthologs are essential for perithecium development. In *C. graminicola*, I have shown that Δ*str1* is blocked at a very early stage of perithecium development. Moreover, striatin mutants of *F. verticillioides* (*fsr1*) and *N. crassa* (*ham3*) are female sterile, and the mutant of *S. macrospora pro11* is arrested in the transition from protoperithecium to perithecium stages. I assume that this functional contrast of fungal striatins between cleistothecia and perithecia developed during the evolution of extant fungi, but further research is needed to test this hypothesis. In *A. nidulans*, StrA is also involved in ascosporogenesis. Although Δ*strA* produced fertile cleistothecia, undifferentiated asci and aberrant ascospores were observed in these cleistothecia. The *N. crassa* Δ*ham3* mutant in a homozygous cross also showed abnormal ascospore production and displayed aberrant meiosis during ascospore formation. These data reveal that fungal striatin orthologs are involved in at least two stages of sexual development.

Conidia of *N. crassa*, *A. nidulans,* and *C. graminicola* are produced following different developmental patterns. Striatin mutants of these fungi produce fewer conidia, indicating that fungal striatins may mediate conidiation regardless of the diverse ontogenesis mechanisms. In *A. nidulans*, over-expression of *strA* produced

conidiophores in a condition where conidiophores are never formed in wild type. This indicates that StrA is a positive regulator of conidiophore production. Collectively these data led me to conclude that fungal striatin orthologs play a role in development of conidiophores or conidiogenous cells.

Virulence

The *F. verticillioides* Δ*fsr1* and *F. graminearum* Δ*fsr1* mutants are dramatically reduced in virulence to maize stalk rot and to barley head blight, respectively. In contrast, Δ*str1* of *C. graminicola* is slightly reduced in virulence. The reduction in virulence may be due in part to slow haphal growth, defective hyphal fusion or other undetermined phenotypes. The impact on virulence may vary with the pathogenic strategies to host defense responses exhibited by each fungal species. Although the mammalian *mob3* ortholog is proposed to be involved in vesicle trafficking, particular in endocytosis that may be required for uptake of nutrients or signaling molecules, there is no significant defect in endocytosis observed in Δ*mob3* of *S. macrospora* and Δ*strA* of *A. nidulans*. The ER localization of *A. nidulans* StrA suggests that fungal striatin may be associated with enzyme biosynthesis or secretion. There is no known secretory defect of several cell wall degrading enzymes in Δ*fsr1* of *F. verticillioides*. Nevertheless, the possibilitiy remains that fungal striatin orthologs mediate secretion of other factors that play a role in virulence. The function of fungal striatin orthologs in virulence remains to be elucidated.

C. graminicola Δ*str1* produces morphologically altered hyphopodia, but appressoria do not deviate from those observed in the wild-type strain. The hyphopodia

that are produced are less lobed and may be reduced in the ability to attach to the host tissue. If the phenotype is conserved in root infection pathogens such as *Gaeumannomyces graminis*, fungal striatin-mediated signaling pathways may have significant impact on virulence of these fungi.

In summary, **I propose that the fungal striatin ortholog localizes to ER and other endomembranes where it regulates hyphal growth, hyphal fusion, conidiation, sexual development and virulence in filamentous fungi.**

FUTURE WORK

I have formulated a working model of the molecular mechanisms of fungal striatin orthologs based on this study and other recently published data (see Chapter I). I hypothesize that a putative protein complex comprised of fungal striatin orthologs, PP2A A/C subunits, Mob3, and Ham2 ortholog localizes to ER and other endomembranes. This putative protein complex coordinates multiple signal transduction pathways including PP2A phosphatase signaling, Calmodulin/Ca^{2+} signaling and MAP kinase signaling. These pathways then regulate hyphal growth, hyphal fusion, conidiation, sexual development and virulence in filamentous fungi (Figure 4.1). Three future projects are proposed based on the working model and are described below.

Define the striatin protein complex in filamentous fungi

To understand the molecular mechanisms of striatin, it is important to identify the interacting proteins. Although a putative protein complex deduced from mammalian

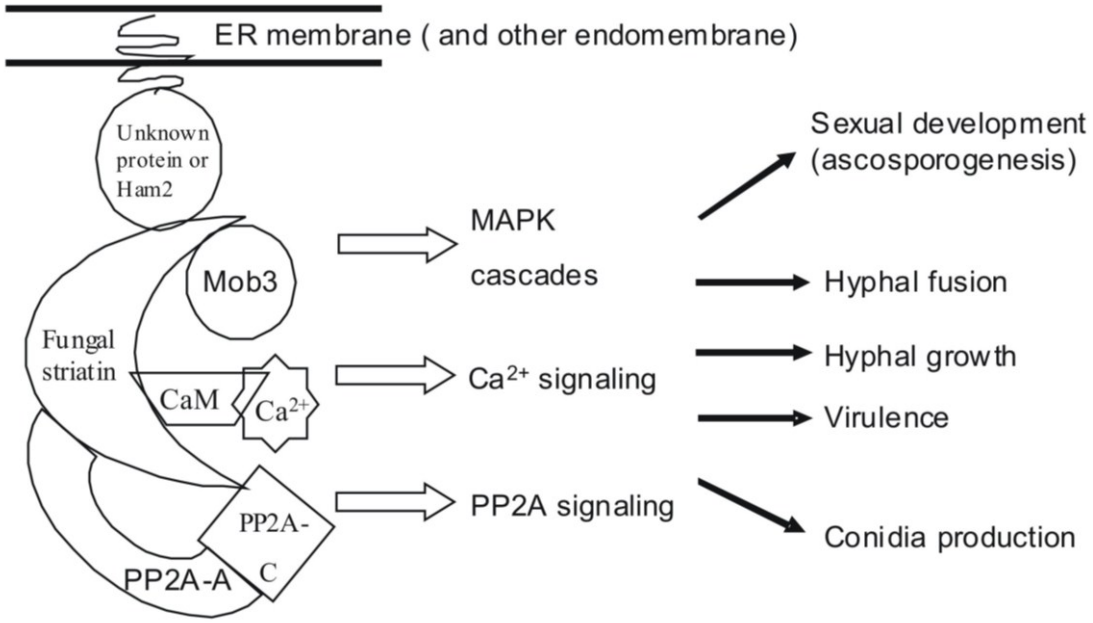

Figure 4.1 A working model of the putative fungal striatin protein complex and potential signal transduction pathways.
Fungal striatin protein complex localizes to ER memberane and other endomembrane, and mediates fungal development through potential signal transduction pathways. CaM: calmodulin; PP2A-A: protein phosphatase 2A-A subunit; PP2A-C: protein phosphatase 2A-C subunit.

and budding yeast models is supported by the observed mutant phenotypes, the evidence of physical protein-protein interactions are still required to confirm the interactions. The mammalian STRIPAK model indicates that additional components involved in forming the protein complex are yet to be identified in fungal systems. A protein affinity-tag coupled with immuno-precipitation (IP) may be used to pull down a stable protein complex for the identification of each component with mass spectrometry. In Appendix C, I describe generation of a *strA*::S-tag strain in *A. nidulans* created for just this purpose. The STRIPAK complex in mammalian model interacts with CTTNBP2 or SLMAP proteins in a mutually exclusive manner (Goudreault et al., 2009). It is possible that the striatin protein complex changes components or interacts with other proteins during different developmental stages. The IP experiments performed in different developmental stages may reveal different striatin protein complexes and will further illustrate how fungal striatin coordinates each specific function by coupling with various proteins. After identification of the fungal striatin interacting proteins, functional characterization of these proteins is critical to understand what functions may be exerted through the component or the signaling pathway. For example, in *N. crassa* Δ*mob3*, Δ*ham2*, Δ*ham3* and Δ*ham4* indicated that Mob3, Ham2 and Ham3 were involved in hyphal fusion and female fertility while Ham4 was only involved in hyphal fusion (Simonin et al., 2010).

Sub-cellular localization of fungal striatin protein complex

The *A. nidulans* StrA protein co-localizes with CnxA in endoplasmic reticulum (ER). It is possible that a small population of StrA population localizes to other endomembrane system (see Chapter II). In addition, the *S. macrospora* Pro22, a potential *S. macrospora* Pro11-interacting protein and a *N. crassa* Ham2 ortholog, is shown to localize to vacuoles (Bloemendal et al., 2010). Two potential *F. verticillioides* Fsr1-interacting proteins are predicted to localize to peroxisomes (Mukherjee and Shim, unpublished data). Thus the question remains, to where does the fungal striatin protein complex localize? Do fungal striatins interact with different protein complexes depending on the sub-cellular localization? The BiFC (bimolecular fluorescence complementation) will help to visualize protein-protein interactions *in vivo* (Kerppola, 2006). To answer this question the interaction of StrA with these major components of the fungal striatin protein complex such as PP2A A/C subunits, Mob3, and Ham2 orthologs in *A. nidulans* can be examined. These results would not only identify the sub-cellular localization of the protein complex, but prove the protein interactions *in vivo*.

Link fungal striatin to kinase signaling pathway

The mammalian STRIPAK complex may interact with TRAF3IP3 which is a protein involved in JNK signaling (Dadgostar and Cheng, 2000; Goudreault et al., 2009). Interestingly, striatin orthologs in fly and goldfish are also known to interact with components of JNK signaling pathway (Chen et al., 2002; Ma et al., 2009). These data suggests that striatin family proteins may also coordinate kinase signaing. In filamentous

fungi, striatin orthologs and other interacting proteins such as Mob3 and Ham2 orthologs are involved in hyphal fusion. The molecular mechanism of hyphal fusion is still not fully understood. It is known that there are three MAP kinase signaling pathways involved in the processes of hyphal fusion in *N. crassa*. These include the pheromone response MAP kinase pathway (NRC-1/MEK-2/MAK-2), the cell wall integrity MAP kinase pathway (MIK-1/MEK-1/MAK-1), and the osmosensing MAP kinase pathway (OS-4/OS-5/OS-2) (Li et al., 2005; Maerz et al., 2008; Pandey et al., 2004; Roca et al., 2005). In mammalian systems, c-Jun is the transcriptional factor activated by the JNK signaling pathway. In fungi, the c-Jun orthologs such as Gcn4 in *S. cerevisiae*, Cpc1 in *N. crassa*, and CpcA in *A. nidulans* were regulated by the cross-control pathway, which is activated by amino-acid starvation conditions (Hinnebusch, 1997; Hoffmann et al., 2000; Paluh et al., 1988). The upstream elements of fungal c-Jun signaling pathway remain largely unknown. Limited data indicate that Gcn4 is regulated by Gcn2 and Ras/PKA signaling pathway in budding yeast (Hinnebusch and Natarajan, 2002). Interestingly, yeast Gcn4 was involved in induction of gene expression of salt-induced genes such as *hal1*. Under normal conditions, *hal1* is repressed by Sko1, a target of Hog1 (a MAP kinase of the osmosensing MAP kinase pathway). Under salt stress conditions, Hog1 releases Sko1 from *hal1* promoter region, allowing Gcn4 binding to the same region to activate the gene expression of *hal1* (Pascual-Ahuir et al., 2001). It is, however, still unkown if Gcn4 is a substrate of Hog1 under salt-stress condition, and if there is any analogous JNK pathway in fungi. Moreover, the mammalian STRIPAK complex contains STK24, STK25, and MST4 that belong to GCK-III subgroup in Ste20 kinase

family (Goudreault et al., 2009). Proteins of ste20 kinase family usually activate the MAP kinase pathway through phosphorylation or protein-protein interaction. Taken together these data lead me to the following hypothesis: fungal striatin othologs also serve as a platform for a MAP kinase pathway. To address this hypothesis, the Ham2 of *N. crassa* could be used as a bait to pull down potential Ham2-interacting proteins because mammalian Ham2 ortholog (STRIP1) was able to pull down MST4 and TRAF3IP3 in flag-tag affinity purification assays.

The emerging data indicate that striatin family proteins play crucial roles in cell development and differentiation in mammals, fungi, and other metazoans. Studies of molecular mechanisms highlight striatin family proteins at the junction of multiple signal transduction pathways. Additional identification and characterization of interacting proteins are still needed to understand the molecular mechanishms of fungal striatin in different developmental processes.

REFERENCES

Araujo-Bazan, L., Penalva, M. A., Espeso, E. A., 2008. Preferential localization of the endocytic internalization machinery to hyphal tips underlies polarization of the actin cytoskeleton in *Aspergillus nidulans*. Mol. Microbiol. 67**,** 891-905.

Asakura, T., Sasaki, T., Nagano, F., Satoh, A., Obaishi, H., Nishioka, H., Imamura, H., Hotta, K., Tanaka, K., Nakanishi, H., Takai, Y., 1998. Isolation and characterization of a novel actin filament-binding protein from *Saccharomyces cerevisiae*. Oncogene. 16**,** 121-130.

Baillat, G., Gaillard, S., Castets, F., Monneron, A., 2002. Interactions of phocein with nucleoside-diphosphate kinase, Eps15, and Dynamin I. J. Biol. Chem. 277**,** 18961-18966.

Baillat, G., Moqrich, A., Castets, F., Baude, A., Bailly, Y., Benmerah, A., Monneron, A., 2001. Molecular cloning and characterization of phocein, a protein found from the Golgi complex to dendritic spines. Mol. Biol. Cell. 12**,** 663-673.

Bailly, Y. J., Castets, F., 2007. Phocein: A potential actor in vesicular trafficking at Purkinje cell dendritic spines. Cerebellum. 6**,** 344-352.

Bartoli, M., Monneron, A., Ladant, D., 1998. Interaction of calmodulin with striatin, a WD-repeat protein present in neuronal dendritic spines. J. Biol. Chem. 273**,** 22248-22253.

Bartoli, M., Ternaux, J. P., Forni, C., Portalier, P., Salin, P., Amalric, M., Monneron, A., 1999. Down-regulation of striatin, a neuronal calmodulin-binding protein, impairs rat locomotor activity. J. Neurobiol. 40**,** 234-243.

Bayram, O., Krappmann, S., Ni, M., Bok, J. W., Helmstaedt, K., Valerius, O., Braus-Stromeyer, S., Kwon, N. J., Keller, N. P., Yu, J. H., Braus, G. H., 2008. VelB/VeA/LaeA complex coordinates light signal with fungal development and secondary metabolism. Science. 320**,** 1504-1506.

Bayram, O., Sari, F., Braus, G. H., Irniger, S., 2009. The protein kinase ImeB is required for light-mediated inhibition of sexual development and for mycotoxin production in *Aspergillus nidulans*. Mol. Microbiol. 71**,** 1278-1295.

Benoist, M., Gaillard, S., Castets, F., 2006. The striatin family: a new signaling platform in dendritic spines. J. Physiol. Paris. 99**,** 146-153.

Berepiki, A., Lichius, A., Shoji, J. Y., Tilsner, J., Read, N. D., 2010. F-actin dynamics in *Neurospora crassa*. Eukaryot. Cell. 9**,** 547-557.

Bergstrom, G. C., Nicholson, R. L., 1999. The biology of corn anthracnose - knowledge to exploit for improved management. Plant Disease. 83**,** 596-608.

Bernhards, Y., Pöggeler, S., 2011. The phocein homologue SmMOB3 is essential for vegetative cell fusion and sexual development in the filamentous ascomycete *Sordaria macrospora*. Curr. Genet. 57**,** 133-149.

Bloemendal, S., Lord, K. M., Rech, C., Hoff, B., Engh, I., Read, N. D., Kuck, U., 2010. A mutant defective in sexual development produces aseptate ascogonia. Eukaryot. Cell. 9**,** 1856-1866.

Blondeau, C., Gaillard, S., Ternaux, J. P., Monneron, A., Baude, A., 2003. Expression and distribution of phocein and members of the striatin family in neurones of rat peripheral ganglia. Histochem. Cell Biol. 119**,** 131-138.

Bourett, T. M., Howard, R. J., 1990. *In vitro* development of penetration structures in the rice blast fungus *Magnaporthe grisea*. Botany. 68**,** 329-342

Bourett, T. M., Howard, R. J., 1992. Actin in penetration pegs of the fungal rice blast pathogen, *Magnaporthe grisea*. Protoplasma. 168**,** 20-26.

Bowman, B. J., Draskovic, M., Freitag, M., Bowman, E. J., 2009. Structure and distribution of organelles and cellular location of calcium transporters in *Neurospora crassa*. Eukaryot. Cell. 8**,** 1845-1855.

Braus, G. H., Krappmann, S., Eckert, S. E., 2002. Sexual development in ascomycetes: Fruit body formation of *Aspergillus nidulans*, In: H. D. Osiewacz (Ed.), Molecular Biology of Fungal Development. Marcel Dekker, New York, pp. 215-244.

Breitman, M., Zilberberg, A., Caspi, M., Rosin-Arbesfeld, R., 2008. The armadillo repeat domain of the APC tumor suppressor protein interacts with Striatin family members. Biochim. Biophys. Acta. 1783**,** 1792-1802.

Bretscher, A., 2003. Polarized growth and organelle segregation in yeast: the tracks, motors, and receptors. J. Cell Biol. 160**,** 811-816.

Brooker, N. L., Leslie, J. F., Dickman, M. B., 1991. Nitrate non-utilizing mutants of *Colletotrichum* and their use in studies of vegetative compatibility and genetic relatedness. . Phytopathology. 81**,** 672-677.

Castets, F., Bartoli, M., Barnier, J. V., Baillat, G., Salin, P., Moqrich, A., Bourgeois, J. P., Denizot, F., Rougon, G., Calothy, G., Monneron, A., 1996. A novel calmodulin-binding protein, belonging to the WD-repeat family, is localized in dendrites of a subset of CNS neurons. J. Cell Biol. 134**,** 1051-1062.

Castets, F., Rakitina, T., Gaillard, S., Moqrich, A., Mattei, M. G., Monneron, A., 2000. Zinedin, SG2NA, and striatin are calmodulin-binding, WD repeat proteins principally expressed in the brain. J. Biol. Chem. 275**,** 19970-19977.

Catlett, N. L., Lee, B. N., Yoder, O. C., Turgeon, B. G., 2002. Split-marker recombination for efficient targeted deletion of fungal genes. Fungal Genet. Newsl. 50**,** 9-11.

Champe, S. P., Nagle, D. L., Yager, L. N., 1994. Sexual sporulation, In: S. D. Martinelli, J. R. Kinghorn (Eds.), *Aspergillus*: 50 Years On. Elsevier, Amsterdam, Netherlands, pp. 429-454.

Chen, H. W., Marinissen, M. J., Oh, S. W., Chen, X., Melnick, M., Perrimon, N., Gutkind, J. S., Hou, S. X., 2002. CKA, a novel multidomain protein, regulates the JUN N-terminal kinase signal transduction pathway in *Drosophila*. Mol. Cell. Biol. 22**,** 1792-1803.

Cho, Y., Cramer, R. A., Jr., Kim, K. H., Davis, J., Mitchell, T. K., Figuli, P., Pryor, B. M., Lemasters, E., Lawrence, C. B., 2007. The *Fus3/Kss1* MAP kinase homolog *Amk1* regulates the expression of genes encoding hydrolytic enzymes in *Alternaria brassicicola*. Fungal Genet. Biol. 44**,** 543-553.

Chung, D. W., Greenwald, C., Upadhyay, S., Ding, S., Wilkinson, H. H., Ebbole, D. J., Shaw, B. D., 2011. *acon-3*, the *Neurospora crassa* ortholog of the developmental modifier, *medA*, complements the conidiation defect of the *Aspergillus nidulans* mutant. Fungal Genet. Biol. 48**,** 370-376.

Cohen, P., 1989. The structure and regulation of protein phosphatases. Annu. Rev. Biochem. 58**,** 453-508.

Correll, J. C., Klittich, C. J. R., Leslie, J. F., 1987. Nitrate nonutilizing mutants of *Fusarium oxysporum* and their use in vegetative compatibility tests. Phytopathology. 77**,** 1640-1646.

Correll, J. C., Klittich, C. J. R., Leslie, J. F., 1989. Heterokaryon self-incompatibility in *Gibberella fujikuroi* (*Fusarium moniliforme*). Mycol. Res. 93**,** 21-27.

Craven, K. D., Velez, H., Cho, Y., Lawrence, C. B., Mitchell, T. K., 2008. Anastomosis is required for virulence of the fungal necrotroph *Alternaria brassicicola*. Eukaryot. Cell. 7**,** 675-683.

Dadgostar, H., Cheng, G., 2000. Membrane localization of TRAF 3 enables JNK activation. J. Biol. Chem. 275**,** 2539-2544.

Delgado-Alvarez, D. L., Callejas-Negrete, O. A., Gomez, N., Freitag, M., Roberson, R. W., Smith, L. G., Mourino-Perez, R. R., 2010. Visualization of F-actin localization and dynamics with live cell markers in *Neurospora crassa*. Fungal Genet. Biol. 47**,** 573-586.

Di Pietro, A., Garcia-MacEira, F. I., Meglecz, E., Roncero, M. I., 2001. A MAP kinase of the vascular wilt fungus *Fusarium oxysporum* is essential for root penetration and pathogenesis. Mol. Microbiol. 39**,** 1140-1152.

Era, A., Tominaga, M., Ebine, K., Awai, C., Saito, C., Ishizaki, K., Yamato, K. T., Kohchi, T., Nakano, A., Ueda, T., 2009. Application of Lifeact reveals F-actin dynamics in *Arabidopsis thaliana* and the liverwort, *Marchantia polymorpha*. Plant Cell Physiol. 50**,** 1041-1048.

Evangelista, M., Pruyne, D., Amberg, D. C., Boone, C., Bretscher, A., 2002. Formins direct Arp2/3-independent actin filament assembly to polarize cell growth in yeast. Nat. Cell Biol. 4**,** 260-269.

Fehrenbacher, K. L., Yang, H. C., Gay, A. C., Huckaba, T. M., Pon, L. A., 2004. Live cell imaging of mitochondrial movement along actin cables in budding yeast. Curr. Biol. 14**,** 1996-2004.

Felenbok, B., 1991. The ethanol utilization regulon of *Aspergillus nidulans*: the *alcA-alcR* system as a tool for the expression of recombinant proteins. J. Biotechnol. 17**,** 11-17.

Fischer-Parton, S., Parton, R. M., Hickey, P. C., Dijksterhuis, J., Atkinson, H. A., Read, N. D., 2000. Confocal microscopy of FM4-64 as a tool for analysing endocytosis and vesicle trafficking in living fungal hyphae. J. Microsc. 198**,** 246-259.

Flipphi, M., Kocialkowska, J., Felenbok, B., 2003. Relationships between the ethanol utilization (*alc*) pathway and unrelated catabolic pathways in *Aspergillus nidulans*. Eur. J. Biochem. 270**,** 3555-3564.

Gaillard, S., Bailly, Y., Benoist, M., Rakitina, T., Kessler, J. P., Fronzaroli-Molinieres, L., Dargent, B., Castets, F., 2006. Targeting of proteins of the striatin family to dendritic spines: role of the coiled-coil domain. Traffic. 7**,** 74-84.

Gaillard, S., Bartoli, M., Castets, F., Monneron, A., 2001. Striatin, a calmodulin-dependent scaffolding protein, directly binds caveolin-1. FEBS Lett. 508**,** 49-52.

Gatch, E. W., Hellmich, R. L., Munkvold, G. P., 2002. A comparison of maize stalk rot occurrence in Bt and non-Bt hybrids. Plant Disease. 86**,** 1149-1155.

Gatch, E. W., Munkvold, G. P., 2002. Fungal species composition in maize stalks in relation to European corn borer injury and transgenic insect protection. Plant Disease. 86**,** 1156-1162.

Gavin, A. C., Bosche, M., Krause, R., Grandi, P., Marzioch, M., Bauer, A., Schultz, J., Rick, J. M., Michon, A. M., Cruciat, C. M., Remor, M., Hofert, C., Schelder, M., Brajenovic, M., Ruffner, H., Merino, A., Klein, K., Hudak, M., Dickson, D., Rudi, T., Gnau, V., Bauch, A., Bastuck, S., Huhse, B., Leutwein, C., Heurtier, M. A., Copley, R. R., Edelmann, A., Querfurth, E., Rybin, V., Drewes, G., Raida, M., Bouwmeester, T., Bork, P., Seraphin, B., Kuster, B., Neubauer, G., Superti-Furga, G., 2002. Functional organization of the yeast proteome by systematic analysis of protein complexes. Nature. 415**,** 141-147.

Godoy, G., Steadman, J. R., Dickman, M. B., Dam, R., 1990. Use of mutants to demonstrate the role of oxalic acid in pathogenicity of *Sclerotinia sclerotiorum* on *Phaseolus vulgaris*. Physiol. Mol. Plant Pathol. 37**,** 179-191.

Goudreault, M., D'Ambrosio, L. M., Kean, M. J., Mullin, M. J., Larsen, B. G., Sanchez, A., Chaudhry, S., Chen, G. I., Sicheri, F., Nesvizhskii, A. I., Aebersold, R., Raught, B., Gingras, A. C., 2009. A PP2A phosphatase high density interaction network identifies a novel striatin-interacting phosphatase and kinase complex linked to the cerebral cavernous malformation 3 (CCM3) protein. Mol. Cell. Proteomics. 8**,** 157-171.

Halaban, R., Svedine, S., Cheng, E., Smicun, Y., Aron, R., Hebert, D. N., 2000. Endoplasmic reticulum retention is a common defect associated with tyrosinase-negative albinism. Proc. Natl. Acad. Sci. USA. 97**,** 5889-5894.

Han, K. H., Han, K. Y., Yu, J. H., Chae, K. S., Jahng, K. Y., Han, D. M., 2001. The *nsdD* gene encodes a putative GATA-type transcription factor necessary for sexual development of *Aspergillus nidulans*. Mol. Microbiol. 41**,** 299-309.

Harris, S. D., Morrell, J. L., Hamer, J. E., 1994. Identification and characterization of *Aspergillus nidulans* mutants defective in cytokinesis. Genetics. 136**,** 517-532.

Hinnebusch, A. G., 1997. Translational regulation of yeast *GCN4*. A window on factors that control initiator-tRNA binding to the ribosome. J. Biol. Chem. 272**,** 21661-21664.

Hinnebusch, A. G., Natarajan, K., 2002. Gcn4p, a master regulator of gene expression, is controlled at multiple levels by diverse signals of starvation and stress. Eukaryot. Cell. 1**,** 22-32.

Ho, Y., Gruhler, A., Heilbut, A., Bader, G. D., Moore, L., Adams, S. L., Millar, A., Taylor, P., Bennett, K., Boutilier, K., Yang, L., Wolting, C., Donaldson, I.,

Schandorff, S., Shewnarane, J., Vo, M., Taggart, J., Goudreault, M., Muskat, B., Alfarano, C., Dewar, D., Lin, Z., Michalickova, K., Willems, A. R., Sassi, H., Nielsen, P. A., Rasmussen, K. J., Andersen, J. R., Johansen, L. E., Hansen, L. H., Jespersen, H., Podtelejnikov, A., Nielsen, E., Crawford, J., Poulsen, V., Sorensen, B. D., Matthiesen, J., Hendrickson, R. C., Gleeson, F., Pawson, T., Moran, M. F., Durocher, D., Mann, M., Hogue, C. W., Figeys, D., Tyers, M., 2002. Systematic identification of protein complexes in *Saccharomyces cerevisiae* by mass spectrometry. Nature. 415**,** 180-183.

Hoffmann, B., Wanke, C., Lapaglia, S. K., Braus, G. H., 2000. c-Jun and RACK1 homologues regulate a control point for sexual development in *Aspergillus nidulans*. Mol. Microbiol. 37**,** 28-41.

Hou, X. S., Goldstein, E. S., Perrimon, N., 1997. *Drosophila* Jun relays the Jun amino-terminal kinase signal transduction pathway to the decapentaplegic signal transduction pathway in regulating epithelial cell sheet movement. Genes Dev. 11**,** 1728-1737.

Howard, R. J., 1997. Breaching the outer barriers—cuticle and cell wall penetration, In: G. Carroll, P. Tudzynski (Eds.), The Mycota V, Plant Relationships. Springer-Verlag, New York, pp. 43-60.

Howard, R. J., Valent, B., 1996. Breaking and entering: host penetration by the fungal rice blast pathogen *Magnaporthe grisea*. Annu. Rev. Microbiol. 50**,** 491-512.

Huckaba, T. M., Gay, A. C., Pantalena, L. F., Yang, H. C., Pon, L. A., 2004. Live cell imaging of the assembly, disassembly, and actin cable-dependent movement of

endosomes and actin patches in the budding yeast, *Saccharomyces cerevisiae*. J. Cell Biol. 167**,** 519-530.

Ito, T., Chiba, T., Ozawa, R., Yoshida, M., Hattori, M., Sakaki, Y., 2001. A comprehensive two-hybrid analysis to explore the yeast protein interactome. Proc. Natl. Acad. Sci. USA. 98**,** 4569-4574.

Janssens, V., Goris, J., 2001. Protein phosphatase 2A: a highly regulated family of serine/threonine phosphatases implicated in cell growth and signalling. Biochem. J. 353**,** 417-439.

Keller, N. P., Bergstrom, G. C., Carruthers, R. I., 1986. Potential yield reductions in maize associated with an anthracnose / European corn borer pest complex in New York. Phytopathology. 76**,** 586-589.

Kemp, H. A., Sprague, G. F., Jr., 2003. Far3 and five interacting proteins prevent premature recovery from pheromone arrest in the budding yeast *Saccharomyces cerevisiae*. Mol. Cell. Biol. 23**,** 1750-1763.

Kerppola, T. K., 2006. Design and implementation of bimolecular fluorescence complementation (BiFC) assays for the visualization of protein interactions in living cells. Nat. Protoc. 1**,** 1278-1286.

Khang, C. H., Berruyer, R., Giraldo, M. C., Kankanala, P., Park, S. Y., Czymmek, K., Kang, S., Valent, B., 2010. Translocation of *Magnaporthe oryzae* effectors into rice cells and their subsequent cell-to-cell movement. Plant Cell. 22**,** 1388-1403.

Kim, H., Han, K., Kim, K., Han, D., Jahng, K., Chae, K., 2002. The *veA* gene activates sexual development in *Aspergillus nidulans*. Fungal Genet. Biol. 37**,** 72-80.

Kim, H., Woloshuk, C. P., 2008. Role of *AREA*, a regulator of nitrogen metabolism, during colonization of maize kernels and fumonisin biosynthesis in *Fusarium verticillioides*. Fungal Genet. Biol. 45**,** 947-953.

Kim, J. S., Raines, R. T., 1993. Ribonuclease S-peptide as a carrier in fusion proteins. Protein Sci. 2**,** 348-356.

Kuo, K., Hoch, H. C., 1996. Germination of *Phyllosticta ampelicida* pycnidiospores: prerequisite of adhesion to the substratum and the relationship of substratum wettability. Fungal Genet. Biol. 20**,** 18-29.

Kwon, Y. H., Hoch, H. C., Staples, R. C., 1991. Cytoskeletal organization in *Uromyces* urediospore germling apices during appressorium formation. Protoplasma. 165**,** 37-50.

Lechward, K., Awotunde, O. S., Swiatek, W., Muszynska, G., 2001. Protein phosphatase 2A: variety of forms and diversity of functions. Acta Biochim. Pol. 48**,** 921-933.

Lee, S. C., Shaw, B. D., 2007. A novel interaction between N-myristoylation and the 26S proteasome during cell morphogenesis. Mol. Microbiol. 63**,** 1039-1053.

Li, D., Bobrowicz, P., Wilkinson, H. H., Ebbole, D. J., 2005. A mitogen-activated protein kinase pathway essential for mating and contributing to vegetative growth in *Neurospora crassa*. Genetics. 170**,** 1091-1104.

Liu, H. L., De Souza, C. P., Osmani, A. H., Osmani, S. A., 2009. The three fungal transmembrane nuclear pore complex proteins of *Aspergillus nidulans* are dispensable in the presence of an intact An-Nup84-120 complex. Mol. Biol. Cell. 20**,** 616-630.

Lu, Q., Pallas, D. C., Surks, H. K., Baur, W. E., Mendelsohn, M. E., Karas, R. H., 2004. Striatin assembles a membrane signaling complex necessary for rapid, nongenomic activation of endothelial NO synthase by estrogen receptor alpha. Proc. Natl. Acad. Sci. USA. 101**,** 17126-17131.

Lu, Q., Surks, H. K., Ebling, H., Baur, W. E., Brown, D., Pallas, D. C., Karas, R. H., 2003. Regulation of estrogen receptor alpha-mediated transcription by a direct interaction with protein phosphatase 2A. J. Biol. Chem. 278**,** 4639-4645.

Ma, H. L., Peng, Y. L., Gong, L., Liu, W. B., Sun, S., Liu, J., Zheng, C. B., Fu, H., Yuan, D., Zhao, J., Chen, P. C., Xie, S. S., Zeng, X. M., Xiao, Y. M., Liu, Y., Li, D. W., 2009. The goldfish SG2NA gene encodes two α-type regulatory subunits for PP-2A and displays distinct developmental expression pattern. Gene Regul. Syst. Bio. 3**,** 115-129.

Maerz, S., Dettmann, A., Ziv, C., Liu, Y., Valerius, O., Yarden, O., Seiler, S., 2009. Two NDR kinase-MOB complexes function as distinct modules during septum formation and tip extension in *Neurospora crassa*. Mol. Microbiol. 74**,** 707-723.

Maerz, S., Ziv, C., Vogt, N., Helmstaedt, K., Cohen, N., Gorovits, R., Yarden, O., Seiler, S., 2008. The nuclear Dbf2-related kinase COT1 and the mitogen-activated protein kinases MAK1 and MAK2 genetically interact to regulate filamentous growth, hyphal fusion and sexual development in *Neurospora crassa*. Genetics. 179**,** 1313-1325.

Maor, R., Puyesky, M., Horwitz, B. A., Sharon, A., 1998. Use of the green fluorescent protein (GFP) for studying development and fungal-plant interaction in *Cochliobolus heterostrophus*. . Mycol. Res. 102**,** 491-496.

McCluskey, K., 2003. The Fungal Genetics Stock Center: from molds to molecules. Adv. Appl. Microbiol. 52**,** 245-262.

Mims, C. W., Vaillancourt, L. J., 2002. Ultrastructural characterization of infection and colonization of maize leaves by *Colletotrichum graminicola*, and by a *C. graminicola* pathogenicity mutant. Phytopathology. 92**,** 803-812.

Moreno, C. S., Lane, W. S., Pallas, D. C., 2001. A mammalian homolog of yeast MOB1 is both a member and a putative substrate of striatin family-protein phosphatase 2A complexes. J. Biol. Chem. 276**,** 24253-24260.

Moreno, C. S., Park, S., Nelson, K., Ashby, D., Hubalek, F., Lane, W. S., Pallas, D. C., 2000. WD40 repeat proteins striatin and S/G(2) nuclear autoantigen are members of a novel family of calmodulin-binding proteins that associate with protein phosphatase 2A. J. Biol. Chem. 275**,** 5257-5263.

Moseley, J. B., Goode, B. L., 2006. The yeast actin cytoskeleton: from cellular function to biochemical mechanism. Microbiol. Mol. Biol. Rev. 70**,** 605-645.

Muimba-Kankolongo, A., Bergstrom, G. C., 2011. Reduced anthracnose stalk rot in resistant maize is associated with restricted development of *Colletotrichum graminicola* in pith tissues. J. Phytopathol. 159**,** 329-341.

Muro, Y., Chan, E. K., Landberg, G., Tan, E. M., 1995. A cell-cycle nuclear autoantigen containing WD-40 motifs expressed mainly in S and G2 phase cells. Biochem. Biophys. Res. Commun. 207**,** 1029-1037.

Nayak, T., Szewczyk, E., Oakley, C. E., Osmani, A., Ukil, L., Murray, S. L., Hynes, M. J., Osmani, S. A., Oakley, B. R., 2006. A versatile and efficient gene-targeting system for *Aspergillus nidulans*. Genetics. 172**,** 1557-1566.

Noselli, S., Agnes, F., 1999. Roles of the JNK signaling pathway in *Drosophila* morphogenesis. Curr. Opin. Genet. Dev. 9**,** 466-472.

Pöggeler, S., Kück, U., 2004. A WD40 repeat protein regulates fungal cell differentiation and can be replaced functionally by the mammalian homologue striatin. Eukaryot. Cell. 3**,** 232-240.

Paluh, J. L., Orbach, M. J., Legerton, T. L., Yanofsky, C., 1988. The cross-pathway control gene of *Neurospora crassa*, *cpc-1*, encodes a protein similar to *GCN4* of yeast and the DNA-binding domain of the oncogene *v-jun*-encoded protein. Proc. Natl. Acad. Sci. USA. 85**,** 3728-3732.

Panaccione, D. G., McKiernan, M., Hanau, R. M., 1988. *Colletotrichum graminicola* transformed with homologous and heterologous benomyl-resistance genes retains expected pathogenicity to corn. . Mol. Plant Microbe Interact. 1**,** 113-120.

Panaccione, D. G., Vaillancourt, L. J., Hanau, R. M., 1989. Conidial dimorphism in *Colletotrichum graminicola*. Mycologia. 81**,** 876-883.

Pandey, A., Roca, M. G., Read, N. D., Glass, N. L., 2004. Role of a mitogen-activated protein kinase pathway during conidial germination and hyphal fusion in *Neurospora crassa*. Eukaryot. Cell. 3**,** 348-358.

Pascual-Ahuir, A., Serrano, R., Proft, M., 2001. The Sko1p repressor and Gcn4p activator antagonistically modulate stress-regulated transcription in *Saccharomyces cerevisiae*. Mol. Cell. Biol. 21**,** 16-25.

Peñalva, M. A., 2005. Tracing the endocytic pathway of *Aspergillus nidulans* with FM4-64. Fungal Genet. Biol. 42**,** 963-975.

Polakis, P., 2000. Wnt signaling and cancer. Genes Dev. 14**,** 1837-1851.

Politis, D. J., 1975. The identity of the perfect state of *Colletotrichum graminicola*. Mycologia. 67**,** 56-62.

Politis, D. J., Wheeler, H., 1973. Ultrastructural study of penetration of maize leaves by *Colletotrichum graminicola*. Physiol. Plant Pathol. 3**,** 465-471.

Potts, J. T., Jr., Young, D. M., Anfinsen, C. B., 1963. Reconstitution of fully active RNase S by carboxypeptidase-degraded RNase S-peptide. J. Biol. Chem. 238**,** 2593-2594.

Prados Rosales, R. C., Di Pietro, A., 2008. Vegetative hyphal fusion is not essential for plant infection by *Fusarium oxysporum*. Eukaryot. Cell. 7**,** 162-171.

Prusky, D., Freeman, S., Dickman, M. B., 2000. *Colletotrichum*: Host Specificity, Pathology, and Host-Pathogen Interaction. APS Press, St. Paul, Minnesota.

Pruyne, D., Legesse-Miller, A., Gao, L., Dong, Y., Bretscher, A., 2004. Mechanisms of polarized growth and organelle segregation in yeast. Annu. Rev. Cell Dev. Biol. 20**,** 559-591.

Pruyne, D. W., Schott, D. H., Bretscher, A., 1998. Tropomyosin-containing actin cables direct the Myo2p-dependent polarized delivery of secretory vesicles in budding yeast. J. Cell Biol. 143**,** 1931-1945.

Punt, P. J., van den Hondel, C. A., 1992. Transformation of filamentous fungi based on hygromycin B and phleomycin resistance markers. Methods Enzymol. 216**,** 447-457.

Qi, X., Mochly-Rosen, D., 2008. The PKCdelta -Abl complex communicates ER stress to the mitochondria - an essential step in subsequent apoptosis. J. Cell Sci. 121**,** 804-813.

Rasmussen, C. G., Glass, N. L., 2007. Localization of RHO-4 indicates differential regulation of conidial versus vegetative septation in the filamentous fungus *Neurospora crassa*. Eukaryot. Cell. 6**,** 1097-1107.

Rasmussen, J. B., Panaccione, D. G., Fang, G. C., Hanau, R. M., 1992. The *PYR1* gene of the plant pathogenic fungus *Colletotrichum graminicola*: selection by intraspecific complementation and sequence analysis. Mol. Gen. Genet. 235**,** 74-80.

Razani, B., Woodman, S. E., Lisanti, M. P., 2002. Caveolae: from cell biology to animal physiology. Pharmacol. Rev. 54**,** 431-467.

Read, N. D., Fleißner, A., Roca, M. G., Glass, N. L., 2010. Hyphal fusion., In: K. A. Borkovich, D. J. Ebbole (Eds.), Cellular and Molecular Biology of Filamentous Fungi. American Society of Microbiology Press, Washington, DC, pp. 274-288.

Riedl, J., Crevenna, A. H., Kessenbrock, K., Yu, J. H., Neukirchen, D., Bista, M., Bradke, F., Jenne, D., Holak, T. A., Werb, Z., Sixt, M., Wedlich-Soldner, R., 2008. Lifeact: a versatile marker to visualize F-actin. Nat. Methods. 5**,** 605-607.

Riedl, J., Flynn, K. C., Raducanu, A., Gartner, F., Beck, G., Bosl, M., Bradke, F., Massberg, S., Aszodi, A., Sixt, M., Wedlich-Soldner, R., 2010. Lifeact mice for studying F-actin dynamics. Nat. Methods. 7**,** 168-169.

Riesgo-Escovar, J. R., Hafen, E., 1997. *Drosophila* Jun kinase regulates expression of decapentaplegic via the ETS-domain protein Aop and the AP-1 transcription factor DJun during dorsal closure. Genes Dev. 11**,** 1717-1727.

Roca, M. G., Arlt, J., Jeffree, C. E., Read, N. D., 2005. Cell biology of conidial anastomosis tubes in *Neurospora crassa*. Eukaryot. Cell. 4**,** 911-919.

Sagot, I., Klee, S. K., Pellman, D., 2002. Yeast formins regulate cell polarity by controlling the assembly of actin cables. Nat. Cell Biol. 4**,** 42-50.

Salin, P., Kachidian, P., Bartoli, M., Castets, F., 1998. Distribution of striatin, a newly identified calmodulin-binding protein in the rat brain: an in situ hybridization and immunocytochemical study. J. Comp. Neurol. 397**,** 41-59.

Sambrook, J., Russell, D. W., 2001. Molecular Cloning: A Laboratory Manual. Cold Spring Harbor Laboratory, Cold Spring Harbor, New York.

Schott, D. H., Collins, R. N., Bretscher, A., 2002. Secretory vesicle transport velocity in living cells depends on the myosin-V lever arm length. J. Cell Biol. 156**,** 35-39.

Seo, J. A., Han, K. H., Yu, J. H., 2004. The *gprA* and *gprB* genes encode putative G protein-coupled receptors required for self-fertilization in *Aspergillus nidulans*. Mol. Microbiol. 53**,** 1611-1623.

Serlupi-Crescenzi, O., Kurtz, M. B., Champe, S. P., 1983. Developmental defects resulting from arginine auxotrophy in *Aspergillus nidulans*. J. Gen. Microbiol. 129**,** 3535-3544.

Sharpless, K. E., Harris, S. D., 2002. Functional characterization and localization of the *Aspergillus nidulans* formin SEPA. Mol. Biol. Cell. 13**,** 469-479.

Shaw, B. D., Chung, D. W., Wang, C. L., Quintanilla, L. A., Upadhyay, S., 2011. A role for endocytic recycling in hyphal growth. Fungal Biol. 115**,** 541-546.

Shaw, B. D., Kuo, K. C., Hoch, H. C., 1998. Germination and appressorium development of *Phyllosticta ampelicida* pycnidiospores. Mycologia. 90**,** 258-268.

Shaw, B. D., Upadhyay, S., 2005. *Aspergillus nidulans swoK* encodes an RNA binding protein that is important for cell polarity. Fungal Genet. Biol. 42**,** 862-872.

Shim, W. B., Sagaram, U. S., Choi, Y. E., So, J., Wilkinson, H. H., Lee, Y. W., 2006. *FSR1* is essential for virulence and female fertility in *Fusarium verticillioides* and *F. graminearum*. Mol. Plant Microbe Interact. 19**,** 725-733.

Simonin, A. R., Rasmussen, C. G., Yang, M., Glass, N. L., 2010. Genes encoding a striatin-like protein (*ham-3*) and a forkhead associated protein (*ham-4*) are

required for hyphal fusion in *Neurospora crassa*. Fungal Genet. Biol. 47**,** 855-868.

Smith, T. F., Gaitatzes, C., Saxena, K., Neer, E. J., 1999. The WD repeat: a common architecture for diverse functions. Trends Biochem. Sci. 24**,** 181-185.

Sohn, K. T., Yoon, K. S., 2002. Ultrastructural study on the cleistothecium development in *Aspergillus nidulans*. Mycobiology. 30**,** 117-127.

Son, S., Osmani, S. A., 2009. Analysis of all protein phosphatase genes in *Aspergillus nidulans* identifies a new mitotic regulator, Fcp1. Eukaryot. Cell. 8**,** 573-585.

Stinnett, S. M., Espeso, E. A., Cobeno, L., Araujo-Bazan, L., Calvo, A. M., 2007. *Aspergillus nidulans* VeA subcellular localization is dependent on the importin alpha carrier and on light. Mol. Microbiol. 63**,** 242-255.

Suelmann, R., Sievers, N., Galetzka, D., Robertson, L., Timberlake, W. E., Fischer, R., 1998. Increased nuclear traffic chaos in hyphae of *Aspergillus nidulans*: molecular characterization of *apsB* and in vivo observation of nuclear behaviour. Mol. Microbiol. 30**,** 831-842.

Sukno, S. A., Garcia, V. M., Shaw, B. D., Thon, M. R., 2008. Root infection and systemic colonization of maize by *Colletotrichum graminicola*. Appl. Environ. Microbiol. 74**,** 823-832.

Taheri-Talesh, N., Horio, T., Araujo-Bazan, L., Dou, X., Espeso, E. A., Penalva, M. A., Osmani, S. A., Oakley, B. R., 2008. The tip growth apparatus of *Aspergillus nidulans*. Mol. Biol. Cell. 19**,** 1439-1449.

Tan, B., Long, X., Nakshatri, H., Nephew, K. P., Bigsby, R. M., 2008. Striatin-3 gamma inhibits estrogen receptor activity by recruiting a protein phosphatase. J. Mol. Endocrinol. 40**,** 199-210.

Toews, M. W., Warmbold, J., Konzack, S., Rischitor, P., Veith, D., Vienken, K., Vinuesa, C., Wei, H., Fischer, R., 2004. Establishment of mRFP1 as a fluorescent marker in *Aspergillus nidulans* and construction of expression vectors for high-throughput protein tagging using recombination in vitro (GATEWAY). Curr. Genet. 45**,** 383-389.

Tolliday, N., VerPlank, L., Li, R., 2002. Rho1 directs formin-mediated actin ring assembly during budding yeast cytokinesis. Curr. Biol. 12**,** 1864-1870.

Tsitsigiannis, D. I., Kowieski, T. M., Zarnowski, R., Keller, N. P., 2004. Endogenous lipogenic regulators of spore balance in *Aspergillus nidulans*. Eukaryot. Cell. 3**,** 1398-1411.

Uetz, P., Giot, L., Cagney, G., Mansfield, T. A., Judson, R. S., Knight, J. R., Lockshon, D., Narayan, V., Srinivasan, M., Pochart, P., Qureshi-Emili, A., Li, Y., Godwin, B., Conover, D., Kalbfleisch, T., Vijayadamodar, G., Yang, M., Johnston, M., Fields, S., Rothberg, J. M., 2000. A comprehensive analysis of protein-protein interactions in *Saccharomyces cerevisiae*. Nature. 403**,** 623-627.

Upadhyay, S., Shaw, B. D., 2006. A phosphoglucose isomerase mutant in *Aspergillus nidulans* is defective in hyphal polarity and conidiation. Fungal Genet. Biol. 43**,** 739-751.

Upadhyay, S., Shaw, B. D., 2008. The role of actin, fimbrin and endocytosis in growth of hyphae in *Aspergillus nidulans*. Mol. Microbiol. 68**,** 690-705.

Utsugi, T., Minemura, M., Hirata, A., Abe, M., Watanabe, D., Ohya, Y., 2002. Movement of yeast 1,3-beta-glucan synthase is essential for uniform cell wall synthesis. Genes Cells. 7**,** 1-9.

Vaillancourt, L. J., Hanau, R. D., 1994. Nitrate-nonutilizing mutants used to study heterokaryosis and vegetative compatibility in *Glomerella graminicola* (*Colletotrichum graminicola*). Exp. Mycol. 18**,** 311-319.

Vaillancourt, L. J., Hanau, R. M., 1991. A method for genetic analysis of *Glomerella graminicola* (*Colletotrichum graminicola*) from maize. Phytopathology. 81**,** 530-534.

Vallim, M. A., Miller, K. Y., Miller, B. L., 2000. *Aspergillus* SteA (sterile12-like) is a homeodomain-C2/H2-Zn+2 finger transcription factor required for sexual reproduction. Mol. Microbiol. 36**,** 290-301.

Veith, D., Scherr, N., Efimov, V. P., Fischer, R., 2005. Role of the spindle-pole-body protein ApsB and the cortex protein ApsA in microtubule organization and nuclear migration in *Aspergillus nidulans*. J. Cell Sci. 118**,** 3705-3716.

Venard, C., Kulshrestha, S., Sweigard, J., Nuckles, E., Vaillancourt, L., 2008. The role of a *fadA* ortholog in the growth and development of *Colletotrichum graminicola in vitro* and *in planta*. Fungal Genet. Biol. 45**,** 973-983.

Venard, C., Vaillancourt, L., 2007a. Colonization of fiber cells by *Colletotrichum graminicola* in wounded maize stalks. Phytopathology. 97**,** 438-447.

Venard, C., Vaillancourt, L., 2007b. Penetration and colonization of unwounded maize tissues by the maize anthracnose pathogen *Colletotrichum graminicola* and the related nonpathogen *C. sublineolum*. Mycologia. 99**,** 368-377.

Vienken, K., Fischer, R., 2006. The Zn(II)2Cys6 putative transcription factor NosA controls fruiting body formation in *Aspergillus nidulans*. Mol. Microbiol. 61**,** 544-554.

Vienken, K., Scherer, M., Fischer, R., 2005. The Zn(II)2Cys6 putative *Aspergillus nidulans* transcription factor repressor of sexual development inhibits sexual development under low-carbon conditions and in submersed culture. Genetics. 169**,** 619-630.

Vogel, H. J., 1964. Distribution of lysine pathways among fungi: evolutionary implications. Am. Nat. 98**,** 435-446.

Walker, J., 1972. Type studies of *Gaeumannomyces graminis* and related fungi. Trans. Br. Mycol. Soc. 58**,** 427-457.

Wang, C. L., Shim, W. B., Shaw, B. D., 2009. Assessing the roles of striatin orthologs in fungal growth, development and virulence. Fungal Genet. Rep. 56**,** Supplement 324.

Watanabe, T., Matsuo, I., Maruyama, J., Kitamoto, K., Ito, Y., 2007. Identification and characterization of an intracellular lectin, calnexin, from *Aspergillus oryzae* using N-glycan-conjugated beads. Biosci. Biotechnol. Biochem. 71**,** 2688-2696.

Wedlich-Soldner, R., Schulz, I., Straube, A., Steinberg, G., 2002. Dynein supports motility of endoplasmic reticulum in the fungus *Ustilago maydis*. Mol. Biol. Cell. 13**,** 965-977.

Wei, H., Requena, N., Fischer, R., 2003. The MAPKK kinase SteC regulates conidiophore morphology and is essential for heterokaryon formation and sexual development in the homothallic fungus *Aspergillus nidulans*. Mol. Microbiol. 47**,** 1577-1588.

Williams, T. M., Lisanti, M. P., 2004. The caveolin proteins. Genome Biol. 5**,** 214.

Yamamura, Y., Shim, W. B., 2008. The coiled-coil protein-binding motif in *Fusarium verticillioides Fsr1* is essential for maize stalk rot virulence. Microbiology. 154**,** 1637-1645.

Yang, H. C., Pon, L. A., 2002. Actin cable dynamics in budding yeast. Proc. Natl. Acad. Sci. USA. 99**,** 751-756.

Yang, L., Ukil, L., Osmani, A., Nahm, F., Davies, J., De Souza, C. P., Dou, X., Perez-Balaguer, A., Osmani, S. A., 2004. Rapid production of gene replacement constructs and generation of a green fluorescent protein-tagged centromeric marker in *Aspergillus nidulans*. Eukaryot. Cell. 3**,** 1359-1362.

Yelton, M. M., Hamer, J. E., Timberlake, W. E., 1984. Transformation of *Aspergillus nidulans* by using a *trpC* plasmid. Proc. Natl. Acad. Sci. USA. 81**,** 1470-1474.

Yin, H., Pruyne, D., Huffaker, T. C., Bretscher, A., 2000. Myosin V orientates the mitotic spindle in yeast. Nature. 406**,** 1013-1015.

Yu, J. H., Hamari, Z., Han, K. H., Seo, J. A., Reyes-Dominguez, Y., Scazzocchio, C., 2004. Double-joint PCR: a PCR-based molecular tool for gene manipulations in filamentous fungi. Fungal Genet. Biol. 41**,** 973-981.

APPENDIX A

DYNAMICS OF F-ACTIN IN *Colletotrichum graminicola* DURING APPRESSORIA AND HYPHOPODIA FORMATION

SUMMARY

Appressoria and hyphopodia are essential for penetration of the host by *Colletotrichum graminicola*, the pathogen of maize stalk rot and leaf anthracnose. To visualize F-actin dynamics in appressoria and hyphopodia, I expressed Lifeact-GFP in a *C. graminicola* wild-type strain. Lifeact, a 17-amino acid peptide, is able to bind F-actin in many living eukaryotic cells. Lifeact-GFP was an effective marker for Spitzenkörper and actin pathes dynamics at hyphal tips, actin rings during septation, and actin cables within hyphae of *C. graminicola*. The retrograde movement of actin cables from the tips of germlings back to the sub-apical region was consistently displayed during germ tube elongation, appressorium formation and hyphopodia development. The concentrated actin cable meshwork was located at the apex of the cell during germ tube emergence. The actin cables shifted to the site of septation during cytokinesis and then redistributed back to the developing cell during appressorium formation. Before penetration, the dynamic actin cables formed a ring and then concentrated in a circle at the penetration pore. F-actin was abundant at the tip of penetration pegs during penetration. Actin cables and actin patches were present at the apex of the swollen invasive hyphae. A time course of hyphopodial development also implicated a similar F-actin dynamic pattern as that displayed during appressorial development.

INTRODUCTION

Appressoria and hyphopodia are specialized penetration structures of phytopathogenic fungi. The rice blast pathogen, *Magnaporthe oryzae*, the grape black rot pathogen, *Phyllostica ampelicida*, and the anthracnose pathogens, *Colletotrichum spp*., infect plant cells mainly through the appressoria (Bergstrom and Nicholson, 1999; Howard and Valent, 1996; Prusky et al., 2000; Shaw et al., 1998). The take-all fungus, *Gaeumannomyces graminis*, penetrates its host using hyphopodia (Walker, 1972). *C. graminicola*, the pathogen of corn stalk rot and leaf anthracnose, infects roots of its host by utilizing through hyphopodia (Sukno et al., 2008). *C. graminicola* appressoria contain lipid bodies, glycogen, ribosomes, small vacuoles, mitochondria and a single nucleus, and are surrounded by an electron-dense wall (Politis and Wheeler, 1973). Once contact is made with the plant epidermal cells, an inner electron translucent wall is deposited around the face of the appressorium that makes contact with the surface. The electron-dense outer wall in contact with the host cell then disappears resulting in a direct contact between the electron translucent wall of the appressoirum and the plant cell wall. The penetration peg develops in this area of direct contact, and breaches the plant cell wall to form the swollen invasive hyphae. Unlike other species of *Colletotrichum*, *C. graminicola* does not contain the appressorial cone surrounding the site of penetration pegs (Mims and Vaillancourt, 2002; Politis and Wheeler, 1973).

Actin is present in cells as monomeric actin and polymeric actin. F-actin is the polymerized form of the monomeric actin. Three types of F-actin containing structures are observed in fungal cells: actin pathches, actin cables, and actin rings (Moseley and

Goode, 2006). Actin patches are endocytic sites or endocytic vesicles surrounded by F-actin (Araujo-Bazan et al., 2008; Huckaba et al., 2004; Shaw et al., 2011; Upadhyay and Shaw, 2008). Actin cables are bundles of F-actin and serve as tracks for type V myosin-dependent organelle transportation and secretory vesicles movements, and myosin-independent movements (Bretscher, 2003; Fehrenbacher et al., 2004; Pruyne et al., 2004; Schott et al., 2002; Utsugi et al., 2002; Yin et al., 2000). Actin rings are involved in septum formation in filamentous fungi, and cytokinesis in budding yeast (Harris et al., 1994; Moseley and Goode, 2006; Rasmussen and Glass, 2007). F-actin is visualized at these sites of cellular morphogenesis and at polarization sites in yeast cell budding, hyphal growth, and germ tube elongation (Berepiki et al., 2010; Delgado-Alvarez et al., 2010; Yang and Pon, 2002). Actin is also involved in the differentiation of appressoria. The rhodamine-conjugated phalloidin treatment revealed that actin cables and actin patches responded to the inductive ridge to change distribution and orientation during the formation of appressoria of *Uromyces appendiculatus* (Kwon et al., 1991). Immuno-fluorescence with anti-actin monoclonal antibody labeled a bright point of localization at the site of penetration pegs, and filaments and 'plaques' of ca. 300 nm in diameter surrounding with penetration pegs of the sonicated appressoria of *M. oryzae* (Bourett and Howard, 1992). However, little is known how actin behaves in live cells in appressoria.

The methods of immunolabeling and rhodamine-conjugated pholloidin staining require the fixation of cells that may alter the organization of F-actin and make it impossible to visualize the dynamics of F-actin in live cells. Fluorescent proteins have been tagged on monomeric actin to visualize the dynamics of F-actin. The GFP-tagged

actin in *Aspergillus nidulans* revealed the dynamics of actin patches in hyphal tips (Taheri-Talesh et al., 2008; Upadhyay and Shaw, 2008). However, these ActA::GFP construct did not label actin cables. Here, I used Lifeact-GFP to visualize the dynamics of F-actin during the development of appressoria and hyphopodia of *Colletotrichum graminicola*. Lifeact is a 17-amino acid peptide derived from the Abp140p (actin binding protein 140) of *Saccharomyces cerevisiae* (Riedl et al., 2008). It has been used to visualize F-actin in other model organisms such as *Arabidopsis thaliana* (Era et al., 2009), *N. crassa* (Berepiki et al., 2010; Delgado-Alvarez et al., 2010), mice (Riedl et al., 2010), and human cell lines (Riedl et al., 2008). In *N. crassa*, comparisons between Lifeact-GFP and other three actin binding proteins (homologs of fimbrin, tropomyosin, and Arp2/3 complex) concluded that Lifeact-GFP not only co-localized with these actin binding proteins, but also labeled the broadest spectrum of F-actin among them (Delgado-Alvarez et al., 2010). Similar to previous studies of F-actin structures and dynamic patterns in filamentous fungi, the *C. graminicola* Lifeact-GFP strains also demonstrate actin patches, actin cables, and actin rings during the hyphal growth, and the dynamic actin patch pattern at the actively growing hyphal tips. Therefore, I used these strains to further visualize F-actin dynamics during appressoria and hyphopodia development.

MATERIALS AND METHODS

Strains and transformation

The *Collectotrichum graminicola* Lifeact-GFP strains generated from this study were derived from the wild-type strain M1.001 (a gift from Dr. Lisa Vaillancourt, University of Kentucky). A Lifeact-GFP plasmid, pAB221 (Berepiki et al., 2010), containing the *ccg1*(p)::Lifeact::C-Gly::GFP construct was co-transformed with pBP15 (Li et al., 2005) containing *hph* gene into strain M1.001. The fungal transformation was preformed as a previously described (Panaccione et al., 1988; Rasmussen et al., 1992). Several candidates that expressed the Lifeact-GFP were acquired and compared with the wild-type strain for growth characteristics. A strain that was comparable wild-type in phenotype and expressed a strong Lifeact-GFP signal was chosen for subsequent studies and named CgAB221-17.

Imaging F-actin in living cells

Falcate conidia were harvested from 2-week-old PDA (potato dextrose agar) cultures incubated at room temperature under continuous light. The conidia suspension was rinsed with sterile water twice before concentrating to 10^4 conidia / ml. To visualize F-actin during hyphal tip growth, conidia were inoculated on a thin layer of Vogle's medium (Vogel, 1964) to avoid the autofluorescence of PDA. After a colony established, a rectangle agar block from the leading edge of the colony was excised and placed on a glass slide for documentation of hyphal growth. To visualize F-actin during appressorium formation, falcate conidia were suspended with sterile water and incubated

on glass cover slips in an aluminum growth chamber as previously described (Kuo and Hoch, 1996; Upadhyay and Shaw, 2006). For induction of hyphopodia, falcate conidia were suspended in liquid Vogel's medium and incubated on a glass cover slide in an aluminum growth chamber. For *in planta* observation, onion epidermal sections of 1 cm^2 from a white onion were peeled from the inner side of scales, and floated on sterile water in a 24-well culture plate. A 10 ul drop of falcate conidial suspension (10^4 conidia / ml) was inoculated on each onion epidermal sheet and incubated at 28°C under continuous light.

Microscopy

Microscopic images were obtained using an Olympus BX51 microscope (Olympus America, Melville, NY, USA) outfitted for wide field fluorescent imaging system and a motorized stage for imaging along the Z-axis. Fluorescent images were taken with a Hamamatsu Orca-ER cooled CCD camera (Hamamatsu, Japan) interfaced with Simple PCI software (Version 5.3.1.081004) (Compix, Imaging Systems, Cranberry Township, PA) that allowed us to acquire time lapsed images and controlled a Prior shutter (Prior Scientific, Rockland, MA, USA) to limit phototoxicity to the cells. The Olympus U-MNIBA2 (Olympus) filter cube containing a dichroic mirror at 505 nm was applied to visualize GFP signal by generating excitation wavelengths from 470 to 480 nm, and emission wavelengths from 510 to 550 nm. Bright field images were acquired from an Olympus DP70 camera interfaced to DP70-BSW software (version 01. 01). Adobe Photoshop version 7.0.1 (Adobe, Mountain View, CA, USA) was used to

compose images for publication.

RESULTS AND DISCUSSION

Lifeact-GFP in hyphal growth and septation

The dynamics of F-actin in hyphal tips have been well documented in *N. crassa* and *A. nidulans* by tagging GFP on actin binding proteins. At hyphal tips, F-actin aggregates in the Spitzenkörper, a vesicle-rich area at the apex of actively growing hyphae. Behind the Spitzenkörper, the F-actin patches enrich at a sub-apical area of hyphae and form a subapical collar (Araujo-Bazan et al., 2008; Berepiki et al., 2010; Delgado-Alvarez et al., 2010; Shaw et al., 2011; Taheri-Talesh et al., 2008; Upadhyay and Shaw, 2008). Considering the functions of actin patches in endocytosis and of the Spitzenkörper in vesicle secretion, these studies proposed an 'Apical Recycling Model' to account for the complementary relationship between exocytosis and endocytosis to support active hyphal growth. As shown in Figure A.1 A, Lifeact-GFP in *C. graminicola* also demonstrated a similar dynamic pattern. The bright F-actin focal point in front of the subapical actin patch collar was presumed as a Spitzenkörper. When the hyphae ceased growing, the Spitzenkörper and the subapical collar disappeared, which is consistent with the notion that Spitzenkörper and sub-apical collar were required for hyphal growth. The dynamic movements of actin cables parallel to hyphae and actin patches localized in cortical region of hyphae are also apparent. This localization pattern of F-actin is revealed in filamentous fungi by immunofluorescence labeling (Araujo-Bazan et al., 2008; Harris et al., 1994; Kwon et al., 1991). Similar to other previous F-

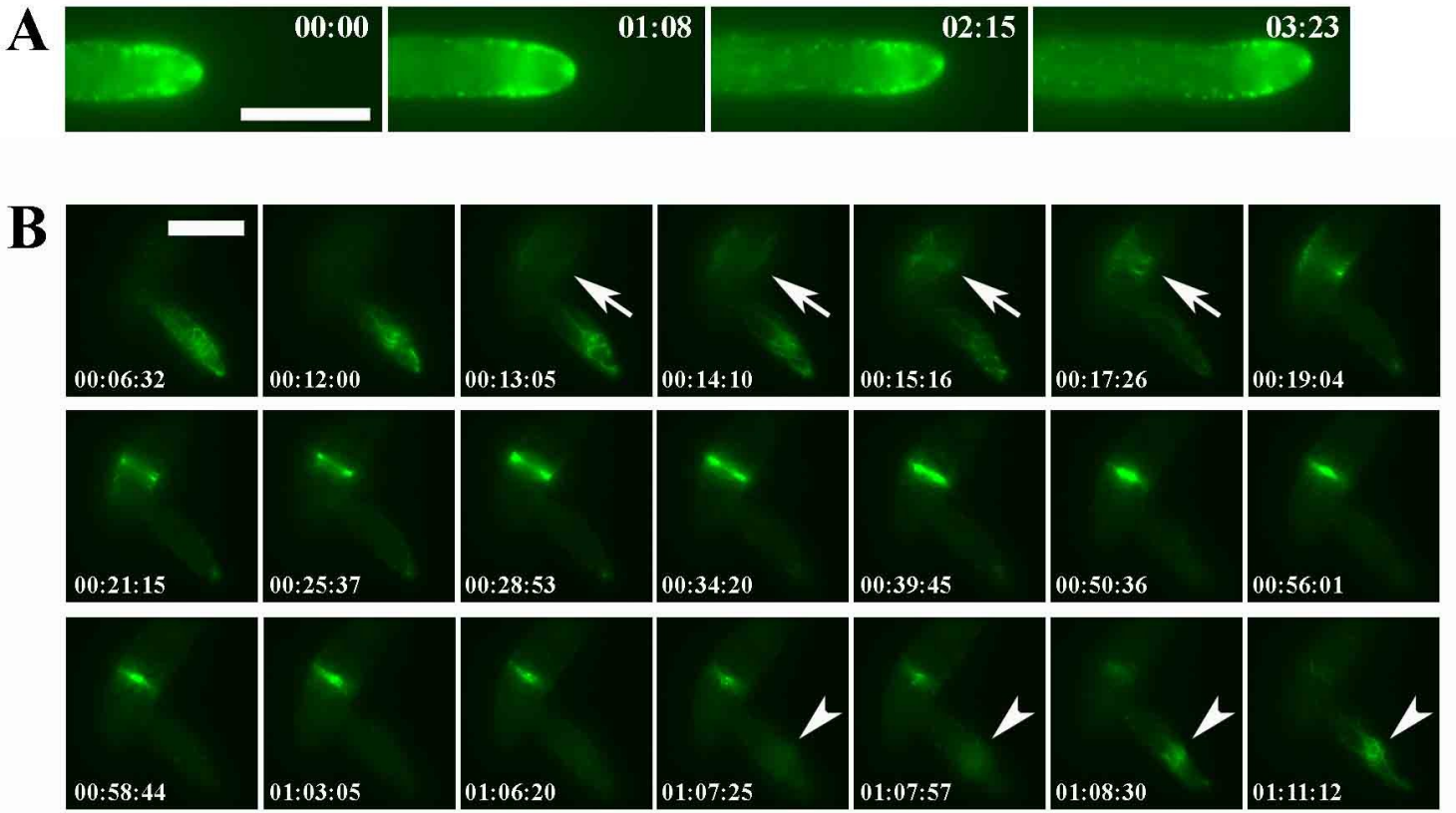

Figure A.1 Dynamics of Lifeact-GFP labeled F-actin during active hyphal growth and septation.
(A) Lifeact-GFP labeled the Spitzenkörper at the apex of a hypha and actin patches that formed a sub-apical collar. (B) Lifeact-GFP labeled actin cables during septum formation in a germling. Several actin cables appeared initially and then condensed at the septation site (arrow). The bright Lifeact-GFP signal indicated the actin contractile ring formed from the sides centripetally toward the center of a hypha. After completion of the the septum the actin cables gradually reform near the apex of the germ tube (arrowhead). Bar = 10 um.

actin studies with Lifeact-GFP (Berepiki et al., 2010; Delgado-Alvarez et al., 2010), this *C. graminicola* Lifeact-GFP also displayed F-actin rings that transiently appeared at the site of septum formation. As shown in a germling, several actin cables gradually appeared around the site of a future septum, and then incorporated to form the contractile ring at the septation site. At the initial stage of septation, the Lifeact-GFP intensely localized at the sides of cell wall, and then extended toward the center of hyphae to form a plate. The plate was split into two thinner layers before dissipating from the sides of a mature septum. The whole processes of septation took around 40- 60 mins (Figure A.1 B). These data indicated that the Lifeact-GFP properly demonstrated the dynamics of F-actin in *C. graminicola*.

F-actin dynamics during appressorial and hyphopodial differentiation

To document the dynamics of F-actin during appressorium formation, Lifeact-GFP was visualized in growing germlings through appressorium formation. Prominent actin cables and patches formed in elongating germ tubes, but were less intense in the conidium. In contrast to the Spitzenkörper based localization at hyphal tips, actin cables form an extensive network at the apex of germlings that displayed a retrograde movement from the tips of the germ tubes along cortex toward the conidium. This meshwork gradually disappated as it moved distal to the tip. After a period of elongation, the sub-apical area of germ tube swelled during elongation and the actin cables continued to display the retrograde movement (Figure A.2 A). Once the shape of appressoria was formed, actin cables began to dissipate. A less defined Lifeact-GFP

Figure A.2 Dynamics of F-actin during appressorium formation.
(A) Actin cables displaying retrograde movement were the major actin structure during germ tube elongation and appressorial enlargement. A Lifeact-GFP signal shifted from the appressoria to the septation site along the periphery of the appressorium (arrows). F-actin then localized to the site of cytokinesis. After spetum formation was complete F-actin again redistributed back into the appressorium. (B) Another germling followed from spetum formation to completion of appressorium development. Following a long quiescent period, a slight increase in the intensity of Lifeact-GFP signal appeared in the central area of appressoria (arrow heads) before actin cables became discernable. A ring formed in the center of the appressorium at the penetration pore. After the fluorescent imaging, this appressorium continued to deposite melanin overnight. Bar = 10 um.

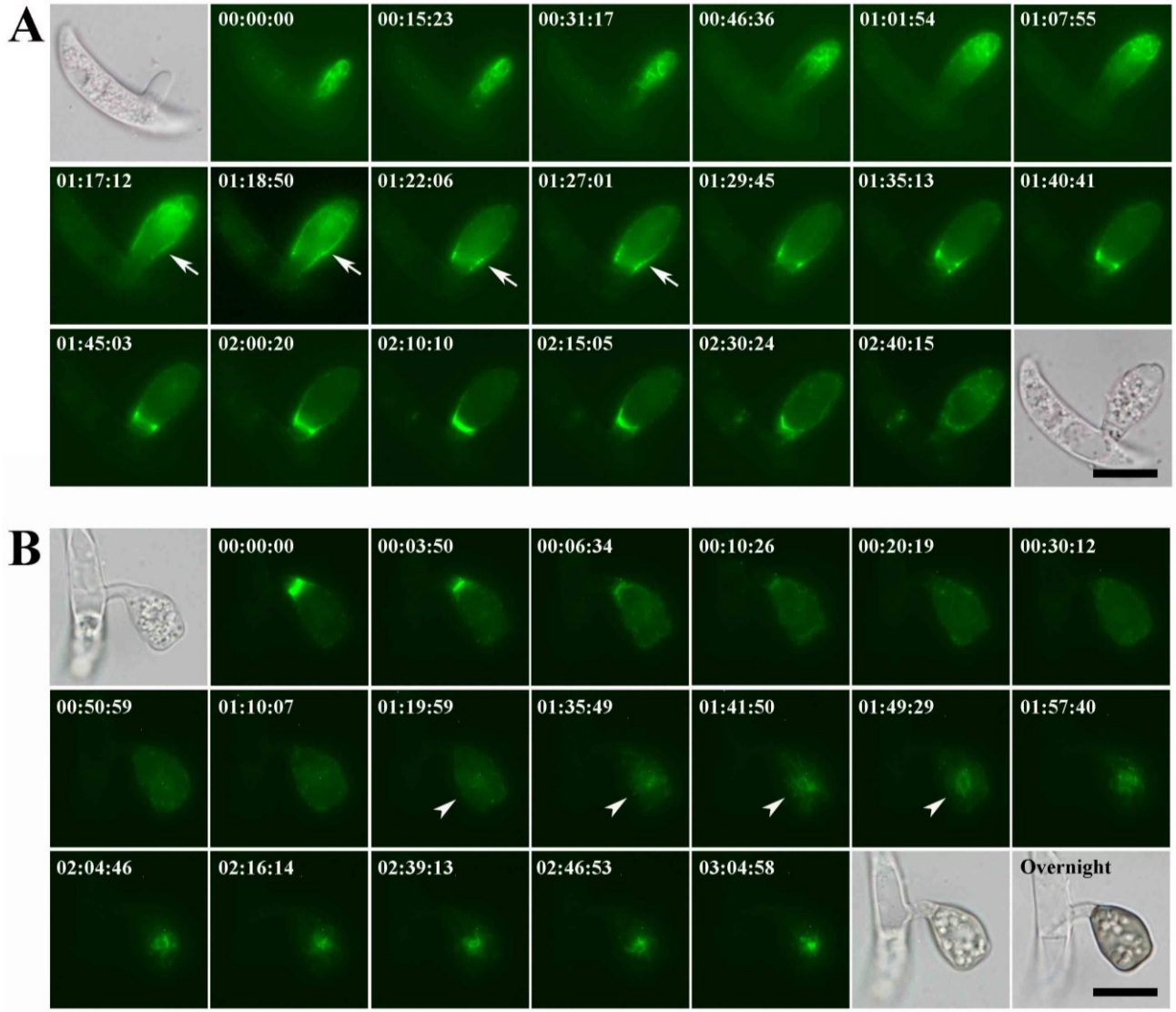
A
00:00:00
00:15:23
00:31:17
00:46:36
01:01:54
01:07:55
01:17:12
01:18:50
01:22:06
01:27:01
01:29:45
01:35:13
01:40:41
01:45:03
02:00:20
02:10:10
02:15:05
02:30:24
02:40:15
B
00:00:00
00:03:50
00:06:34
00:10:26
00:20:19
00:30:12
00:50:59
01:10:07
01:19:59
01:35:49
01:41:50
01:49:29
01:57:40
02:04:46
02:16:14
02:39:13
02:46:53
03:04:58
Overnight

signal around the central area of appressoria then shifted along the cell periphery to the base of the appressoria where a septum began to form (Figure A.2 A, arrows). The signal shift occurred over a 7- to 10-min period.

The process of septum formation at the base of appressoria was similar to that described above. Subsequently, the Lifeact-GFP signal shifted from the newly formed septum back to the appressoria along the periphery of the cell. During the following 50 min, actin cables and patches formed a loose network evenly distributing at the cortex, and there was no significant change in signal intensity (Figure A.2 B, from time point 00:20:19 to 01:10:07). Although the Lifeact-GFP signal intensity in appressoria was low during this period of time, it was still more apparent than that in the conidial compartment and the basal part of germ tube. Next, an accumulation of Lifeact-GFP signal appeared at the central area of appressoria (Figure A.2 B, arrow heads). Actin cables then gradually appeared at the center of the appressorium near the face in contact with the substratum. The actin cables were oriented toward the central region and periodically formed a ring structure. The ring became more concentrated over time (Figure A.2 B, from time point 02:04:46 to 03:04:58). The F-actin later concentrated at a circle area that co-localized to the un-melanized penetration pore in bright field (See below). Over night, the completion of a melanized appressorium indicated the cell was healthy despite expression of Lifeact-GFP and long-term exposure with intense light from the microscope (Figure A.2 B).

The *C. graminicola* hyphopodium is more varied in shape than the appressorium. It is usually derived from hyphae and is able to penetrate root cells and leaf sheaths

(Sukno et al., 2008). Our observations indicated that actin cables and patches also played an important role in shaping hyphopodial development. A retrograde movement of actin cables from the front edge of hyphae was more prominent while differentiating a hyphopodium. A lobed hyphopodium developed at the end of the differentiated hypha and physically contacted the hard glass surface. Similar to appressoria, actin cables assembled in the central area of hyphopodia and then concentrated in a circle area. After several hours, the hyphopodium was melanized, but left an un-melanized circular area that was presumed to be the penetration pore (Figure A.3). Although it is unknown if the formation of hyphopodia and appressoria are controlled by the same signaling pathways, this data suggested that they shared a similar developmental processes.

The retrograde movement of actin cables from growing tips consistently occurred during the development of germ tubes, appressoria and hyphopodia of *C. graminicola*, indicating that the movement may play a crucial role in cell differentiation. The same phenomenon was also observed in *N. crassa* and *S. cerevisiae* (Berepiki et al., 2010; Yang and Pon, 2002). In budding yeast, the movement is proposed to be due to assembly of new materials at the end of actin cables. In this model, cable elongation occurs at the apex resulting in the retrograde movement of the actin meshwork at sites of greatest growth activity. The Myo2p-dependent secretory vesicles are delivered along the actin cables to the cable assembly sites in a direction opposite of the retrograde movement (Moseley and Goode, 2006; Pruyne et al., 1998; Schott et al., 2002; Yang and Pon, 2002). If this model is also functional in *C. graminicola*, it suggests that the secretory vesicles were delivered along actin cables toward the leading edges of growing tips. This

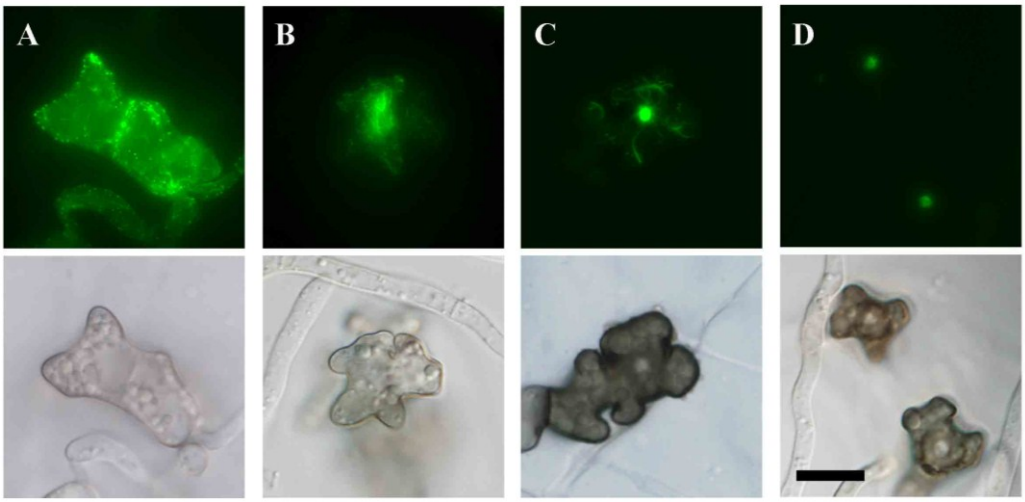

Figure A.3 F-actin subcellular localization during hyphopodium formation.
Actin cables and actin patches were distributed throughout the developing hyphopodium (A). Once the hyphopodial shape was set, actin cables redirected to the center of the hyphopodium (B). In a melanized hyphopodium, F-actin gradually concentrated in a ring at the penetration pore (C & D). Bar = 10 um.

suggestion matched with our observations that the intense Lifeact-GFP signal was always observed at the growing tips or leading edges, and more intense signal corresponded with more significant growth, supporting the hypothesis that retrograde directed actin cables support growth.

Formins are required for the assembly of actin filaments and of actin rings in budding yeast (Evangelista et al., 2002; Sagot et al., 2002; Tolliday et al., 2002). A formin homolog of *A. nidulans*, SepA, was also required for septum formation and localized to septation sites (Sharpless and Harris, 2002). These data indicate that new actin filaments were assembled during sepation. The *C. graminicola* Lifeact-GFP signal apprears to shift during appressorium formation and septation indicated that pre-existing actin elements were involved in septum formation. During the Lifeact-GFP signal shift from the germ tube apex to the septation site in the conidium, the less defined Lifeact-GFP signal of actin elements appeared to be formed from the pre-existing actin cables. Since Abp140p is an actin binding protein that attaches to actin at a ratio of 1 to 30 (Asakura et al., 1998), I speculated that the shifting actin elements were in the form of actin filaments which unbundled from the pre-existed actin cables, and reassembled to actin cables at a new place. Since actin filaments are very small, a group of Lifeact-GFP actin filaments may appear as hazy GFP signal. The long actin cables then appear around the septation site and may be bundled from these pre-existing unbundled actin filaments instead of from newly generated filaments at septation site. These data raise the questions of how the pre-existing actin elements were useful since the new actin filament will be assembled at sites?; what coordinates the un-bundling and bundling of actin

filaments?; and how the actin elements were delivered along the the cell cortex?

F-actin functions in penetration

To further document the dynamics of F-actin during penetration, I inoculated the *C. graminicola* Lifeact-GFP strain on onion epidermal cells. Actin cables and patches were present in conidia and germ tubes during germination, but mostly in the appressorium during formation. Actin cables formed a ring at the site of penetration. The ring area was not melanized in mature appressoria when observed through bright field microscopt. The penetration pore formed at sites where appressoria was in tight contact with onion epidermal cells. A fine penetration peg developed from the penetration pore. F-actin was present in the penetration peg and intensely localized at the apex, but the forms of F-actin were not observable. After penetrating through the cell wall, the apex of penetration peg swelled to form a swollen invasive hypha. Actin cables and some actin patches were discernable during these developmental processes (Figure A.4).

While actin cables formed a ring at the presumed penetration pore there was no visible change to the appressoria in bright field images (data not shown). However, according to established data on the the developmental processes and the ultrastructure of appressoria formation of *C. graminicola*, an inner crescent of electron translucent wall material was deposited at surface in contact with the substratum after the shape of the appressorium was set. The electron translucent wall resembled the 'bilayer pore wall overlay' in *M. oryzae* appressoria (Bourett and Howard, 1990), though only one layer was resolved in *C. graminicola* appressoria. Later, the outer electron-dense wall at

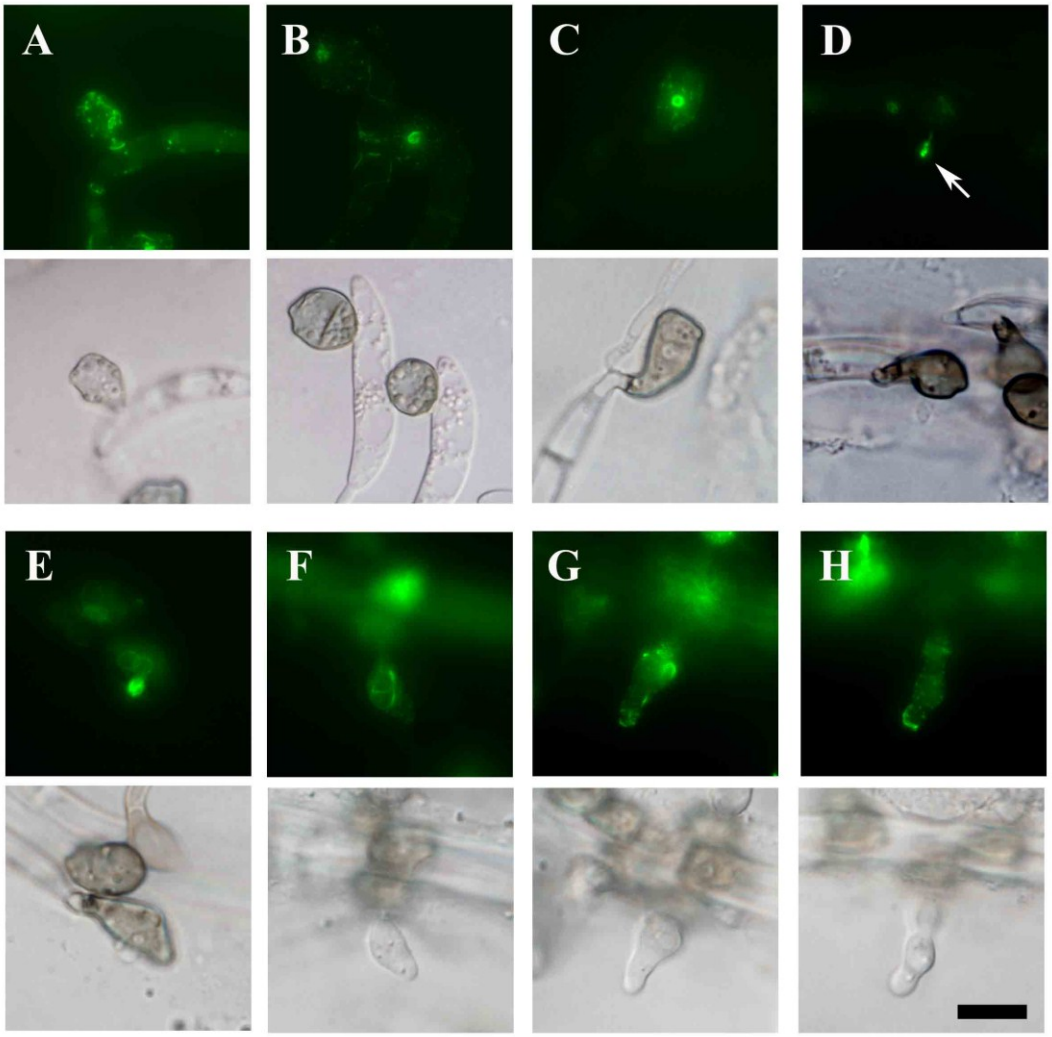

Figure A.4 F-actin subcellular localization during penetration of onion epidermal cells. F-actin localized at the cell periphery while appressoria were formed (A). F-actin gradually concentrated at an unmelanized ring (B & C). A penetration peg was formed beneath this ring. F-actin was concentrated at the tip of the penetration peg (D). After penetration through the cell wall, actin cables and actin patches were found at the cell apex, as the pentration peg swelled into an invasive hyphae the actin distribution became less concentrated (E-H). Bar = 10 um.

region of the penetration pore disappear (Politis and Wheeler, 1973). The penetration peg develops from a region inside the crescent of electron translucent wall. Similar to *M. oryzae*, the inner electron translucent wall of appressoria was continuous to the wall surrounding penetration pegs and invasive hyphae (Bourett and Howard, 1990; Politis and Wheeler, 1973). Since actin cables are involved in hyphal growth and septum formation, I speculate that the actin cables were functional in depositing the electron translucent wall for preparing penetration, and further played a role in the dissolution of the outer electron-dense wall and in the formation of penetration pore. Although hyphopodia are morphologically distinct from appressoria, both structures share many characteristics. I predict that hyphopodia also contain a layer of inner electron translucent wall in their ultrastructure, and require F-actin to deposite the electron translucent wall and to form the penetration pore.

APPENDIX B

THE CYTOLOGY OF *Fusarium* - MAIZE STALK ROT PATHOGENESIS

To visualize the fungus *in planta*, a sGFP-tagged transformant (Fv-GFP) expressing free sGFP in the cytosol was acquired from Dr. Won-Bo Shim (Texas A&M University). This Fv-GFP strain displayed similar culture phenotypes and pathogenicity to wild type and was selected to represent the wild-type strain for cytological studies (data not shown). A conidium suspension of the Fv-GFP strain was inoculated on the wounded basal inter-node for 6, 9, 12 days. The Fv-GFP strain was observed in free-hand sections of stalk tissue. *F. verticillioides* intracellularly and intercellularly colonized and broke down the parenchyma cells surrounding the inoculation site (Figure B.1 A and B). Compared with parenchyma cells, the vascular bundles possessing thick cell walls were more recalcitrant to fungal digestion than parenchyma (Figure B.1 D). Microconidium sporulation inside plant tissue was also observed in this area (Figure B.1 C, arrow). Colonization by the fungus involved extending hyphae between the intercellular spaces without penetrating the plant cells. Fungal hyphae also spread through the vascular bundles. It was noted that the spread of mycelia utilizing the vascular bundle is faster than from intercellular space. Maize also responded to fungal invasion by depositing occlusions in the vascular bundle along cell walls and in intercellular spaces, which was accompanied by a discoloration of those tissues.

The wild type and Δ*fsr1* strains caused necrotic parenchyma tissue around inoculation sites. Wild type caused larger lesions than did the Δ*fsr1* strain. Discolored

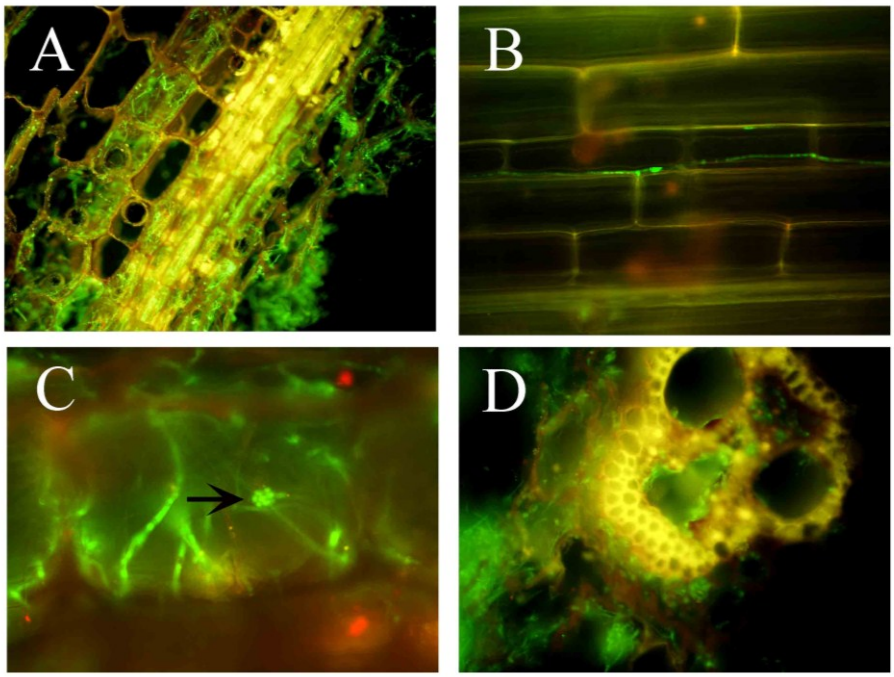

Figure B.1 Representative micrographs of wild-type *F. verticillioides* (Fv-GFP) colonizing maize stalks.
F. verticillioides colonized maize stalk intracellularly (A) and intercellularly (B), and sporulated (arrow) in colonized tissue (C). The vascular bundles possessing thick cell wall were more tolerant to fungal digestion than parenchyma (D).

vascular bundles were extended from necrotic regions infected by wild type and Δ*fsr1* strains. Tissue isolation assays revealed that the wild type and Δ*fsr1* strains were colonized in necrotic and non-necrotic tissues (Figure B.2). To re-confirm this preliminary result that the Δ*fsr1* strain was isolated from non-necrotic tissues, a GFP-tagged Δ*fsr1* may help to track the presence of the mutant strain. Accordingly, I generated a free GFP-tagged Δ*fsr1* strain (Δ*fsr1*-GFP) to visualize the role of *fsr1* during the course of colonization and disease expression. Briefly, a *gpdA*(p)::sGFP construct was amplified from plasmid gGFP (Maor et al., 1998) with primer sGFP/R (5'CTCATGTTTGACAGCTTATCATCGGA3') and primer gGFP/P6 (5'CGTCTGGACCGATGGCTGTG3'), and then cloned in psGFP with pGEM-T easy vector background. The psGFP and pBP-G containing geneticin resistance gene were co-transformed into Δ*fsr1* strain. The Δ*fsr1*-GFP strain (ΔFvfsr1-sGFP1) displayed strong GFP signal and possessed comparable pathogenecity and colonial characteristics to the Δ*fsr1* strain. The Δ*fsr1*-GFP strain is ready to examine the colonization ability of *F. verticillioides* in *fsr1* mutation background.

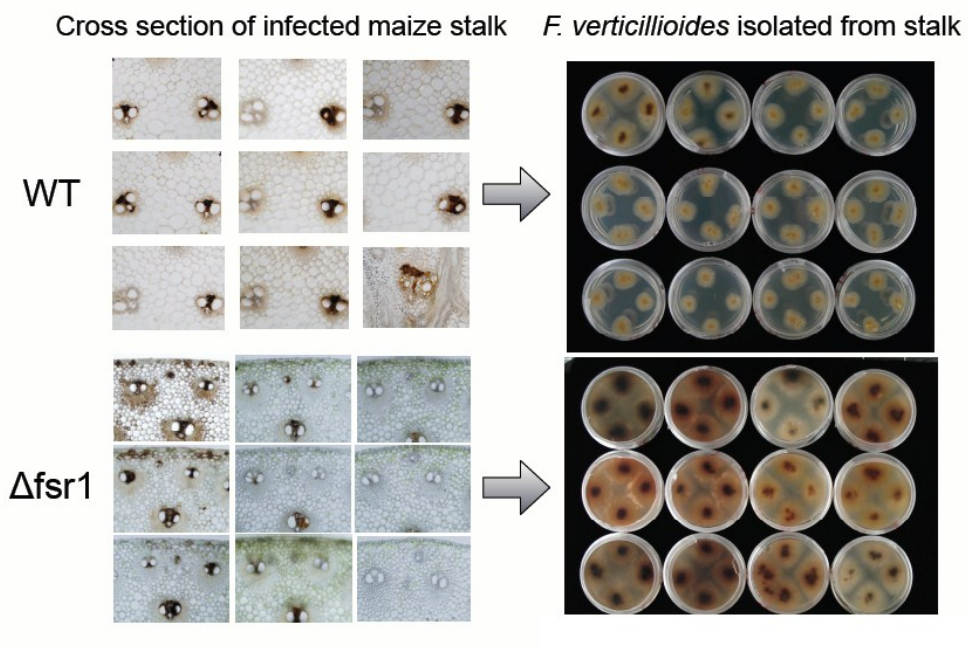

Figure B.2 Cross section of maize stalks infected by wild type and Δ*fsr1 F. verticillioides*.
Wild type and Δ*fsr1* stains were able to be isolated from discolored (necrotic) and non-discolored tissues.

APPENDIX C

Aspergillus nidulans StrA::S-tag STRAINS AND BiFC VECTORS FOR *Fusarium verticillioides*

Generation of StrA::S-stag strains

RNase A (pancreatic ribonuclease A) catalyzes the cleavage of RNA. RNase S, a short version of RNase A, consists of S-peptide (1-20 aa) and S-protein (21-124 aa), and has a comparable enzymatic activity as RNase A. The S-Tag (KETAAAKFERQHMDS) was derived from S-peptide and necessary to form a fully functional complex with S-protein (Potts et al., 1963). The small size of S-Tag has a high sensitivity of detection and is excessively soluble with little net charge at neutral pH (Kim and Raines, 1993). These properties make the S-Tag unlikely to interfere the proper folding and function of a fused target protein. Therefore, S-Tag has been widely used in protein purification. In addition, S-Tag was also applied to search for interacting proteins of a protein of interest in *A. nidulans* (Liu et al., 2009).

As a step toward identifying the fungal striatin-interacting proteins, I have generated strains that have S-Tag at the C-terminus of *A. nidulans* StrA expressed from its native locus. The strain generation strategy and primers used were the same as those for generating the StrA::eGFP strains (see Chapter II). Instead of amplifying eGFP::*pyrG*-AF construct from pFN03, the S-tag::*pyrG*-AF construct was amplified from pHL-81 with the same primers (Liu et al., 2009), fused with other amplicons, and cloned into pGEM-T easy vector, resulting pStrA-S-tag8. The pStrA-S-tag8 was transformed into

TN02A25. Transformants containing S-tag at the *strA* native locus were selected for examining the StrA::S-tag expression. The StrA::S-tag expression was verified by western blot with the S-tag antibody (Thanks to Dr. Shengli Ding Texas A&M University for assistance) (Figure C.1).

I also constructed DNA fragments that will be used to fuse S-tag to the C-terminus of *F. verticillioides fsr1* with the split-marker method. A 1514-bp 3'-end coding region of *fsr1* without stop codon was amplified from wild-type *F. verticillioide* M3125 with primer Fvfsr1F1 (5'ACCGCCCTGATACCGATGCTTT3') and primer Fvfsr1R-S-tag (5'GGCACCGGCTCCAGCGCCTGCACCAGCTCCTCGTGCAAACACCTTGACCAC3'), which contains 30-bp overlapping with the N-terminus of an S-tag amplicon. The S-tag amplicon including a GA-5 linker at N-terminus and 3' UTR was amplified from pHL-81 with primer GFP-F (5'GGAGCTGGTGCAGGCGCT3') and primer NS-Hph (5'GTAATCATGGTCATAGCTGTTTCCACAGGCCACATCGGTGCTGTAT3'), which contains 24-bp overlapping with an amplicon containing *hph* gene. The amplicon was amplified from pBP15 with primer M13R-F (5'GGAAACAGCTATGACCATGATT3') and primer M13F-R (5'TTGTAAAACGACGGCCAGTGA3'). The three amplicons were fused in a 3'*fsr1*::S-tag::*hph* construct by fusion PCR. A 1732-bp fragment from the 3'UTR of *fsr1* was amplified from the wild-type strain with primer Fvfsr1DF (5'TACGCGCGCTCACTGGCCGTCGTTTTACAAAAAAGGGTACGGGGTGGTGGTG3') and primer Fvfsr1DR1 (5'ACTGTCGGGGCTGCTGTTTGAC3'). The 3'*fsr1*::S-

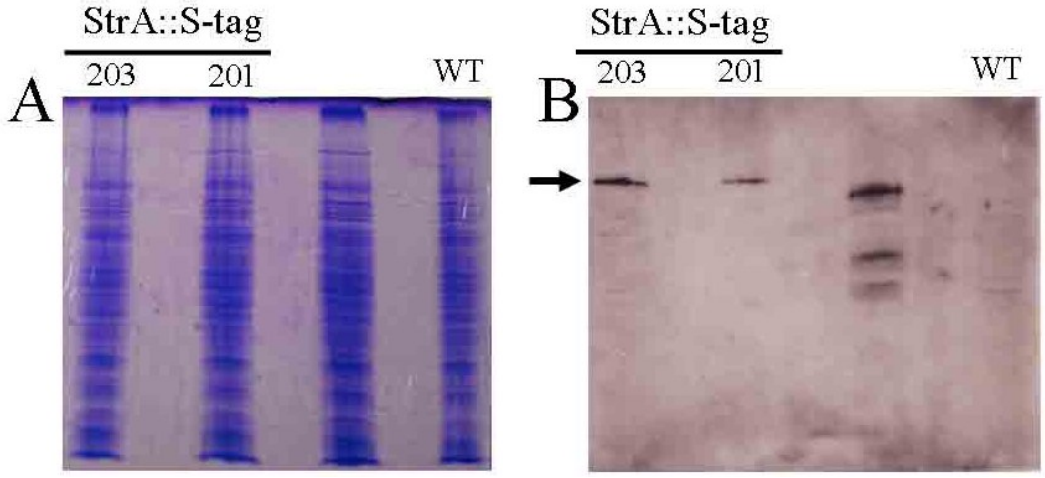

Figure C.1 Expression of StrA::S-tag.
Two transformants (StrA::S-tag 201 & 203) containing S-tag tagged StrA (arrow) were detected with S-tag antibody while wild-type strain did not.

tag::*hph* construct and the 3'UTR of fsr1 were further fused into a final amplicon with fusion PCR. The first split-marker cassette containing a 1149-bp fragment from the 3'end of the coding region of *fsr1*, a S-tag, and a N-terminal part of *hph* gene was amplified from the final amplicon with nested primer Fvfsr1F2 (5'GGTCACGCAGGAGCAATTCTGT3') and primer HY-R (5'GGATGCCTCCGCTCGAAGTA3'). The cassette was cloned into pGEM-T easy vector and named pfsr1-Stag-NSM1. The second split-marker cassette including a C-terminal part of hph gene and a 1328-bp fragment from the 3'UTR of *fsr1* was amplified from the final amplicon with primer YG-F (5'CGTTGCAAGACCTGCCTGAA3') and nested primer Fvfsr1R2 (5'CCTTCCGAACCTCTGTGATCTTGC3'), and cloned to form pfsr1-Stag-SM2. The two cassettes were ready to be amplified for transformation.

BiFC vectors for *Fusarium verticillioides*

One of the best ways to confirm the protein interaction is to see the proteins interacting with each other in living cells. BiFC (bimolecular fluorescence complementation) assay applies "split YFP" on two potential interacting proteins in living cells. If the two tagged proteins interact, they may bring two split fluorescent components together, resulting in reconstituting fluorescence (Kerppola, 2006). Our lab received two vectors (pDV7 and pDV8) containing *apsB* from Dr. Reihard Fisher (Karlsruhe Institute of Technology). Each contains one of the N- or C- terminus of *yfp* under the control of *alcA* promoter and a *pyr4* selection marker for using in *A. nidulans*. To verify two vectors contain compatible truncated constructs, I transformed pDV7 into

A773 strain and PDV8 into TN02A25, resulting in A773DV7-1 and TNDV8-1 strains, respectively. Progeny (AnapsB-Bifc12G) of A773DV7-1 X TNDV8-1 containing both N-*yfp*::*apsB* and C-*yfp*::*apsB* displayed YFP signal while the progeny only containing one construct did not (data not shown). Similar to a previous report that ApsB forms a homo-dimer and localized to the spindle pole bodies in *A. nidulans* (Suelmann et al., 1998; Veith et al., 2005). This result verified the two vectors for the BiFC assay.

To apply BiFC assay on *F. verticillioides*, new vectors need to be made and essentially have the substitutive promoter and selective markers, and restriction sites that are available to insert the genes of interest following the truncate *yfp* constructs. A 846-bp short functional version of *gpdA* promoter was amplified from plasmind gGFP with primer GPDA-F1 (5'CGGTGCCTGGATCTTCCTAT3') and primer GPDA-R (5'GATGGGAAAAGAAAGAGAAAAGAAA3') (Kim and Woloshuk, 2008). The N-*yfp* was amplified from pDV7 with primer L-gpd-NYFP-F (5'CTTTTCTCTTTCTTTTCCCATC**GGTACC**ATGGTGAGCAAGG3') which contains 22 bp overlapping with the *gpdA* promoter and a *Kpn*I restriction site, and primer L-NYFP-R (5'-C**GGCGCGCC**CGTGGCGATGGA-3') which contained an *Asc*I restriction site. Similarly, the C-*yfp* was amplified from pDV8 with primer L-gpd-CYFP-F

(5'CTTTTCTCTTTCTTTTCCCATCC**GGTACC**ATGGCCGACAAGCAGAAGAAC G3') which contained 22-bp overlapping with the *gpdA* promoter and a *Kpn*I restriction site, and primer L-CYFP-R (5'C**GGCGCGCC**GTGGTTCATGACCTTCTGTTTC3') which contained an *Asc*I restriction site. The *gpdA* promoter was fused with N-*yfp* and

C-*yfp* by fusion PCR, respectively, to acquire *gpdA*::N-*yfp* and *gpdA*::C-*yfp* constructs. The *hph* gene was amplified from pBP15 with primer L-NYFP-Hph-F (5'CCATCGCCACG**GGCGCGCCG**TTAATTAACGATAACTGATATTGAAGGAG C3') which contained 20 bp overlapping with the *gpdA*::N-*yfp* construct and an *Asc*I and a *Pac*I restriction sites, and primer M13F-R (5'TTGTAAAACGACGGCCAGTGA3'). The *gen* gene was amplified from pBP-G with primer L-CYFP-Gen-F (5'GGTCATGAACCAC**GGCGCGCCG**TTAATTAAGCGGCTTCGAATCGTGGCT A3') which contained 22 bp overlapping with the *gpdA*::C-*yfp* construct and an *Asc*I and a *Pac*I restriction sites, and primer M13R-F (5'GGAAACAGCTATGACCATGATT3'). The *gpdA*::N-*yfp* construct and *hph* gene were further fused by fusion PCR and amplified with nest primer GPDA-F (5'AGAGACGGACGGTCGCAGAG3') and nest primer M13F-R1 (5'GACGGTATCGAT**AAGCTT**GAT3') which contained a *Hind*III restriction site. The resultant amplicon was cloned into pGEM-T easy vector, named pNm3 (*gpdA*::*Kpn*I::N-*yfp*::*Asc*I::*Pac*I::*gen*::*Hind*II) . The *gpdA*::C-*yfp* construct and *gen* gene were fused by fusion PCR, amplified with nest primer GPDA-F and nest primer M13F-R1, and then cloned into pGEM-T easy, resulting pCm3 (*gpdA*::*Kpn*I::C-*yfp*::*Asc*I::*Pac*I::*gen*::*Hind*II). In short, the coding region of two potential interacting proteins can be amplified with a 5'end primer containing an AscI restriction site and a 3'end primer containing a PacI restriction site, and cloned into pNm3 or pCm3, respectively. The resultant plasmids derived from pNm3 and pCm3 are ready to be transformed in pairs to examine the homo- and hetero- protein-protein interactions.

Hex1, a candidate of *F. verticillioides* Fsr1-interacting protein, has been identified from Dr. Won-Bo Shim's lab by Y2H screen. The BiFC technique was chosen to further verify the interaction in living cell. To insert genes of interst, the pNm3 and pCm3 were designed to contain an *Asc*I and a *Pac*I restriction sites that are juxtaposed to each other and placed directly behind either the N- or C- terminus of *yfp* in each vector. Accordingly, the N- or C- terminus of YFP will tag on the N-terminus of proteins encoded by the inserted genes of interest. The *F. verticillioides fsr1* was amplified with primer Fvfsr1AscF (5'TT**GGCGCGCC**AATGGGCCCTAATGCTGGCAACG3') and primer Fvfsr1PacR2 (5' CC**TTAATTAA**TTGAGGCATCGGAATGAGGTCAGG 3'), and then cloned in pFsr1-Bifc. The *hex1* was amplified with primer FvHex1F (5'TT**GGCGCGCC**AATGATACGCAAGCGAGATACTATAGA3') and primer FvHex1R (5'CC**TTAATTAA**GGAGCTCAGGTATAACTCCTAAGCCTT3'), and then cloned in pHex1-Bifc. Both fsr1 and hex1 were released from their vectors by digesting with *Asc*I and *Pac*I, and cloned into *Asc*I- and *Pac*I-digested pNm3 or pCm3, resulting in four vectors pNmfsr1, pCmhex1, pNmhex1, and pCmfsr1 (Figure C.2). Thus, a pair of BiFC vectors (pNmfsr1 & pCmhex1 or pNmhex1 & pCmfsr1) can be co-transformed into *F. verticillioides* to examine the YFP expression using the fluorescence microscope.

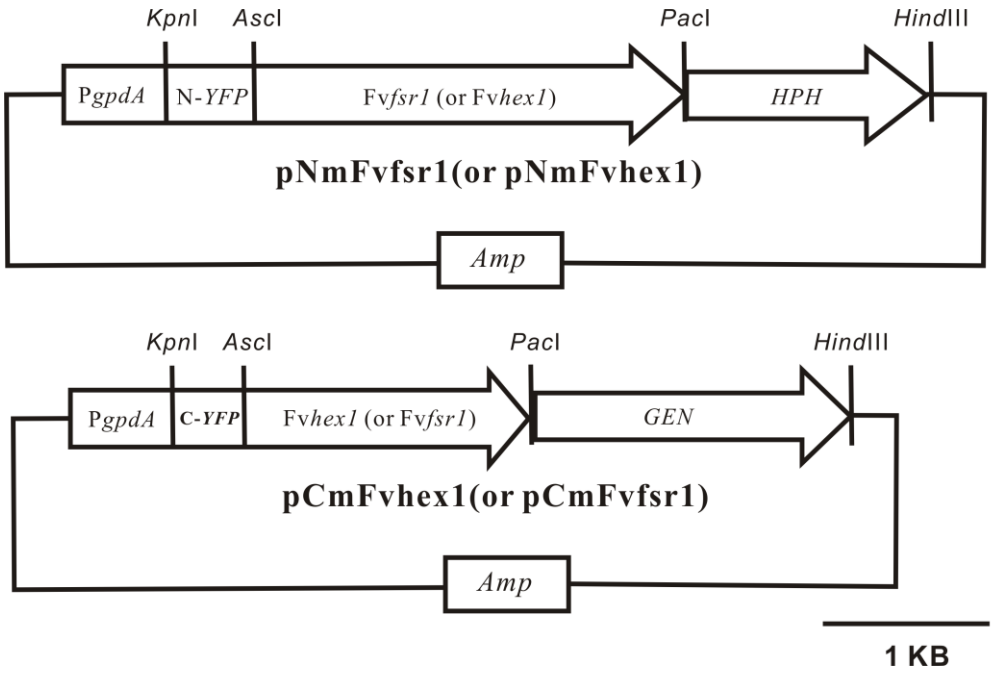

Figure C.2 BiFC vectors for Fv*fsr1* and Fv*hex1*.
N-terminal or C-terminal truncated YFP were tagged at the N-terminus of Fv*fsr1* or Fv*hex1* and expressed by *gpdA* promoter. Hygomycin and Geneticin resistant genes were used as selective markers respectively. The BiFC expression constructs with selective markers were cloned in the pGEM-easy vector.

VITA

Name: Chih-Li Wang

Address: Department of Plant Pathology and Microbiology
c/o Dr. Brian Shaw
2132 TAMU
Texas A&M University
College Station, Texas 77843-2132

Email Address: chih-tamu@tamu.edu

Education: B.A. Plant Pathology, National Chung Hsing University, Taichung, Taiwan
M.S., Plant Pathology, National Chung Hsing University, Taichung, Taiwan

Selected Publications:

Shaw, B.D., Chung, D.W., Wang, C.L., Quintanilla, L.A., and Upadhyay, S. 2011. A role for endocytic recycling in hyphal growth. Fungal Biology, 115: 541-546.

Wang, C.L., Shim, W.B., and Shaw, B.D. 2010. *Aspergillus nidulans* striatin (StrA) mediates sexual development and localizes to the endoplasmic reticulum. Fungal Genetics and Biology 47: 789-799.

Wang, C.L., Chang, P.F.L., Lin Y.H., Malkus A., and Ueng P.P. 2009. Group I introns in SSU ribosomal DNA of several *Phaeosphaeria* species. Botanical Studies 50: 167-177.

Wang, C.L, Malkus A., Zuzga S.M., Chang P.F.L., Cunfer B.M., Arseniuk E., and Ueng P.P. 2007. Diversity of the tri-functional histidine biosynthesis gene (*his*) in cereal *Phaeosphaeria* species. Genome 50: 595-609.

Chen, C.Y., Wang, C.L., and Huang J.W. 2006. Two new species of *Kirschsteiniothelia* from Taiwan. Mycotaxon 98: 153-158.

Wang, C.L. and Hsieh, H.Y. 2006. Occurrence and pathogenicity of stem canker of guava in Taiwan caused by *Botryosphaeria rhodina*. Plant Pathology Bulletin 15: 219-230.

Hsieh, W.H., Chen, C.Y., and Wang, C.L. 2000. Taiwan ascomycetes — Pyrenomycetes and Loculoascomycetes. China graphics, Taichung, Taiwan, 244pp.